Advanced Engineering Research

Theoretical and scientific-practical journal

Vol. 22

no. 4

2022

ISSN 2687-1653

1 Mechanics

2 Machine Building and Machine Science

3 Information Technology, Computer Science, and Management

DOI 10.23947/2687-1653

vestnik-donstu.ru

Advanced Engineering Research

Vol. 22, no. 4

Theoretical and scientific-practical journal

Published since 1999

Quarterly
October-December 2022

ISSN 2687-1653
DOI: 10.23947/2687-1653

Founder and publisher ─ Federal State Budgetary Educational Institution of Higher Education

Don State Technical University (DSTU)

The journal was known as Vestnik of Don State Technical University (until August 2020)

Included in the list of peer-reviewed scientific editions where the basic research results of doctoral, candidate's theses should be published (State Commission for Academic Degrees and Titles List) in the following research areas:

1.1.8 – Deformable Solid Mechanics (Engineering Sciences)
1.1.8 – Deformable Solid Mechanics (Physicomathematical Sciences)
1.2.2 – Mathematical Simulation, Numerical Methods and Program Systems (Engineering Sciences)
2.3.5 – Software and Mathematical Support of Machines, Complexes and Computer Networks (Engineering Sciences)
2.5.3 – Machine Friction and Wear (Engineering Sciences)
2.5.5 – Technology and Equipment of Mechanical and Physicotechnical Processing (Engineering Sciences)
2.5.6 – Engineering Technology (Engineering Sciences)
2.5.8 – Welding, Allied Processes and Technologies (Engineering Sciences)

The journal is indexed and archived in the Russian Science Citation Index (RSCI), in the International Database EBSCO (Academic Search Ultimate Magazines and Journals), Dimensions, CyberLeninka, ROAD, GoogleScholar. The journal is a member of Directory of Open Access Journals (DOAJ), Association of Science Editors and Publishers (ASEP) and CrossRef.

Certificate of mass media registration ЭЛ № ФС 77 – 78854 of 07.08.2020 is issued by the Federal Service for Supervision of Communications, Information Technology, and Mass Media

The issue is prepared by:

Inna V. Boyko, Marina P. Smirnova (English version)

Founder's, Publisher's and Printery Address:

Gagarin Sq. 1, Rostov-on-Don, 344003, Russia. Phone: +7 (863) 2-738-372

E-mail: vestnik@donstu.ru http://vestnik-donstu.ru/

CONTENTS

MECHANICS

UDC 531.01

https://doi.org/10.23947/2687-1653-2022-22-4-296-305

Original article

Development of Properties Control Methods for Magnetorheological Medium to Regulate the Stiffness of Exoskeleton Variable-Length Link

Alexander O. Blinov[1] ✉, **Andrey V. Borisov**[1], **Larisa V. Konchina**[1], **Marina A. Novikova**[1], **Anatoly V. Chigarev**[2]

[1] National Research University "MPEI", Smolensk Branch, 1, Energeticheskii proezd, Smolensk, Russian Federation

[2] Belarusian State University, 4, Nezavisimosti Avenue, Minsk, Republic of Belarus

✉ alex-blinov67@yandex.ru

Abstract

Introduction. The article investigated one of the problems of creating exoskeletons — controlling the properties of magnetic rheological fluid in links of variable length with adjustable stiffness. Based on the research of domestic and foreign authors, the development and urgency of the topic was evaluated. The disadvantage of known exoskeleton models has been specified, i.e., the use of absolutely solid links, whose dynamics does not convey the dynamics of the human musculoskeletal system. The scientific research aimed at the formation of a new direction in the development of exoskeletons that accurately simulate the biomechanics of movements.

Materials and Methods. Different states of structures of variable-length links with a magnetorheological fluid were studied. It has been noted that the links work on the principle of magnetic shock absorbers and consist of a piston rod, electromagnetic coils, and a housing filled with magnetorheological fluid. The ordering effect of an external magnetic field on the particles of a magnetorheological fluid was visualized and mathematically presented. The significance of such factors as time, charge density, magnetic field strength, as well as vectors of electric and magnetic induction, electric intensity and electric current density for this system was shown. The input parameter affecting the behavior of the magnetorheological fluid was determined. This was the magnetic field intensity. It was shown that the viscosity of the liquid varied depending on the shape of the magnetic particles (oblong or oblate ellipsoid).

Results. The dependences that were fundamental for solving the task were investigated and visualized. The magnetic field strength and the angle between the vector directed along a straight line connecting the centers of two micron particles, and the vector of the external magnetic field strength were taken as the basic parameters. It was shown how the magnetic moment, voltage and its antisymmetric part depended on them. It was established that to control the properties of a magnetorheological fluid, it was required to change:

– the external magnetic field intensity;

– the angle between the external magnetic field intensity and the orientation vector between the dipoles.

Two values of force were compared: one – for a given link design, and the other — fixed when walking in the lower leg of a person. The consistency of these indicators was established.

Discussion and Conclusion. The scientific research results allowed us to present:

– a method for controlling the properties of a magnetorheological fluid by an external magnetic field;

– a variable-length link model with adjustable stiffness.

The results obtained can be used in modeling multilink structures to create comfortable exoskeletons that interact synchronously with the human musculoskeletal system as a single human-machine system. The development is applicable to solving significant social and economic problems.

Keywords: exoskeleton, magnetorheological fluid, variable-length link, adjustable stiffness, magnetic induction, magnetic field strength, magnetorheological fluid intensity, magnetic moment.

Acknowledgements. The authors would like to thank the reviewers for valuable comments that contributed to the improvement of the article.

Funding information. The study was conducted with the financial support of the Russian Science Foundation (grant no. 22–21–00491), https://rscf.ru/project/22-21-00491/

For citation. A. O. Blinov, A. V. Borisov, L. V. Konchina, M. A. Novikova, A. V. Chigarev. Development of Properties Control Methods for Magnetorheological Medium to Regulate the Stiffness of Exoskeleton Variable-Length Link. Advanced Engineering Research, 2022, vol. 22, no. 4, pp. 296–305. https://doi.org/10.23947/2687-1653-2022-22-4-296-305

Introduction. Previously performed modeling allowed us to identify changes in the lengths of the links of the human musculoskeletal system, their sizes, movement speeds, as well as to determine the forces in the kinematic chain [1]. This made it possible to formulate requirements for the properties and modes of functioning of the exoskeleton link that repeats the basic biomechanical properties of the corresponding user link. The study aims at developing a model of a variable-length link with adjustable stiffness to create comfortable exoskeletons of a new generation that adequately reproduce the actions of the human musculoskeletal system. Exoskeletons are used in medical and rehabilitation centers to verticalize the position of the patient's body, in cosmonautics when creating spacesuits and rehabilitation suits.

Magnetic fields acting on a magnetorheological medium can be used to control models of links with adjustable stiffness. Exoskeletons with adjustable stiffness of variable length links will provide stable, safe, comfortable human locomotion. The implementation of drives for controlled configuration changes in such models is of practical value, which determines the urgency of the study.

From 2010 to 2020, the number of publications with the keyword “exoskeleton” in the database “Russian Science Citation Index” increased ten times (there were less than 50 and became more than 500). Since 2015, the number of patents for exoskeletons and their components has been growing, specialized software is being registered more often. Currently, there is no data on the links of variable-length exoskeletons with adjustable stiffness. Solutions with soft electric pumps and a pneumatic ring generator are mentioned, but they do not use magnetorheological fluids[1]. There is a description of an actuator with a magnetorheological fluid, whose viscosity changes under the influence of a magnetic field [2–4][2]. It is proposed to use magnetorheological materials to create exoskeleton drives[3]. In [4–6], the use of magnetorheological fluid in the creation of an exoskeleton knee joint drive was studied. The torque in this joint has a damping effect when walking [7]. Magnetorheological drives were considered in [8–9]. An exoskeleton, whose links can be adjusted in length and stiffness, has not yet been developed.

Materials and Methods. It is assumed that the exoskeleton link will work on the principle of magnetic shock absorbers [10]. The link consists of a rod with piston *AE*, housing *CB*, filled with a magnetorheological fluid, and electromagnetic coils (Fig. 1).

[1] Soft Robots Were Equipped with Electrophoretic Logic Circuits. planet-today.ru. URL: https://planet-today.ru/novosti/nauka/item/110728-myagkikh-robotov-osnastili-elektroflyuidnymi-logicheskimi-skhemami (accessed: 10.09.2022).
[2] Psomopoulou E, et al. A Simple Controller for a Variable Stiffness Joint with Uncertain Dynamics and Prescribed Performance Guarantees. Proc. IEEE/RSJ International Conference on Intelligent Robots and Systems. 2012. P. 5071–5076. 10.1109/IROS.2012.6385859
[3] Jinzhou Chen, Wei-Hsin Liao. Design and Control of a Magnetorheological Actuator for Leg Exoskeleton. In: Proc. IEEE International Conference on Robotics and Biomimetics (ROBIO). 2007. P. 1388–1393. 10.1109/ROBIO.2007.4522367

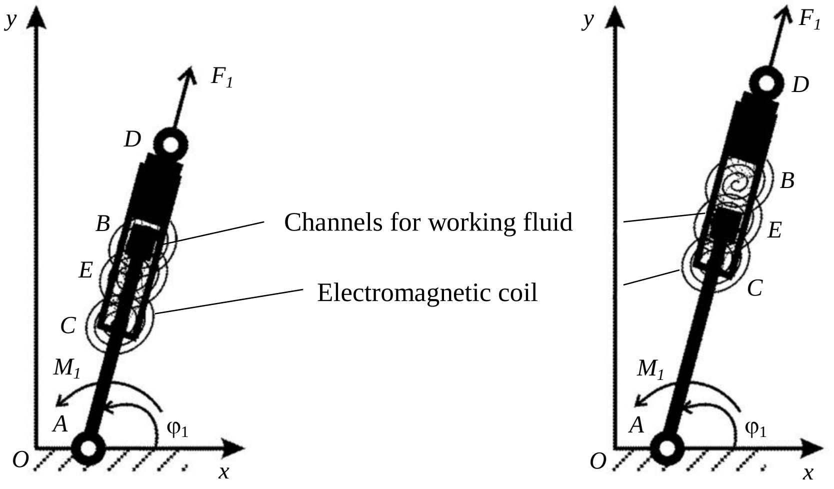

a) *b*)

Fig. 1. Construction of a variable-length link with a magnetorheological fluid:

a — link in a compressed state in the phase of support on it; *b* — link in a stretched state in the transfer phase (the authors' figure)

At points *A* and *D*, there are hinges that provide connection and relative rotation of the links in the exoskeleton. The magnetic field is created by an electromagnetic coil and acts on the magnetorheological fluid inside the link. The magnetic particles of the liquid are ordered under the electromagnetic-field effect, and the rheological properties change.

The properties of the magnetorheological fluid are due to polarization; therefore, magnetic particles line up along the lines of force (Fig. 2).

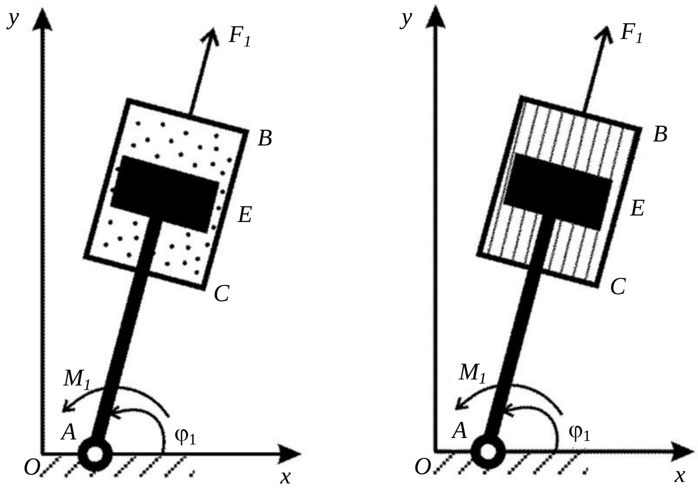

a) *b*)

Fig. 2. Magnetorheological fluid particles in the cylindrical part of the link:

a — magnetic particles are randomly arranged without the application of an external magnetic field; *b* — aligned chains of oriented magnetic particles along the lines of force under the action of an external magnetic field (the authors' figure)

Under the influence of an external electromagnetic field, polarization and magnetization occur in a magnetorheological fluid. For such fluid, Maxwell's equations have the form:

$$rot\vec{E} = \frac{\partial \vec{B}}{\partial t}, div\vec{B} = 0,$$
$$rot\vec{H} = \vec{j} + \frac{\partial D}{\partial t}, div\vec{D} = \rho_e. \quad (1)$$

Here, $\vec{D}$ — electric induction vector; $\vec{B}$ — magnetic induction vector; t — time; $\vec{E}$ — electric intensity vector; $\vec{H}$ — magnetic field strength; ρ_e — charge density; $\vec{J}$ — electric current density vector.

The electric current density vector is related to the electric field strength:

$$\vec{J} = \gamma \times \vec{E}, \tag{2}$$

where γ — specific conductivity of the substance.

A magnetic particle in a magnetorheological fluid is a dipole, i.e., a system of two opposite charges equal in modulus Q, located at distance l from each other. The moment of a pair of forces acting from the side of the field on an elementary dipole is equal to

$$\vec{M}_d = \vec{d} \times \vec{H}, \tag{3}$$

where $\vec{d}$ — elementary dipole moment.

$$\vec{d} = |Q|\vec{l}, \tag{4}$$

where $\vec{l}$ — dipole arm — vector drawn along the axis of the dipole from a negative charge to a positive one and equal to the distance between the charges l.

Magnetic induction vector $\vec{B}$ is related to magnetization vector $\vec{M}$, which characterizes, from a macroscopic point of view, the ordered distribution in the body of magnetic dipoles:

$$\vec{B} = \mu_0(\vec{H} + \vec{M}). \tag{5}$$

At low values of magnetization, it is directly proportional to the magnetic field strength:

$$\vec{M} = \chi\vec{H}. \tag{6}$$

After the transformations:

$$\vec{B} = \mu\mu_0\vec{H}, \tag{7}$$

where $\chi = \mu - 1$ — magnetic susceptibility of matter; $\mu_0 = 1.26 \cdot 10^{-6} H/m$ [11] — absolute magnetic permeability in vacuum; μ — relative magnetic permeability.

In [11–13], for the magnetic susceptibility of matter χ, the results of experimental studies of a kerosene-based magnetorheological fluid with different concentrations of magnetite particles in the range $\chi \in [1.04; 9.20]$ at a relative concentration $\varphi \in [0.211; 1]$ are given.

Thus, the input parameter that determines the behavior of a magnetorheological fluid is the magnetic field strengt $\vec{H}$, which is generated by a coil wound on a variable-length link element. The field strength is a piecewise given step function. Magnetorheological fluids are magnetized in relatively small magnetic fields $H \in [100; 100{,}000]\ A/m$.

Let the magnetorheological fluid under the movement of the rod inside the link body (Fig. 2) realize a simple shear flow with velocity gradient $\dot{\gamma}$, and the intensity of the external magnetic field $\vec{H}$ be directed at an angle ψ to the gradient of the flow velocity. Suppose that magnetic particles have the shape of ellipsoids with the ratio of two semi-axes $\frac{a}{b} = 2$ and $b = c$.

The intensity of the magnetorheological fluid can be estimated based on the results obtained in works [12–14]:

$$\begin{gathered}
\sigma = \sigma_s + \sigma_a, \\
\sigma_a = \frac{\varphi_L \Gamma_m}{2 n_c \nu_L}, \\
\sigma_s = n_f \dot{\gamma} \Big\{ 1 + \varphi_L + \Big[\alpha_n + \frac{1}{2}(\zeta_n + \beta_n \lambda_n) + \\
+ \frac{1}{2}\beta_n \cos(2\theta_n) + (\chi_n - 2\beta_n\lambda_n) sin^2(\theta_n)\cos^2(\theta_n) \Big] \Big\}.
\end{gathered} \tag{8}$$

Mechanics

Here, σ_s — symmetric stress component; σ_a — antisymmetric stress component; φ_L — volume fraction of micron particles equal to $\varphi_L = 0.0127$; n — number of particles in the chain; n_c — maximum number of particles in the chain; $\alpha_n, \ldots, \lambda_n$ — kinetic coefficients given in works [12, 13]; Γ_m — magnetic moment tending to build a chain of particles along the field; ν_L— volume of a micron particle; $\dot{\gamma}$ — shear rate; n_f — viscosity of magnetorheological fluid; θ — angle between the vector directed along a straight line connecting the centers of two micron particles and the vector of the external magnetic field strength.

As can be seen from formula (6), the stress tensor of a magnetorheological fluid in a magnetic field is asymmetric. The symmetrical part of the stress depends on the viscosity of the magnetorheological fluid. The direction and magnitude of the applied external magnetic field affect significantly the viscosity of the magnetorheological fluid. The viscosity coefficient may be less or greater than the initial value, depending on the direction of the applied field and the shape of the particles. This coefficient in the magnetic field varies for two reasons. The first reason is related to the retardation of particle rotation in the field, which causes an increase in the coefficient value. The second reason is the orienting influence of an external magnetic field on suspended particles. Depending on the direction of the field, the viscosity coefficient may decrease or increase. As an example, consider an external magnetic field that is applied along the direction of fluid flow. If its magnetic particles have the shape of oblong ellipsoids, then the viscosity decreases. If these are oblate ellipsoids, the viscosity increases.

Magnetic moment Γ_m, which tends to build a chain of particles along the field, is calculated by the formula [12, 13]:

$$\Gamma_m = 2{,}25\mu_0 H^2 \nu_L (n-1)\left(\chi_f + 1\right)\sin\theta\cos\theta. \tag{9}$$

Here, ν_L — micron particle volume; $\nu_L = \pi d_L^3/6$; d_L — micron particle diameter; $d_L = 1\cdot 10^{-6}$ m; θ — angle between the vector connecting the centers of two micron particles and the vector of the external magnetic field; χ_f — magnetic susceptibility of the carrier ferrofluid (assume that it is constant and always equal to the initial value $\chi_f = 3.05$).

Research Results. We build a graph of the magnetic moment Γ_m from the magnetic field strength H and angle θ.

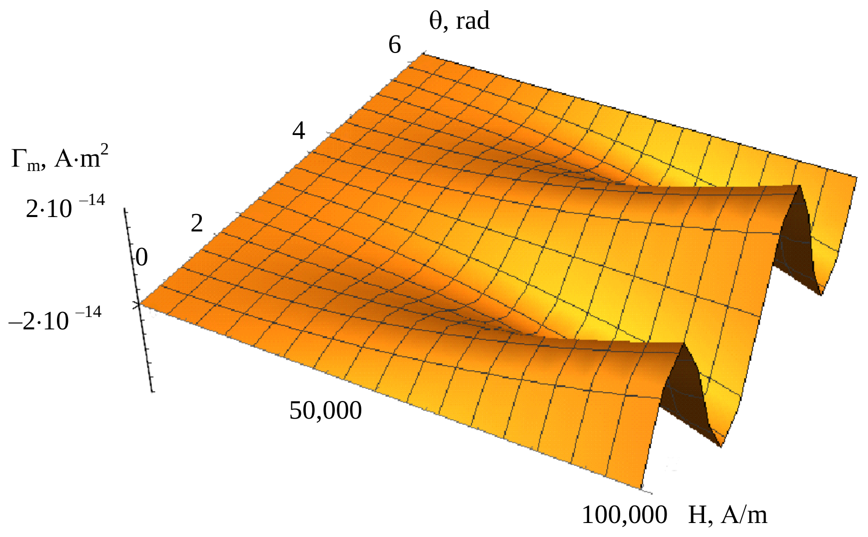

Fig. 3. Dependence of magnetic moment Γ_m on magnetic field strength H and angle θ (the authors' figure)

According to Figure 3, it is possible to judge the behavior of magnetic moment Γ_m at different values of the magnetic field strength and the angles between the field and the dipoles, to estimate the antisymmetric part of voltage σ_a. Using formulas (8) and (9), we obtain:

$$\sigma_a = \frac{\varphi_L 2{,}25\mu_0 H^2 \nu_L (n-1)\left(\chi_f + 1\right)\sin\theta\cos\theta}{2n_c}. \tag{10}$$

Taking into account works [12–14], as a result of solving the equation at $H = 10^5$ A/m, we obtain $n_c \approx 60$. The viscosity of the magnetorheological fluid is assumed to be equal to $n_f = 1.36$ Pa $\cdot$ s [11].

The results of calculations of the antisymmetric part of the voltage are graphically presented in Figure 4.

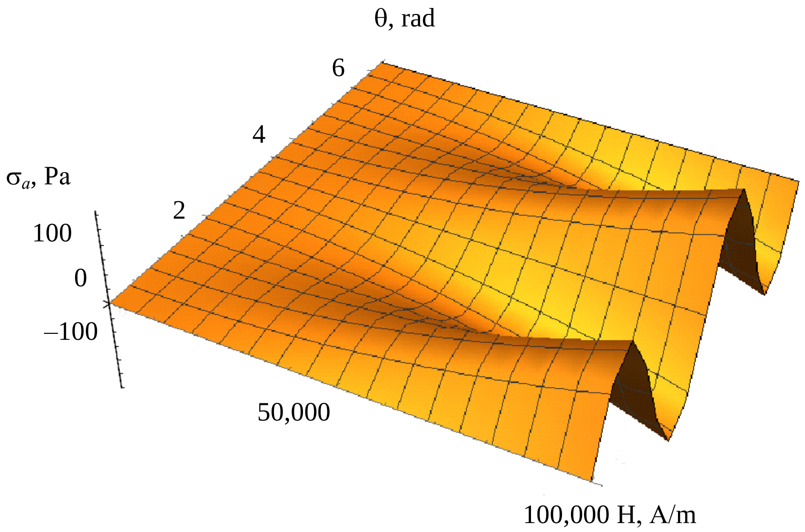

Fig. 4. Dependence of the antisymmetric part of stress σ_a on magnetic field strength H and angle θ (the authors' figure)

The graph shows that with an increase in the strength of the applied external magnetic field, the strength of the magnetorheological fluid monotonically grows taking into account angle θ. Dependence σ_a on angle θ shows that the intensity of the magnetorheological fluid reaches:

– maximum values at angles that are multiples of $\frac{\pi}{4}$;

– zero values at angles that are multiples of $\frac{\pi}{2}$.

Consider the symmetric part of stress σ_s. In (8), there are kinetic coefficients for it. Let us calculate them using the expressions from [12, 13], where they are shown in an analytical form. The number of particles in the chain is assumed to be equal to $n = 30$ as the arithmetic mean, based on the estimate of the maximum number of particles. Let us determine qualitatively, in the first approximation, shear rate $\dot{\gamma}$ between the outer layer of fluid near the wall of the link housing and the inner layer near the rod. At that, we will proceed from the requirements for the design of the exoskeleton link for the human lower leg model. In this case, we are talking about the maximum value of the rate of change in the length of a person's lower leg, with which the exoskeleton link should work synchronously. According to [15], the rate of change in the length of the lower leg is equal to $\dot{l} = 0.6$ m/s. The distance between the body and the rod of the link is assumed to be equal to d = 0.01 m. Then, the shear rate is $\dot{\gamma} = 60\ s^{-1}$. This does not contradict the results of other authors: $\dot{\gamma} \in [0; 100]\ s^{-1}$. In the future, such an assessment will require clarification based on experiments, since no solutions or experimental results suitable for modeling exoskeletons or anthropomorphic robots have been found in the literature.

The results of calculations of the symmetric part of the stress are presented graphically in Figure 5.

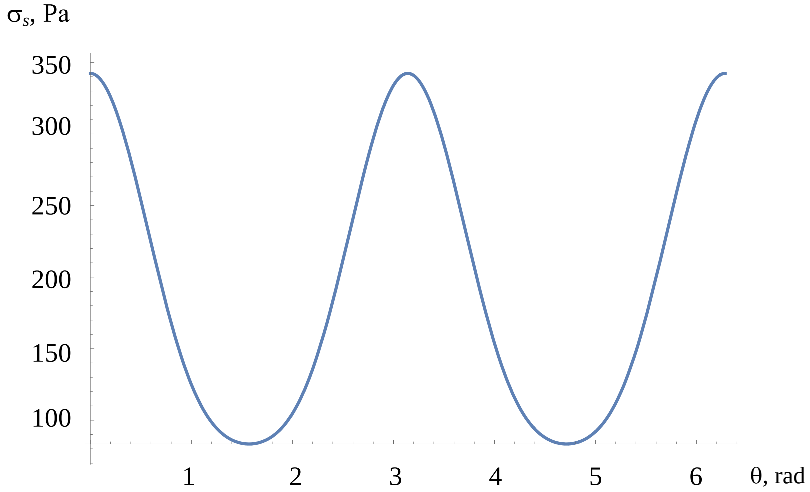

Fig. 5. Dependence of the symmetrical part of stress σ_s on angle θ (the authors' figure)

The intensity of the magnetorheological fluid as the sum of the symmetric and antisymmetric parts is shown in Figure 6. Its cross-section at a fixed value of the magnetic field strength is shown in Figure 7.

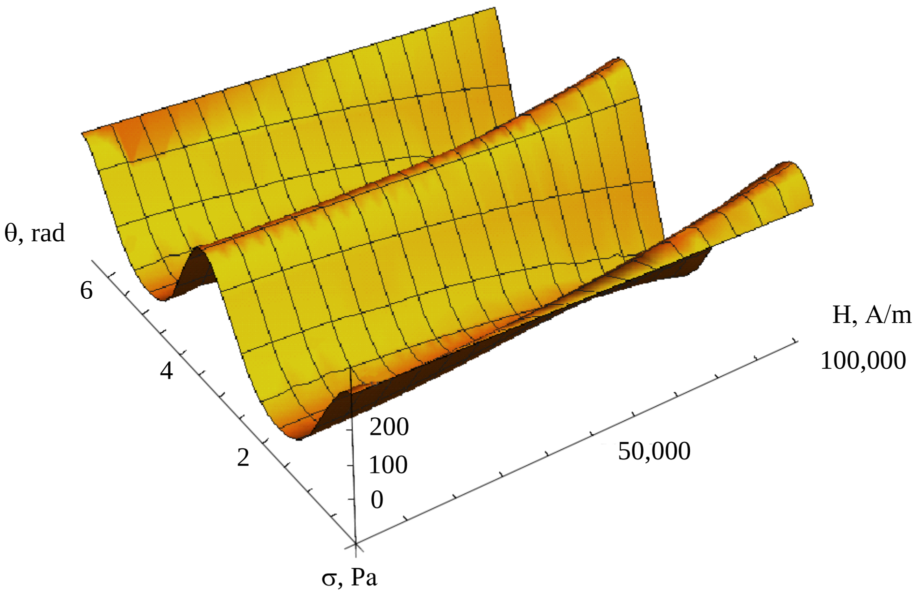

Fig. 6. Dependence of stress σ on magnetic field strength H and angle θ (the authors' figure)

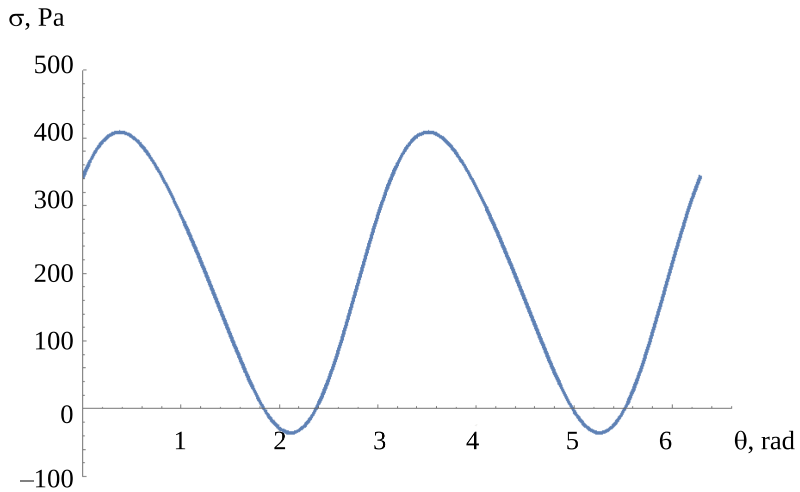

Fig 7. Dependence of stress σ on angle θ at fixed magnetic field strength value $H = 10^5$ A/m (the authors' figure)

Maximum value $\sigma_{max} = 408.6$ Pa is reached at $\theta = 0.37$ rad. Thus, to control the properties of a magnetorheological fluid, it is required to change the angle between the intensity of the external magnetic field and the orientation vector between the dipoles. It is also necessary to change the intensity of the external magnetic field.

The inner diameter of the housing in which the rod is located is assumed to be equal to $D = 0.2$ m. As the first approximation, assume that the calculated stresses are normal. Now, it is possible to determine the force with which the magnetorheological fluid acts in a variable-length link with adjustable stiffness:

$$F_{mrf} = \sigma A = \frac{\sigma \pi D^2}{4}. \tag{11}$$

Figure 9 shows a graph constructed at a fixed value of the magnetic field strength H for two control parameters: H and angle θ (Fig. 8).

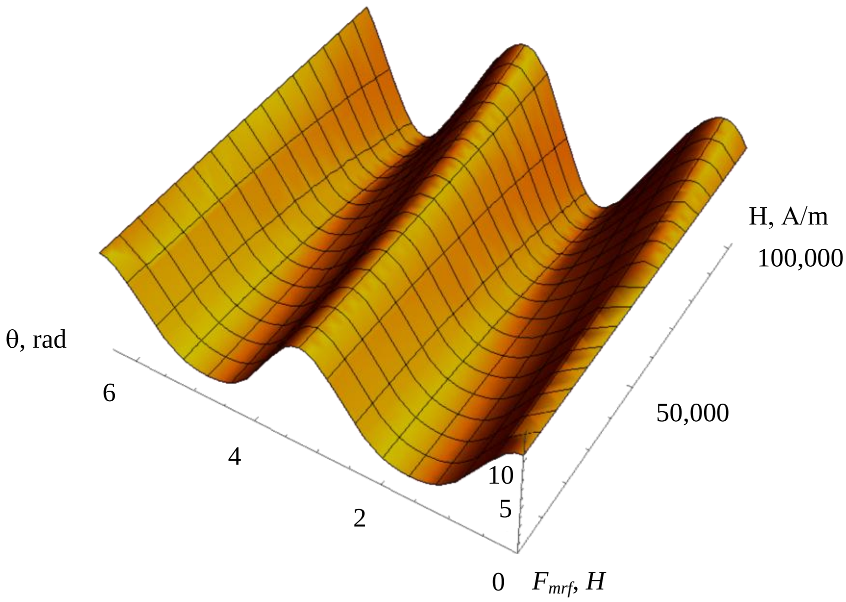

Fig. 8. Dependence of force F_{mrf} on the magnetic field strength H and angle θ (the authors' figure)

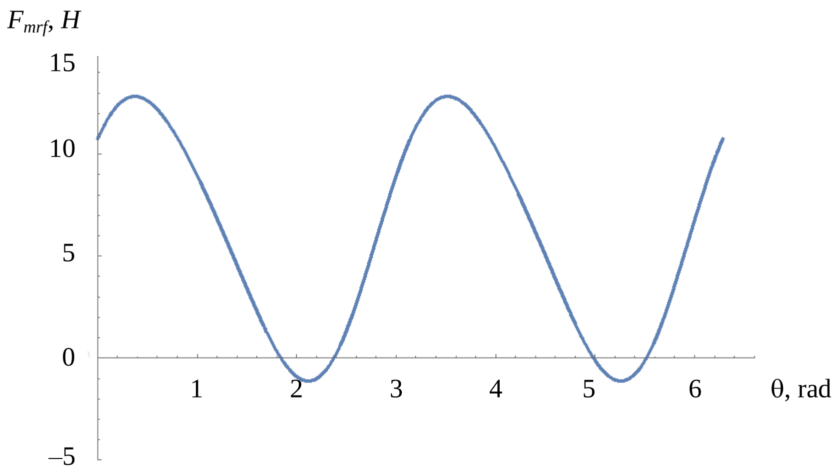

Fig. 9. Dependence of force F_{mrf} on angle θ at fixed value of the magnetic field strength $H = 10^5$ A/m (the authors' figure)

Maximum value ${F_{mrf}}_{max} = 12.8$ H is reached at $\theta = 0.37$ rad. This corresponds to the values at which, according to [14], the exoskeleton link functions. To further increase the force from the side of the magnetorheological fluid, it is required to increase the intensity of the external magnetic field.

Thus, in order for the particles to orient themselves along the field lines in the required way, you need to apply a magnetic field of the appropriate intensity and orientation.

Discussion and Conclusions. The research work results allow us to propose a method of controlling the effect of an external magnetic field on the properties of a magnetorheological fluid. For the first time, a model of a variable-length exoskeleton link with adjustable stiffness, which functions due to a magnetorheological medium, is proposed. The concept can be used to create:

– comfortable exoskeletons with links of variable length, hinges and connections;

– spacesuits and similar special equipment;

– transport systems in the form of anthropomorphic robots that provide convenient movement in rough terrain.

A widespread use of anthropomorphic robotic systems of a new generation (mechatronic modules synchronized with the movements of the human musculoskeletal system) will solve important social and economic problems:

– improve the quality of life of people with motor disabilities;

– contribute to the development of high technologies in various branches of the domestic industry.

References

1. Borisov AV, Kaspirovich IE, Mukharlyamov RG. On Mathematical Modeling of the Dynamics of Multilink Systems and Exoskeletons. Journal of Computer and Systems Sciences International. 2021;60:827–841. https://doi.org/10.1134/S106423072104002X

2. Bougrinat Y, Achiche S, Raison M. Design and Development of a Lightweight Ankle Exoskeleton for Human Walking Augmentation. Mechatronics. 2019;64:102297. https://doi.org/10.1016/j.mechatronics.2019.102297

3. Jinzhou Chen, Wei-Hsin Liao. Design, Testing and Control of a Magnetorheological Actuator for Assistive Knee Braces. Smart Materials and Structures. 2010;19:035029. 10.1088/0964-1726/19/3/035029

4. Carlson J. Magnetorheological Fluid Actuators. In book: Adaptronics and Smart Structures: Basics, Materials, Design, and Applications. Hartmut Janocha (ed.) Saarbrücken: Springer; 1999. P. 180–195.

5. Ahmadkhanlou F, Zite JL, Washington GN. A Magnetorheological Fluid-Based Controllable Active Knee Brace. Proceedings SPIE. 2007;6527:652700. https://doi.org/10.1117/12.715902

6. Dollar AM, Herr H. Lower Extremity Exoskeletons and Active Orthoses: Challenges and State-of-the-Art . IEEE Transactions on Robotics. 2008;24:144–158. 10.1109/TRO.2008.915453

7. Taesik Lee, Dongyoung Lee, Buchun Song, et al. Design and Control of a Polycentric Knee Exoskeleton Using an Electro-Hydraulic Actuator. Sensors. 2020;20:211. https://doi.org/10.3390/s20010211

8. Laflamme S. Online Learning Algorithm for Structural Control Using Magnetorheological Actuators. Massachusetts: Institute of Technology; 2007. 88 p. URL: https://dspace.mit.edu/bitstream/handle/1721.1/39271/170931934-MIT.pdf?sequence=2

9. Glowinski S, Krzyzynski T, Bryndal A, et al. A Kinematic Model of a Humanoid Lower Limb Exoskeleton with Hydraulic Actuators. Sensors. 2020;20:6116. https://doi.org/10.3390/s20216116

10. Yusupbekov HA, Sobirov MM, Yuldashev AR. Active Suspension of a Car with Variable Shock Absorbers. Nauka, tekhnika i obrazovanie. 2020;66:18–27.

11. Lebedev AV. Viscosity of Magnetic Fluids Must Be Modified in Calculations of Dynamic Susceptibility. Journal of Magnetism and Magnetic Materials. 2017;431:30–32. https://doi.org/10.1016/j.jmmm.2016.09.110

12. Zubarev AY, Iskakova LY, Chirikov DN. On the Nonlinear Rheology of Magnetic Fluids. Colloid Journal. 2011;73:320–333.

13. Zubarev AY, Chirikov DN. Magnetorheological Properties of Ferrofluids Containing Clustered Particles. Colloid Journal. 2013;75:567–576.

14. Blinov A, Borisov A, Konchina L, et al. Applying the Models of Magneto-Rheological Substances in the Study of Exoskeleton Variable-Length Link with Adjustable Stiffness. Journal of Applied Informatics. 2022;17:133–142. https://doi.org/10.37791/2687-0649-2022-17-2-133-142

15. Borisov AV, Chigarev AV. Mathematical Models of Exoskeleton. Dynamics, Strength, Control. Cham: Springer; 2022. 232 p. https://doi.org/10.1007/978-3-030-97733-7

Received 23.09.2022.
Revised 20.10.2022.
Accepted 24.10.2022.

About the Authors:

Blinov, Alexander O., teaching assistant of the Technological Machines and Equipment Department, National Research University “MPEI”, Smolensk Branch (1, Energeticheskii proezd, Smolensk, 214013, RF), ORCID, alex-blinov67@yandex.ru

Borisov, Andrey V., professor of the Technological Machines and Equipment Department, National Research University “MPEI”, Smolensk Branch (1, Energeticheskii proezd, Smolensk, 214013, RF), Dr.Sci. (Phys.-Math.), associate professor, ScopusID, ORCID, BorisowAndrej@yandex.ru

Konchina, Larisa V., associate professor of the Technological Machines and Equipment Department, National Research University “MPEI”, Smolensk Branch (1, Energeticheskii proezd, Smolensk, 214013, RF), Cand.Sci. (Phys.-Math.), associate professor, ORCID, la_kon@mail.ru

Novikova, Marina A., senior lecturer of the Technological Machines and Equipment Department, National Research University “MPEI”, Smolensk Branch (1, Energeticheskii proezd, Smolensk, 214013, RF), ORCID, mar.novikova@ro.ru

Chigarev, Anatoly V., professor of the Mechanics and Mathematics Faculty, Belarusian State University (4, Nezavisimosti Avenue, Minsk, 220030, Belarus), Dr.Sci. (Phys.-Math.), professor, ORCID, chigarevanatoli@yandex.by

Claimed contributorship:
A. O. Blinov: research objectives and tasks setting; computational analysis; plotting; text preparation; formulation of conclusions. A. V. Borisov: academic advising; analysis of the research results; the text revision; correction of the conclusions. L. V. Konchina: composing a system of differential equations in partial derivatives and recording relationships that determine the magnetorheological fluid behavior. M. A. Novikova: graphic representation of a variable-length exoskeleton link with adjustable stiffness and its functioning, selection of numerical parameters of the model. A. V. Chigarev: basic concept formulation; participation in the analysis of results and preparation of conclusions.

Conflict of interest statement
The authors do not have any conflict of interest.

All authors have read and approved the final manuscript.

MECHANICS

UDC 539.42
https://doi.org/10.23947/2687-1653-2022-22-4-306-314

Original article

Strength Calculation of the Coupling of the Floor Slab and the Monolithic Reinforced Concrete Frame Column by the Finite Element Method

Peter P. Gaidzhurov ✉, **Victor A. Volodin**
Don State Technical University, 1, Gagarin Sq., Rostov-on-Don, Russian Federation
✉ gpp-161@yandex.ru

Abstract

Introduction. The given model does not allow obtaining data on the distribution of the stress tensor components in the zone of intersection of the floor and the column. Therefore, the problem of improving the strength calculation technique at the joints of floors and columns is urgent. This study aims at developing the concept of fragmentation of the frame to assess the load-bearing capacity of the floors. As a rule, a frame-rod design scheme is used under the finite element modeling of high-rise buildings made of monolithic reinforced concrete. Numerical experiments using volume-rod and volume-plate models of a repeating structural fragment were performed on a test example of a six-span three-storey monolithic reinforced concrete frame. Practical recommendations have been developed for the refined strength calculation of the floors of monolithic reinforced concrete frames of multistorey buildings.

Materials and Methods. Computational experiments were performed using the ANSYS Mechanical software package, in which the finite element method was implemented in the form of a displacement method. A plate-rod ensemble of finite elements was used to simulate the stress-strain state of a monolithic reinforced concrete frame. The refined calculation of the coupling zone of the floor slab and column under static loading was performed using solid, beam, truss and plate elements.

Results. An engineering technique has been developed for numerical analysis of the stress-strain state of the coupling of the floor and the column of the reinforced concrete monolithic frame under static loading. The most accurate result was provided by a finite element model constructed using beam finite elements as reinforcing rods.

Discussion and Conclusions. The developed technique of numerical modeling of the coupling of the floor and the column made it possible to estimate the real strength margin of this node, taking into account the real geometry of reinforcing grids, as well as to clarify the bearing capacity of a monolithic reinforced concrete frame under various loading scenarios.

Keywords: finite element method; solid, beam, truss, plate finite elements; girderless floor with a capless joint; model of coupling of a floor slab and a column; models of discrete floor reinforcement.

Acknowledgements. The authors would like to thank the reviewers, whose critical assessment of the submitted materials and suggestions contributed to a significant improvement in the quality of this article.

For citation. P. P. Gaidzhurov, V. A. Volodin. Strength Calculation of the Coupling of the Floor Slab and the Monolithic Reinforced Concrete Frame Column by the Finite Element Method. Advanced Engineering Research, 2022, vol. 22, no. 4, pp. 306–314. https://doi.org/10.23947/2687-1653-2022-22-4-306-314

Introduction. Currently, the design of high-rise buildings made of monolithic reinforced concrete is based on a frame-link structural scheme, which, to a certain extent, enables to provide the "survivability" of the building in case of progressive (avalanche-like) destruction [1, 2]. Note that in the domestic construction science, the term "progressive destruction" is understood as the process of collapse of support structures on several floors of the building or on one floor with an area of more than 80 m^2. This phenomenon occurs as a result of the simultaneous destruction, as a rule, of one support element, followed by a rapidly increasing destruction of the entire building or part of it according to the "domino" scenario.

The main structural elements of monolithic reinforced concrete frames of multistorey buildings are repeated fragments of columns and girderless floors connected by capless joints [1].

Despite many years of experience in designing buildings with braced frames, there are cases of progressive destruction of these objects in world practice. The reasons for such phenomena are mainly due to errors in the design of the interface zone of floors and columns in combination with violation of the established rules of operation of buildings. This study aims at developing an engineering technique for strength calculation of the braced frame of a multistorey building made of monolithic reinforced concrete, taking into account the volumetric nature of the stress state in the area of the floor and column.

In finite element modeling of bending reinforced concrete structures, an approach is usually used that involves the representation of concrete by two-dimensional or three-dimensional finite elements (FE), whose construction is based on the principles of elasticity theory. Reinforcing rods, as a rule, are modeled by beam or truss rods of the appropriate dimension. According to the method of ensembling solid and rod FE, the following schemes of reinforcement representation are distinguished [2, 3]: discretely distributed, in which the coordinates of nodes of different types of elements coincide (Fig. 1 *a*); reinforcement using the so-called built-in finite elements (Fig. 1 *b*). In the latter case, the coordinates of the nodes of different-type FE do not coincide, and the procedure of "condensation" of the elements of the stiffness matrices of the rod element on adjacent nodes of the solid (basic) element is specified (Fig. 1 *c*). Note that the computational technology of embedded FE is applicable exclusively for solving the problem of generalized plane stress state. Moreover, basic FE should be isoparametric and polyquadratic, and the built-in FE should be straight-line truss-type (Fig. 1 *c*).

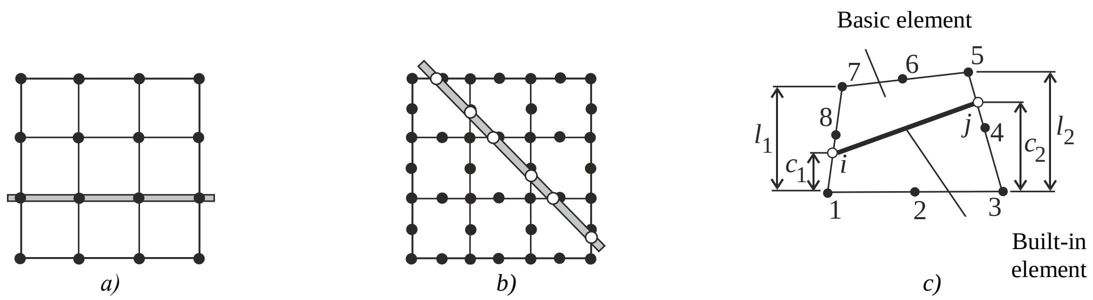

Fig. 1. Reinforcement modeling schemes: *a* — discretely distributed;
b — with built-in rod elements; *c* — basic and built-in elements (the authors' figure)

In the Russian practice of strength calculation of monolithic buildings and structures made of reinforced concrete, customized software complexes LIRA-CAD and SCAD-Office are mainly applied [4, 5]. They use the technology of the ensembling of plate and beam FE for the construction of braced frames. At that, the so-called rigid inserts are automatically introduced in the areas of the interface of floors and columns. They are star-shaped spaced beam elements with artificially high bending stiffness (Fig. 2). The geometry of the rigid insert corresponds to the transverse dimensions of the column section. This approach makes it possible to give a more physical character to the distribution of bending moments in the floor FE.

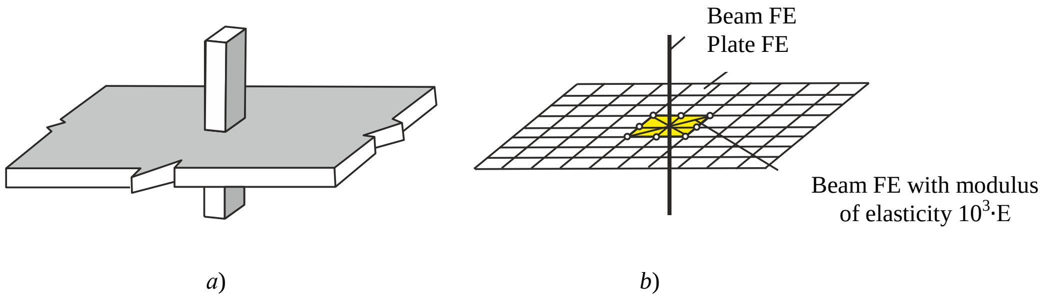

Fig. 2. Modeling of the floor and column interface zone:
a — interface zone; *b* — design scheme of the interface zone with a rigid insert (the authors' figure)

An alternative to rigid inserts with beam FE with excessive rigidity is the procedure of co-opting (binding) the degrees of freedom of the nodes of plate elements adjacent to the node of the rod element, with the corresponding nodal displacements and rotation angles of the FE rod elements. Naturally, with this approach, it is required to provide for the thickening of the grid to the dimensions of the cross sections of the columns at the junctions of the plate and rod FE. Note that the considered approach can also be programmatically automated.

Materials and Methods. At present, developers of finite element software complexes, when constructing stiffness matrices of plate and shell finite elements, widely use the MITC (Mixed Interpolation of Tensorial Components) algorithm, based on the procedure of independent (separate) approximation of bending and shear deformations. This procedure aims at eliminating the effect of "jamming" or false shift.

To model the columns of monolithic reinforced concrete frames, rectilinear two-node beam FE with six nodal dofs are used, which include three displacements in the direction of local axes and corresponding angular displacements.

The ANSYS Mechanical software package provides a four-node plate FE, SHELL63, and a two-node beam FE, BEAM188[1], for calculating spatial braced frames. The analysis of the three-dimensional stress-strain state of reinforced concrete structures was performed using a special eight-node element SOLD65.

Research Results. Let us calculate the stress-strain state of a monolithic three-storey reinforced concrete frame with a column pitch of 5×7 m. Floor height — 4.7 m; column cross-section size — 0.4×0.4 m; floor thickness — 0.2 m. Elasticity modulus, Poisson's ratio, specific gravity of floor materials — $E = 2.7\times10^4$ MPa; $\upsilon = 0.2$; $\gamma = 2{,}440$ kg/m^3; columns — $E = 3\times10^4$ MPa; $\upsilon = 0.2$; $\gamma = 2{,}500$ kg/m^3. The calculated values of concrete resistance to axial compression and stretching are: $R_b = 25.5$ MPa, $R_{bt} = 2.37$ MPa, respectively.

We assume that constant evenly distributed load $q = 2$ kPa acts on all the floors of the frame. Calculations are carried out taking into account the own weight of the frame. We believe that the bases of the columns of the first floor of the frame are rigidly fixed.

At the first stage of the calculation of the floor and the frame columns, we model, respectively, plate SHELL63 and beam BEAM188 FE.

Table 1 shows the results of comparative calculations of the ceiling of the first floor of the frame. Calculations were carried out with a grid step on the floors of 0.2 m and 0.5 m. The columns were divided into 6 FE in both cases. In Table 1 and further, the following is indicated: u_z — maximum deflection; M_x, M_y — bending moments relative to global axes. The third row of Table 1 shows the calculation data of the frame with rigid inserts (grid pitch 0.2 m). Rigid inserts with side dimensions of 0.4×0.4 m were modeled by SHELL63 plate FE with elasticity modulus $10^3 \cdot E$.

Note that values $M_{x\,max}$, $M_{y\,max}$, given in Table 1, refer to small local zones of coupling of columns and floors. Values $M_{x\,min}$ and $M_{y\,min}$ are distributed along the perimeter of the frame between the rows of edge columns.

[1] Basov KA. ANSYS: spravochnik pol'zovatelya. Moscow: DMK Press; 2005. 640 p. (In Russ.)

A similar calculation of the frame was performed using LIRA-CAD software package. The value of the maximum deflection on the ground floor under similar loading and mechanical constants of the material, obtained using the LIRA-CAD software package, was u_z = –3.06 mm, which is comparable to the calculation in ANSYS u_z = –3.49 mm with a grid step on the floors of 0.2* (Table 1). When calculating using LIRA-CAD complex, at the step of constructing an "analytical model" at the points of intersection of columns and floors, "punching contours" were included, affecting indirectly the bending stiffness of the floors in the direction of its increase.

Table 1

Values of extreme bending moments in the interface zone of the first floor ceiling and column when using SHELL63

Grid pitch, m	Number of unknowns	u_z , m	M_X , kN·m		M_Y , kN·m	
			min	*max*	*min*	*max*
0.5	103,032	–0.004908	–13.1	37.2	–20.6	45.3
0.2	583,200	–0.005409	–15.2	70.2	–22.5	99.7
0.2*	583,200	–0.003492	–10.8	106	–17.5	106

Table 2 shows values of the extreme bending moments for the ceiling of the first floor, obtained using ANSYS (grid pitch 0.2* m) and LIRA-CAD (grid pitch 0.395 m). It should be noted that in LIRA-CAD complex, a scale of linear bending moments has been introduced to quantify values M_x and M_y, i.e., the resulting moments are reduced to a strip of plate with a width of 1 m.

Table 2

Comparison of extreme values of bending moments in the interface zone of the first-floor ceiling and column, calculated using ANSYS and LIRA-CAD

Software package	M_x, kN·m		M_y, kN·m	
	min	*max*	*min*	*max*
ANSYS	–10.8	106	–17.5	106
LIRA-CAD	–31.5	8.37	–42.2	12.9

From the data in Table 2, it can be seen that the extreme moments of the same name obtained using ANSYS and LIRA-CAD differ significantly in magnitude. This circumstance is explained by the presence of local zones of concentration of internal forces at the interface points of plate and rod FE in the investigated finite element model. Moreover, the accepted dimensions of the plate FE in both complexes do not allow us to accurately simulate the gradients of changes in bending moments in the specified concentration zones.

Analyzing the results of the calculation of the frame according to the plate-rod scheme, we come to the conclusion that this model does not enable to study a detailed picture of the stressed state of the structure. In particular, it is not possible to analyze the zones of tensile normal stresses σ_x, σ_y σ_z, that occur at the junctions of columns and floors. In this regard, the task of constructing a computational model of a repeating fragment of the frame is urgent. That allows performing a numerical study of the volumetric stress-strain state, including reinforcement. Figure 3 shows the floor framing plan with selected repeating fragments *a*, *b*, *c*. The area of the repeating fragment *a* is the object of further study.

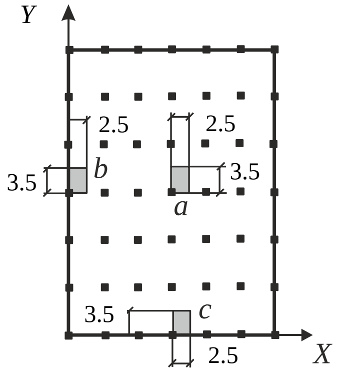

Fig. 3. Repeating fragments *a*, *b*, *c* of floor framing (the authors' figure)

To simulate the volumetric stress-strain state of a repeating fragment, we used an eight-node SOLID185 type FE with three degrees of freedom in the node.

Figure 4 shows the design scheme of the repeating fragment *a* of the frame under consideration. The above calculation scheme refers to the first floor of the frame. Here, the concentrated force P =72.6 kN was taken from the diagram of longitudinal forces obtained using a plate-rod model of the frame. In this case, the concentrated force P was converted to a statically equivalent pressure $q_к$ = 453.5 kPa, acting on a site of 0.2×0.2 m (1⁄4 part of the column section). Static boundary conditions $\bar{u}_X$, $\bar{u}_Y$, $\bar{u}_Z$ were imposed on the FE nodes with regard to the cyclic symmetry of the pattern of floor deformation. The corresponding finite element model of the fragment, built on the basis of SOLID185 solid FE, is shown in Figure 5. In this case, the grid step of the solid FE was assumed to be 0.1 m. We applied pressure on the floor fragment and 1/4 of the column using SURF154[2].

The comparison results of the stiffness properties of the plate-rod and solid finite element models of the frame fragment under consideration in the form of displacement distribution patterns u_Z are shown in Figure 6. The distribution patterns u_Z in Figure 6 *b* and Figure 6 *c* correspond to the calculations of the fragment with and without taking into account force P. As can be seen from the presented results, the calculation without taking into account force P (Fig. 6 *c*) gives the displacement values closest to the data of the plate-rod model. Further numerical experiments will be carried out taking into account the loading of the fragment column by pressure $q_к$.

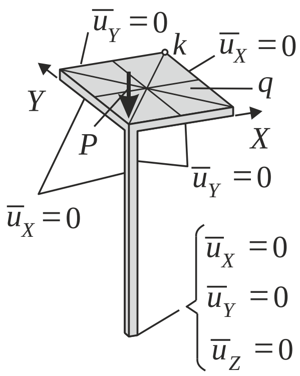

Fig. 4. Fragment calculation scheme (the authors' figure)

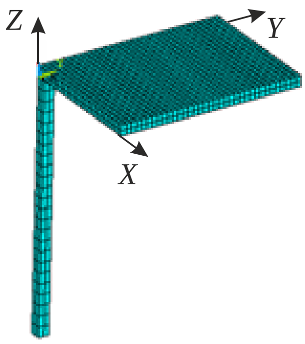

Fig. 5. Finite element fragment model (the authors' figure)

[2] Basov KA. ANSYS: spravochnik pol'zovatelya. Moscow: DMK Press; 2005. 640 p. (In Russ.)

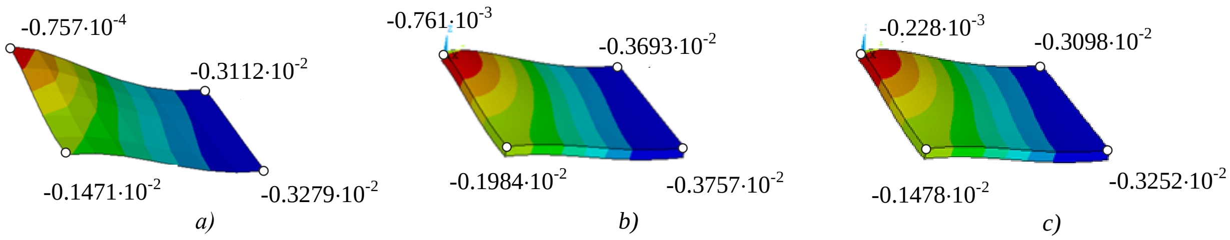

Fig. 6. Calculation results of displacement u_z for two models:*a* — plate-rod model;
b — solid model taking into account force *P*; *c* — solid model without taking into account force *P* (the authors' figure)

Let us study the effect of reinforcement on the stress-strain state of the frame fragment under consideration. We assume that the floor is girderless and capless. Let us consider three schemes for modeling the reinforcement of the part of the floor belonging to the fragment: 1 — discrete reinforcement using rod FE (BEAM188); 2 — discrete reinforcement using truss FE (LINK180); 3 — distributed reinforcement using plate FE (SHELL63). It should be noted that reinforcement modeling by means of truss FE is also suitable for calculating prestressed reinforced concrete structures[3] [1, 6, 7].

The structural elements of the discrete reinforcement of the frame fragment are shown in Figure 7. The material of the reinforcing rods is steel ($E = 2\times10^5$ MPa; $\nu = 0.28$; $\gamma = 7{,}800$ kg/m^3).

Reinforcing grids are made of rods of the following diameter: background reinforcement (along the entire floor plane) — 10 mm; reinforcement of girders — 12 mm; reinforcement of the column cap — 16 mm. The diameters of the rods for transverse reinforcement of girders and column caps have values similar to the above. The reinforcing rods of the column with a diameter of 12 mm are located at the corners of the section.

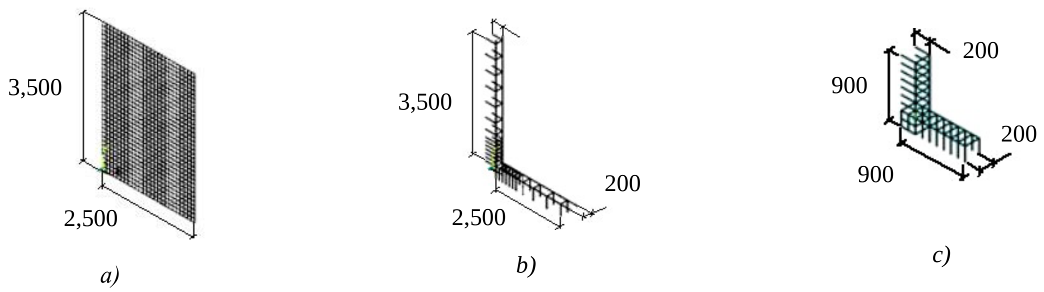

Fig. 7. Structural elements of discrete reinforcement:
a — background upper/lower reinforcement; *b* — girder reinforcement;
c — column cap reinforcement (the authors' figure)

The assigned values of the diameters of the reinforcing rods were taken on the basis of the prototype [8–10]. To model the reinforcement, we used either beam or truss FE.

An alternative to the discrete reinforcement model is an approach based on the principle of "smearing", the so-called distributed reinforcement model. In general, the principle of "smearing" is the introduction of the reduced modulus of elasticity, which is a function of the elastic moduli of the components of an inhomogeneous material and their volume concentrations. However, the calculation practice [1] has shown that for reinforced concrete structures working on bending, the introduction of specific reinforcing layers equivalent to the volume occupied by reinforcing rods gives more realistic results. The geometry of such layers mimics the geometry of reinforcing steel grids. For the frame fragment under consideration, Figure 8 shows equivalent reinforcing layers modeled by SHELL63-type plate FE.

[3] CS 52-101-2003. Concrete and Reinforced Concrete Structures without Prestressing. Moscow, 2004.

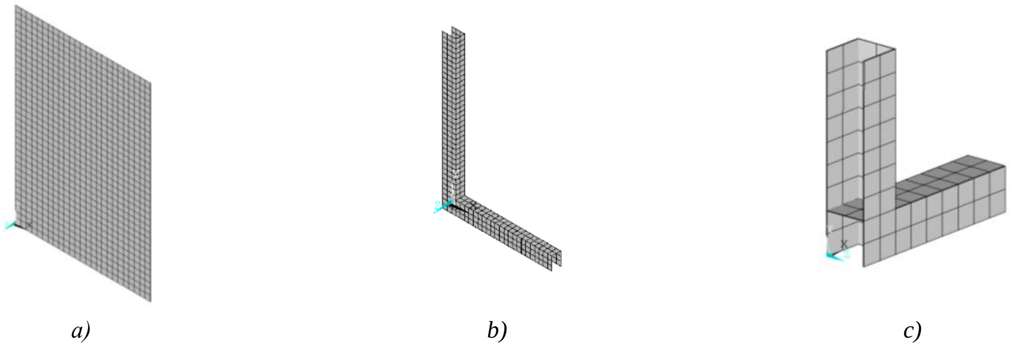

Fig. 8. Equivalent reinforcing layers: *a* — layer for background reinforcement (upper/lower); *b* — girder reinforcement layers; *c* — column cap reinforcement layers (the authors' figure)

Based on the condition of equality of the volumes of reinforcing elements and the coincidence of the geometry of the reinforcement zones, we obtain the following thicknesses for the equivalent reinforcing layers: a layer of background reinforcement — 1.6 mm; layers of girder reinforcement — 1.1 mm, 0.74 mm, 1.2 mm, 0.78 mm; layers of column cap reinforcement — 5 mm, 2.7 mm.

During the computational experiment, the dependence of deflection u_z at point *k* and maximum tensile stresses $\sigma^+_{x\ max}$, $\sigma^+_{y\ max}$, $\sigma^+_{z\ max}$ on the adopted reinforcement scheme of the fragment under study was investigated (Fig. 4). Table 3 shows the calculation results.

Table 3

Values of deflections and stresses in various methods of reinforcement modeling

Reinforcement modeling	u_z at point *k*, mm	$\sigma^+_{x\ max}$, MPa	$\sigma^+_{y\ max}$, MPa	$\sigma^+_{z\ max}$, MPa
Nonreinforced	–3.32	3.26	4.40	1.44
BEAM188	–2.81	2.77	3.76	1.08
LINK180	–2.92	2.75	3.74	1.06
SHELL63	–2.06	1.19	1.74	0.513

The analysis of the results has shown that the use of plate FE causes a significant underestimation of the maximum tensile stresses. The data obtained using beam and truss FE are practically the same, which is explained by the low bending stiffness of the reinforcing rods.

It is important to emphasize that for the considered loading option, when using rod FE (BEAM188 and LINK180), in the column – floor interface zone, the strength condition for stresses $\sigma^+_{x\ max}$ and $\sigma^+_{y\ max}$ is not fulfilled.

Figure 9 shows a visualization of the cracking process in the floor slab obtained through modeling concrete with SOLIDS65 solid eight-node FE. It should be noted that only microcracks appear in the floor, whose boundary is in good agreement with the shear stress field σ_{xy} in the floor plane (Fig. 10).

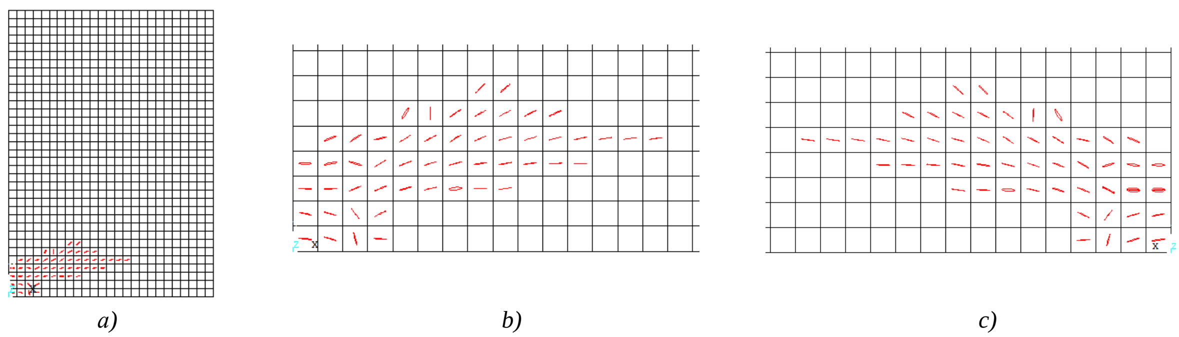

Fig. 9. Visualization of cracking process in the floor slab:
a — general view of the fragment; *b* — view of the crack formation zone from above;
c — view of the crack formation zone from below (the authors' figure)

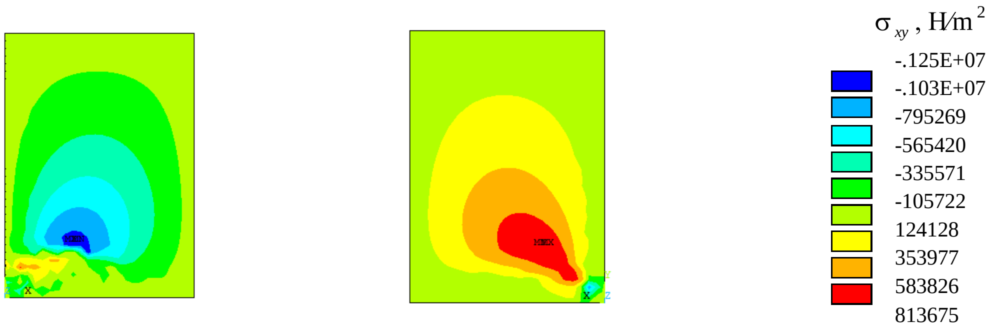

a) *b)* *c)*

Fig. 10. Stress distribution pattern in the floor:
a — view of the fragment from above; *b* — view of the fragment from below; *c* — stress scale (the authors' figure)

To simulate the physical nonlinearity of concrete, the Willam-Warnke model [11] was used with the following parameters: the coefficient of shear force transmission at an open crack — 0.3; the coefficient of shear force transmission at a closed crack — 0.7; the tensile crack reduction factor — 0.6.

Discussion and Conclusions

1. Based on the performed linear-elastic calculation of a monolithic frame made of reinforced concrete, it has been validated that the plate-rod model widely used in design practice does not allow quantifying the values of tensile normal stresses in the areas of conjugation of floor slabs and columns in the areas of interface of floor slabs and columns.

2. A technique has been developed for numerical modeling of the volumetric stress-strain state at the interface zone of floor and column of a monolithic reinforced concrete frame, which provides estimating the actual margin of safety of this node, as well as to specify the bearing capacity of the corresponding building or structure under various loading scenarios.

References

1. Frederick S. Merritt, Jonathan T. Ricketts. Building Design and Construction Handbook. McGraw Hill Professional, 2000. 1600 p.

2. Wolanski AJ. Flexural Behavior of Reinforced and Prestressed Concrete Beams Using Finite Element Analysis. Marquette University, Milwaukee; 2004. 87 p.

3. Hyo-Gyoung Kwak, Filippou FC. Finite Element Analysis of Reinforced Concrete Structures under Monotonic Loads. University of California, 1990. 124 p.

4. Gorodetskiy AS, Batrak LG, Gorodetskiy DA. Raschet i proektirovanie konstruktsii vysotnykh zdanii iz monolitno-go zhelezobetona (problemy, opyt, resheniya i rekomendatsii, komp'yuternye modeli, informatsionnye tekhnologii). Kyiv: Fakt; 2004. 106 p. (In Russ.)

5. Perelmuter AV, Slivker VL. Raschetnye modeli sooruzhenii i vozmozhnost' ikh analiza. Moscow: DMK Press; 2009. 596 p. URL: https://znanium.com/catalog/product/1910747 (accessed: 14.09.2022). (In Russ.)

6. Samokhvalova EO, Ivanov AD. Styk kolonny s bezbalochnym beskapitel'nym perekrytiem v monolitnom zdanii. Magazine of Civil Engineering. 2009;3:33–37. (In Russ.)

7. FIP Handbook on Practical Design: Examples of the Design of Concrete Structures. Thomas Telford Limited, London; 2010. 188 p.

8. Lukin AV, Modestov VS. Finite Element Modeling and an Analysis of the Stress-Strain State of Reinforced Concrete Structures. St. Petersburg Polytechnic University Journal: Physics and Mathematics. 2014;201:35–46.

9. Gaigerov PP, Al-Jabobi Sami Fahl, Al-Yaj Mahmoud Abdo Hasa. Finite Element Modeling of Force Transmission the Tension of the Steel Tendon on the Concrete. University News. North-Caucasian Region. Technical Sciences

Series. 2017;2:73–78.

10. Gaigerov PP, Iskhakova ER, Al-Jabobi Sami Fahl, et al. Definition of Camber Long-Span Reinforced Concrete Girders in pre-Stressed Reinforcement Finite Element. University news. North-Caucasian region. Technical Sciences Series. 2017;4:86–91.

11. Karpenko NI. Nauka, tekhnika i obrazovanie Obshchie modeli zhelezobetona. Moscow: Stroiizdat; 1996. 416 p. (In Russ.)

Received 31.10.2022.

Revised 22.11.2022.

Accepted 29.11.2022.

About the Authors:

Gaidzhurov, Peter P., professor of the Engineering Mechanics Department, Don State Technical University (1, Gagarin sq., Rostov-on-Don, 344003, RF), Dr.Sci. (Eng.), ORCID, gpp-161@yandex.ru

Volodin, Victor A., post-graduate student of the Engineering Mechanics Department, Don State Technical University (1, Gagarin sq., Rostov-on-Don, 344003, RF), ORCID, vik25vol@bk.ru

Claimed contributorship:

P. P. Gaidzhurov: task statement; choice of solution method; construction of mathematical and computer model; discussion of the results. V. A. Volodin: critical review of literary sources on the research topic; computational analysis; discussion of the conclusions.

Conflict of interest statement

The authors do not have any conflict of interest.

All authors have read and approved the final manuscript.

MACHINE BUILDING AND MACHINE SCIENCE

UDC 624.04:531.391.3
https://doi.org/10.23947/2687-1653-2022-22-4-315-322

Original article

Analytical Estimation of the Natural Oscillation Frequency of a Planar Lattice

Mikhail N. Kirsanov
National Research University (MPEI), 14, Krasnokazarmennaya St., Moscow, Russian Federation

Abstract

Introduction. A new scheme of a flat statically determinate regular lattice is proposed. The lattice rods are hinged. The study aims at deriving a formula for the dependence on the number of panels of the first natural oscillation frequency of nodes endowed with masses, each of which has two degrees of freedom in the lattice plane. The rigidity of all rods is assumed to be the same, the supports (movable and fixed hinges) — nondeformable. Another objective of the study is to find the dependence of the stresses in the most compressed and stretched rods on the number of panels in an analytical form.

Materials and Methods. The approximate Dunkerley's method was used to determine the lower bound for the lattice natural frequency. The lattice rigidity was found in analytical form according to Maxwell-Mohr formula. The rod stresses and the reactions of the supports were determined from the equilibrium equations compiled for all lattice nodes. Generalization of the result to an arbitrary number of panels was performed by induction using Maple symbolic math operators for analytical solutions to a number of problems for lattices with different number of panels.

Results. The lower analytical estimate of the first oscillation frequency was in good agreement with the numerical solution for the minimum frequency of the oscillation spectrum of the structure. Formulas were found for the stresses in four most compressed and stretched rods and their linear asymptotics. All required transformations were made in the system of Maple symbolic math.

Discussion and Conclusions. The obtained dependence of the first frequency of lattice oscillations on the number of panels, mass and dimensions of the structure has a compact form and can be used as a test problem for numerical solutions and optimization of the structure.

Keywords: lattice, natural frequency, Dunkerley's estimate, induction, Maxwell–Mohr formula, Maple, lower frequency estimate, analytical solution, rod stresses, asymptotics.

Funding information. The research is done with the financial support from RFFI within the frame of research project no. 22–21–00473.

Acknowledgments. The author would like to thank the reviewers, whose critical evaluation of the submissions and suggestions for improvement contributed significantly to the quality of this article.

For citation. M. N. Kirsanov. Analytical Estimation of the Natural Vibration Frequency of a Planar Lattice. Advanced Engineering Research, 2022, vol. 22, no. 4, pp. 315–322. https://doi.org/10.23947/2687-1653-2022-22-4-315-322

Introduction. Lattice structures are widely used in mechanical engineering as load-bearing or enclosing elements. The procedure of calculating the natural frequencies of lattice vibrations is traditionally based on numerical evaluations, which, as a rule, use the finite element technique with application-specific packages. Analytical methods are used much less frequently. The development of mathematical packages of symbolic mathematics (Maple, Wolfram Mathematica, Derive, Maxima, etc.) enables to search for such solutions for regular systems in which it is possible to take into account the order of regularity (the number of periodic structures of the construct, specifically, the number of panels) in the solution. The study aims at finding analytical dependence of the lower boundary of the first part of the lattice structure on the number of panels. The dependence of the solution on the number of panels expands significantly the scope of the formula and makes it possible to optimize the design by any parameter. For the first time, R. Hutchinson and N. Fleck were engaged in the problem of the existence and calculation of statically definable regular truss systems [1, 2]. In [3, 4], such constructions were studied in connection with optimization problems. There are also analytical solutions in the form of finite formulas for the programs of regular planar [5–7] and spatial trusses [8]. Reference book [9] provides formulas for deflections and displacements of supports for flat trusses and lattices with an arbitrary number of panels. In [10–13], lower estimates of the first natural frequency of flat trusses were obtained, found by induction for an arbitrary order of a regular structure.

There is another line of analytical research of structures [14–16]. In these works, the solution is in the Maple system in the form of trigonometric series.

In this paper, the induction method has been used, which consists in generalizing a number of separate calculations of lattices with a consistently increasing number of panels for the case of an arbitrary number of panels. All transformations used Maple symbolic math operators. The object of the study was a new scheme of a regular statically definable flat lattice of rectangular shape in the form of an asymmetric truss on two supports. The task was to deduce the analytical dependence of the fundamental vibration frequency of the structure on the number of panels. The derived formula can be used in optimization problems and for estimating numerical solutions of such large-order structures, for which numerical calculations may contain errors associated with the round-off accumulation.

Materials and Methods. There are $5(n+1)$ nodes, including three support nodes (one for fixing the left support, two — for the right bars modeling a fixed hinge), in a truss with length $(2n-1)a$ and height $4h$. The number of rods, including three support rods, is $N=10n+4$. The truss is statically definable. When calculating the vibration frequencies of the structure, it is assumed that the mass of the truss is concentrated in the nodes.

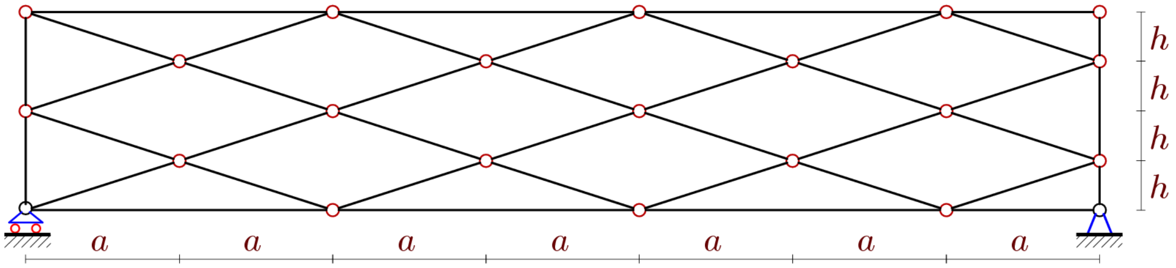

Fig. 1. Lettice diagram, *n*=4 (the author's figure)

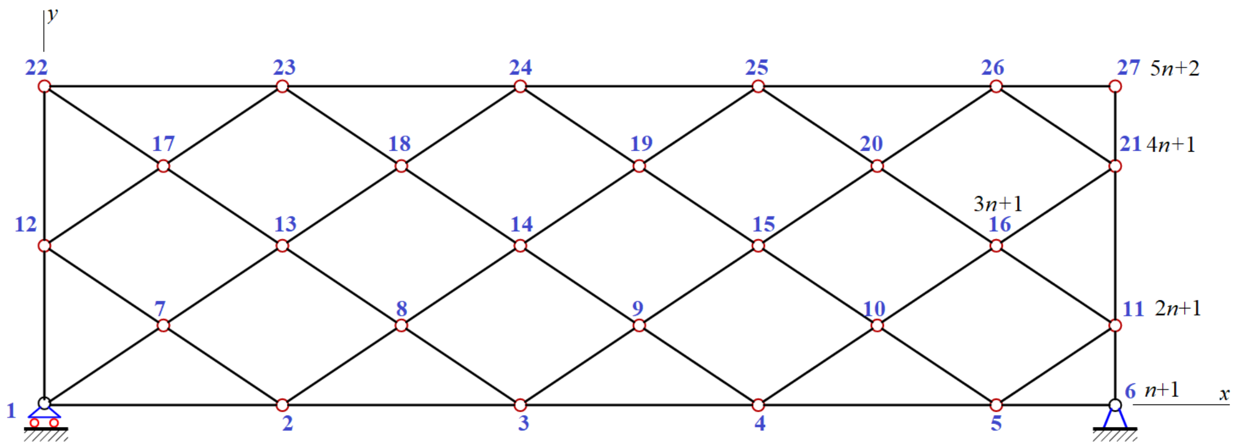

Fig. 2. Lattice numbering, *n*=5 (the author's figure)

The force calculation is performed in the Maple system according to the program [17]. The nodes and rods of the truss are numbered (Fig. 2). The origin of coordinates is in the left support. Coordinates are set in cycles.

The lattice structure is established by the order of connection of the rods in the nodes. To do this, special lists $\Phi_\alpha=[i_1,i_2]$ of numbers i_1, i_2 of the rod ends $\alpha=1,..,N$ are introduced. The rods of the lower outer contour, specifically, have the following node numbers at the ends: $\Phi_i = [i, i+1],\ i = 1,..,n.$ The numbers of the ends of the other rods of the lattice are set in the same way. The system of equilibrium equations of nodes in projections on the coordinate axis is compiled in matrix form $\mathrm{GS} = \mathrm{B}$, S — vector of all rod stresses, including three reactions of the supports, B — vector of external nodal loads. System matrix G consists of guiding cosines of stresses. In this case, the same stress is applied to different rod ends and are multidirectional:

$$G_{2\Phi_{i,2}-1,i} = -l_{x,i} / l_i, G_{2\Phi_{i,2},i} = -l_{y,i} / l_i;$$
$$G_{2\Phi_{i,1}-1,i} = l_{x,i} / l_i, G_{2\Phi_{i,1},i} = l_{y,i} / l_i,\ i = 1,..., N,$$

where $l_{x,i} = x_{\Phi_{i,1}} - x_{\Phi_{i,2}}$, $l_{y,i} = y_{\Phi_{i,1}} - y_{\Phi_{i,2}}$ — projections of conditional vectors of rods on the coordinate axis, $l_i = \sqrt{l_{x,i}^2 + l_{y,i}^2}$ — length of rod *i*=1,..,*N*.

The lattice rod stresses can be obtained from solving a system of equations in symbolic or numerical form.

Research Results. Consider the stress state of the lattice in the case of loading at all angles by vertical stresses *P* (Fig. 1). Figure 3 shows a distribution pattern in the rods of the structure. The thicknesses of the segments in the Figure are conditionally proportional to the modules of the corresponding stresses. Compressed rods are highlighted in blue, stretched rods — in red. The stress values are attributed to magnitude *P* of the load on the node, rounded to two significant digits. The most stretched rod was expected to be in the middle of the lower belt, the most compressed one — in the lower rod on the right side of the structure.

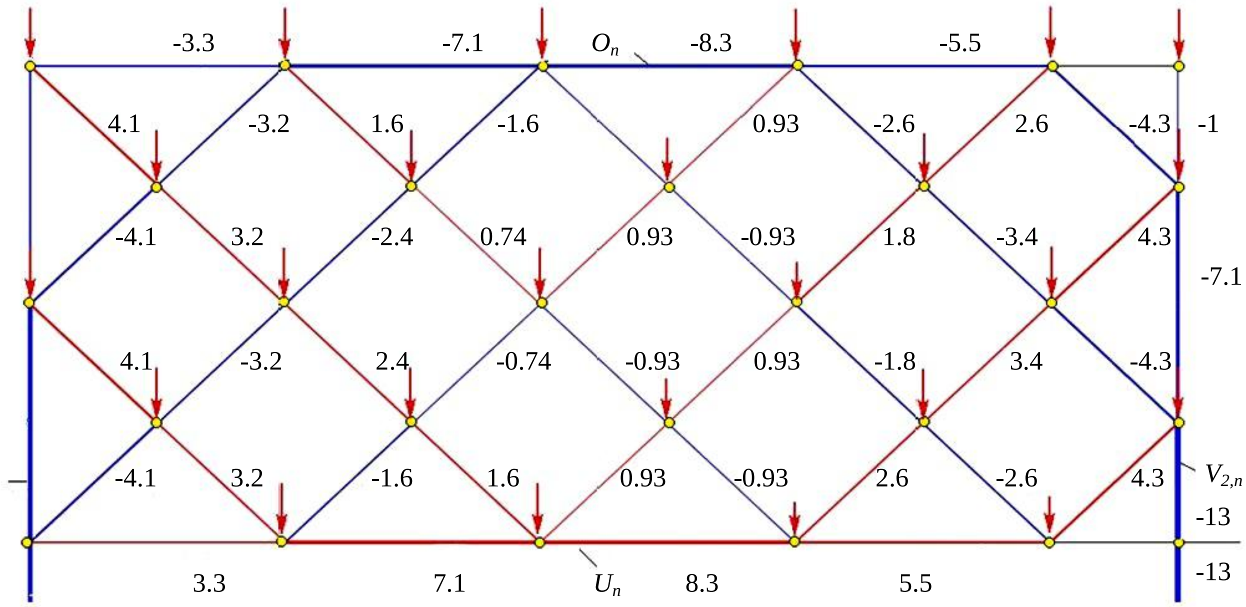

Fig. 3. Stress distribution on the lattice rods, $a = 4m, h = 3m, n = 5$ (the author's figure)

The analytical dependences of the stresses in the most compressed and stretched rods on the number of panels are obtained by induction from the generalization of the sequences of individual solutions. Say, for stress $V_{1,n}$ in the lower rod of the left side of the lattice, the sequence of values for lattices of order *n* = 1, 2, 3, ... has the form: $V_{1,n} / P = -2,\ -12,\ -28,\ -54,\ -84,\ -126,\ -170,\ -228,\ -286,\ -360,...$. The recurrent equation for the common term of this sequence is given by operator rgf_findrecur of the Maple system:

$$V_{1,n} = V_{1,n-1} + 2V_{1,n-2} - 2V_{1,n-3} - V_{1,n-4} + V_{1,n-5}.$$

Solving the equation using rsolve operator:

$$V_{1,n} = -P(30n^2 - 2(7-(-1)^n)n - (-1)^n + 1) / (8(2n-1)).$$

Other expressions for critical stresses are found in the same way:

$$O_n = -Pa(20n^3 - 30n^2 + 5 - 4(\cos\varphi + \sin\varphi)(1-2n) - \cos(2\varphi))/(32(2n-1)h);$$
$$U_n = -O_n;$$
$$V_{2,n} = -P(5n^2 - n - 1)/(2n-1),$$

where $\varphi = \pi n/2$. It is of interest to note that stresses $V_{1,n}$ and $V_{2,n}$ do not depend on the size of *a* and *h*.

The analytical form of solutions allows us to find their asymptotics using Maple operator limit:

$$\lim_{n\to\infty} V_{1,n} = -3P_{sum}/8,\ \lim_{n\to\infty} V_{2,n} = -3P_{sum}/8;$$
$$\lim_{n\to\infty} O_n/n = -\lim_{n\to\infty} U_n/n = -aP_{sum}/(16h),$$

where $P_{sum} = 5nP$ — total load on the lattice. For stresses $V_{1,n}$ and $V_{2,n}$ in the rods on the sides of the lattice, the asymptotes are horizontal, for stresses O_n and U_n on the upper and lower belts, they are inclined.

Natural frequency. Of the entire spectrum of natural vibration frequencies of a structure, the first, lowest frequency is the most important for assessing its dynamic behavior. Its value is included in most solutions to the problems of structural dynamics. This value is required, among other things, to assess the seismic characteristics of the structure. The lower bound of the first frequency for regular structures in the form of a dependence on the number of panels can be obtained analytically.

When determining the natural vibration frequencies of the structure, a simplified model of the inertial properties of the truss is adopted. It is assumed that the rods of the lattice have no mass, and the entire mass is distributed evenly across the nodes. Neglecting the movement of the supports, we get the total number of degrees of freedom equal to $K = 10n$. Donkerley's formula [13] for estimating the lower bound of the first frequency has the form:

$$\omega_D^{-2} = \sum_{p=1}^{K} \omega_p^{-2}, \tag{1}$$

where ω_p — partial frequencies of the structure. Partial frequencies of mass vibrations are determined from the equation:

$$m\ddot{y}_p + D_p y_p = 0,\ p=1,...,K. \tag{3}$$

Here, $y_p = y_p(t)$ — coordinate of node *p;* $\ddot{y}_p$ — acceleration; D_p — rigidity, inverse compliance $\delta_p = 1/D_p$. Compliance can be calculated using the Maxwell-Mohr formula:

$$\delta_p = 1/D_p = \sum_{\alpha=1}^{N} \left(S_\alpha^{(p)}\right)^2 l_\alpha/(EF), \tag{4}$$

where $S_\alpha^{(p)}$ — stress in the rod with number α from the action of the vertical unit force applied to node *p*, where the mass is located. The rigidity rate and partial frequency depend on the place where the mass is located. For harmonic vibrations $y_p = U_p\sin(\omega t + \varphi)$ from (3), $\omega_p = \sqrt{D_p/m}$ follows. The substitution of this expression in (4) gives a formula for estimating the first frequency only by partial frequencies of mass vibrations:

$$\omega_D^{-2} = \sum_{p=1}^{K} \omega_p^{-2} = m\sum_{p=1}^{K}\delta_p = m(\Delta_{n,v} + \Delta_{n,h}). \tag{5}$$

The amounts for vibrations in the vertical $\Delta_{n,v}$ and horizontal $\Delta_{n,h}$ directions are separately allocated. Successive calculation of the vibration frequencies of lattices of various orders shows that coefficient $\Delta_{n,v}$ in (5) has the form:

$$\Delta_{1,v} = (14h)/(EF);$$
$$\Delta_{2,v} = (44a^3 + 75c^3 + 250h^3)/(9EFh^2);$$
$$\Delta_{3,v} = (24a^3 + 25c^3 + 36h^3)/(EFh^2);$$
$$\Delta_{4,v} = 2(154a^3 + 175c^3 + 176h^3)/(7EFh^2);$$
$$\Delta_{5,v} = 2(1254a^3 + 1125c^3 + 791h^3)/(27EFh^2).$$

In general, for vertical partial frequencies:

$$\Delta_{n,v} = \left(C_1a^3 + C_2c^3 + C_{3y}h^3\right)/\left(EFh^2\right). \tag{6}$$

For partial frequencies horizontally:

$$\Delta_{n,v} = \left(C_4a^3 + C_5c^3 + C_{6y}h^3\right)/\left(EFa^2\right). \tag{7}$$

Using Maple operator rgf_findrecur, we obtain a homogeneous recurrent equation of the seventh order to determine the coefficient for a^3:

$$C_{1,n} = 3C_{1,n-1} - C_{1,n-2} - 5C_{1,n-3} + C_{1,n-4} + C_{1,n-5} - 3C_{1,n-6} + C_{1,n-7}\ .$$

The solution to the equation is given by rsolve operator:

$$C_1 = (n^4 - 2n^3 + 61n^2 - 6(3(-1)^n + 10)n + 9(-1)^n - 9)/18. \tag{8}$$

Other coefficients are found in the same way:

$$\begin{aligned} C_2 &= 25n(n-1)/6; \\ C_3 &= (136n^2 + 2(9(-1)^n - 14)n - 9(-1)^n - 15)/(6(2n-1)). \end{aligned} \tag{9}$$

Similarly:

$$\begin{aligned} C_4 &= (164n^3 - (36\cos(2\varphi) + 142)n^2 + (24\cos(2\varphi) - 24\sin\varphi + 24\cos\varphi + 20)n - \\ &\quad -3\cos(2\varphi) + 12\sin\varphi - 12\cos\varphi + 27)/(2n-1)/12; \\ C_5 &= (10n^3 - 5n^2 + 15n + 8)/(2(2n-1)); \\ C_6 &= (36n^3 - (28 + 8\cos(2\varphi))n^2 + (128 + 22\cos(2\varphi) + 24\cos\varphi - 24\sin\varphi)n - \\ &\quad -12\cos\varphi - 9\cos(2\varphi) + 109 + 12\sin\varphi)/(2n-1)^2/2, \end{aligned} \tag{10}$$

where $\varphi = \pi n/2$.

As a result, the expression for the lower estimate of the first frequency follows from (5–7):

$$\omega_D^{-2} = m\left(\left(C_1a^3 + C_2c^3 + C_3h^3\right)/h^2 + \left(C_4a^3 + C_5c^3 + C_6h^3\right)/a^2\right)/(EF). \tag{11}$$

Estimation of the solution error (11) is possible from comparison to the minimum frequency of the entire spectrum of lattice natural frequencies obtained numerically. The spectrum of a system with many degrees of freedom is found from solving the eigenvalue problem of the matrix. Differential equations of mass dynamics of a structure with a number of degrees of freedom K are written in matrix form:

$$m\mathrm{I}_K\ddot{\mathrm{Y}} + \mathrm{D}_K\mathrm{Y} = 0, \tag{12}$$

where D_K — truss rigidity matrix, Y — mass displacement vector, I_K — unity matrix. Let B_K be the matrix, inverse of D_K. Multiplying (12) from the left by B_K, gives the equation:

$$m\mathrm{B}_K\ddot{\mathrm{Y}} + \mathrm{I}_K\mathrm{Y} = 0. \tag{13}$$

Connection $\ddot{\mathrm{Y}} = -\omega^2\mathrm{Y}$ is valid for harmonic vibrations with frequency ω. Hence, from (13), the problem of eigenvalues follows: $\mathrm{B}_K\mathrm{Y} = \lambda\mathrm{Y}$, where $\lambda = 1/(\omega^2 m)$ — the eigenvalues of matrix B_K. The elements of the compliance matrix are found from the Maxwell-Mohr formula. To calculate the eigenvalues of a matrix in the Maple system, Eigenvalues operator from LinearAlgebra package is used. In general, the solution to this problem can be obtained only in numerical form.

Example. The steel lattice has panel length $a = 2m$, height $h = 1$ m, masses in nodes $m = 300\,kg$, rod rigidity $EF = 0.8\cdot10^5\,kN$. Figure 4 shows the dependences of the first frequency on the number of panels obtained numerically and analytically.

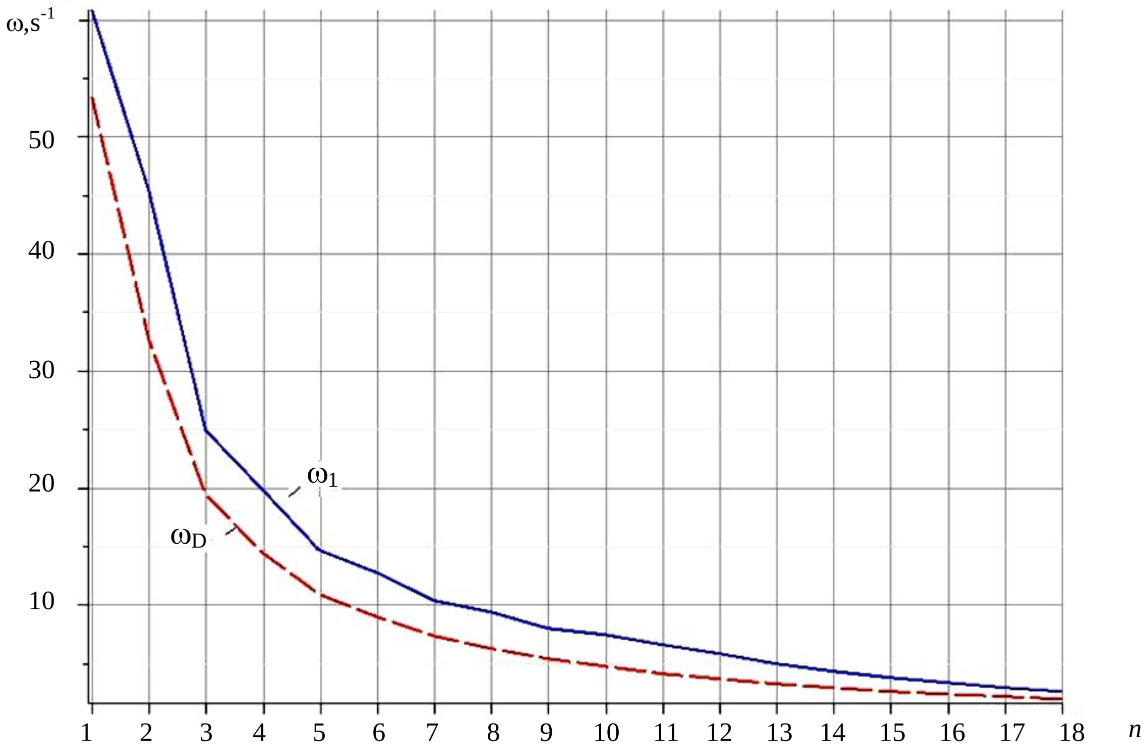

Fig. 4. Comparison of the first natural vibration frequency of lattice ω_1 and its lower analytical estimate ω_D depending on the number of panels (the author's figure)

Relative error $\varepsilon = (\omega_1 - \omega_D)/\omega_1$, depending on the number of panels (Fig. 5), shows that with an increase in the number of panels, the error, starting from n =1, increases, and then monotonously and quickly decreases. This is particularly important when using the obtained formula through calculating lattices with a large number of panels, for which the numerical count starts to gain an error associated with the accumulation of rounding errors, and the cost of computer resources is growing rapidly.

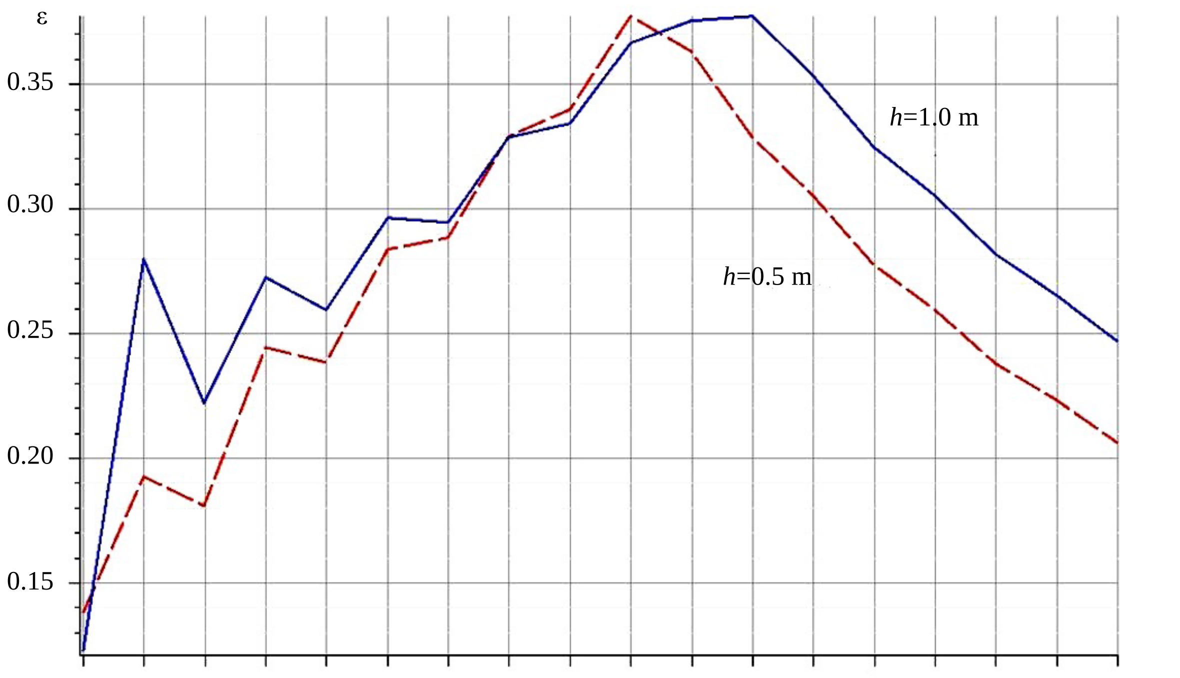

Fig. 5. The error of the analytical solution for the natural frequency depending on the number of panels and height h (the author's figure)

Discussion and Conclusions. A scheme of a statically definable plane lattice was proposed. The task was to obtain an analytical expression of the lower bound of the first natural vibration frequency of a lattice truss for an arbitrary number of panels in the structure. The solution was obtained by induction in the Maple system. The presence of extrema on the constructed curves made it possible to optimize the number of lattice panels by choosing the highest accuracy of the estimate and selecting the required vibration frequency. The proposed study took into account horizontal mass vibrations. Considering horizontal vibrations somewhat complicated the final calculation formula, making it more cumbersome. In addition to the Donkerley's method used, there was a more accurate Rayleigh energy method for evaluating the first frequency, which gave an estimate of the first frequency from above. However, even this solution in the case under consideration had an unnecessarily cumbersome appearance and was not given here.

References

1. Hutchinson RG, Fleck NA. Microarchitectured Cellular Solids — the Hunt for Statically Determinate Periodic Trusses. ZAMM Journal for Applied Mathematics and Mechanics. 2005;85:607–617. https://doi.org/10.1002/zamm.200410208

2. Hutchinson RG, Fleck NA. The Structural Performance of the Periodic Truss. Journal of the Mechanics and Physics of Solids. 2006;54:756–782. https://doi.org/10.1016/J.JMPS.2005.10.008

3. Kaveh A. Optimal Analysis of Structures by Concepts of Symmetry and Regularity. Vienna: Springer; 2013. 463 p. https://doi.org/10.1007/978-3-7091-1565-7

4. Kaveh A, Zolghadr A. Truss Optimization with Natural Frequency Constraints Using a Hybridized CSS–BBBC Algorithm with Trap Recognition Capability. Computers & Structures. 2012;102–103:14–27. https://doi.org/10.1016/J.COMPSTRUC.2012.03.016

5. Ovsyannikova VM. Dependence of Deformations of a Trapezous Truss Beam on the Number of Panels. Structural Mechanics and Structures. 2020;26:13–20.

6. Ilyushin AS. The Formula for Calculating the Deflection of a Cmpound Externally Statically Indeterminate Frame. Structural Mechanics and Structures. 2019;22:29–38.

7. Qiao Dai. Analytical Dependence of Planar Truss Deformations on the Number of Panels. AlfaBuild. 2021;17:1701.

8. Kirsanov MN. The Stress-Strain State of a Rectangular Covering Spatial Truss. Construction of Unique Buildings and Structures. 2020;91:9104.

9. Kirsanov M. Trussed Frames and Arches: Schemes and Formulas. UK: Cambridge Scholars Publishing Lady Stephenson Librar; 2020. 178 p.

10. Petrichenko EA. Lower Bound of the Natural Oscillation Frequency of the Fink Truss. Structural Mechanics and Structures. 2020;26:21–29.

11. Petrenko VF. The Natural Frequency of a Two-Span Truss. AlfaBuild. 2021;20:2001.

12. Vorobev OV. Bilateral Analytical Estimation of the First Frequency of a Plane Truss. Construction of Unique Buildings and Structures. 2020;92:9204.

13. Vorobyev O. About Methods of Obtaining Analytical Solution for Eigenfrequencies Problem of Trusses. Structural Mechanics and Structures. 2020;24:25–38.

14. Goloskokov DP, Matrosov AV. Approximate Analytical Solutions in the Analysis of Thin Elastic Plates. AIP Conference Proceedings. 2018;1959:070012.

15. Goloskokov DP, Matrosov AV. Approximate Analytical Approach in Analyzing an Orthotropic Rectangular Plate with a Crack. Materials Physics and Mechanics. 2018;36:137–141.

16. Goloskokov DP, Matrosov AV. Comparison of Two Analytical Approaches to the Analysis of Grillages. In: Proc. 2015 Int. Conf. "Stability and Control Processes" in Memory of V.I. Zubov (SCP). 2015. P. 382–385. 10.1109/SCP.2015.7342169

17. Buka-Vaivade K, Kirsanov MN, Serdjuks DO. Calculation of Deformations of a Cantilever-Frame Planar Truss Model with an Arbitrary Number of Panels. Vestnik MGSU. 2020;15:510–517. 10.22227/1997-0935.2020.4.510-517

Received 16.09.2022.
Revised 14.10.2022.
Accepted 16.10.2022.

About the Author:

Kirsanov, Mikhail N., professor of the Department of Robotics, Mechatronics, Dynamics and Machine Strength, National Research University “MPEI” (14, Krasnokazarmennaya St., Moscow, 111250, RF), Dr.Sci. (Phys.-Math.), ResearcherID, ScopusID, ORCID, C216@ya.ru

Conflict of interest statement

The author does not have any conflict of interest.

The author has read and approved the final manuscript.

MACHINE BUILDING AND MACHINE SCIENCE

Check for updates

UDC 621.778.1
https://doi.org/10.23947/2687-1653-2022-22-4-323-330

Original article

On the Control of the Technical Condition of Elevator Ropes Based on Artificial Intelligence and Computer Vision Technology

Alexey V. Panfilov ✉, **Alexander R. Yusupov**, **Anatoly A. Korotkiy**, **Boris F. Ivanov**

Don State Technical University, 1, Gagarin Sq., Rostov-on-Don, Russian Federation

✉ panfilov@ikcmysl.ru

Abstract

Introduction. The safety problem and the situation with accidents during the operation of elevator installations are elucidated. The role of elevator rope defects as a factor of dangerous incidents is indicated from the point of view of statistics. The malfunctions of the elevator mechanical equipment related to the defective indices of the ropes are listed. There is a difference in the documentary fixation of defective indices and rejection rates of ropes of lifting structures.

Materials and Methods. The well-known approaches to the control of ropes of lifting structures were described. It was emphasized that visual inspection control (VIC) was required to identify such rejection rates of steel elevator ropes as geometry change, corrosion and wear, wire breaks, temperature exposure, etc. The rejection rate was presented in the form of a mathematical system. The technical condition of elevator ropes during the operation was integrally assessed by the totality of identified defects at a fixed length. The decision to create a software and hardware complex (PAC) for the practical implementation of visual and measuring control was validated.

Results. The developed PAC VIC laboratory sample consisted of a hardware part, a video stream processing module, communicator for the server connectivity, specially designed software, and a client mobile application. PAC VIC implemented the following functions:

– automatic detection and classification of the major significant rope defects based on a deep convolutional artificial neural network;

– demonstration of a three-dimensional image of a rope and an image scanning algorithm with distortion compensation, according to which the metric characteristics of defects were fixed;

– integral assessment of the technical condition of the rope according to the totality of detected defects;

– color interpretation of the actual technical condition of the rope with subsequent transmission to the user's mobile device.

Preliminary tests have shown the suitability of the PAC VIC for identifying defects. The reliability of the results for the identification and qualification of defects exceeded 80 %. Work on deep learning of the system continues.

Discussion and Conclusions. PAC VIC of elevator ropes provides eliminating the risks of visual control caused by the psychophysical state of a person. It works remotely and contactless. The solution proposed by the authors automatically evaluates the rejection rates according to five criteria: external wire breaks, surface wear, rope diameter change, undulation, traces of temperature exposure. An important result of the VIC of steel ropes using computer vision and artificial intelligence is an increase in reliability and safety during the operation of elevator equipment.

Keywords: defects, elevator ropes, rejection rates, visual inspection control, hardware-software package, artificial neural networks, computer vision.

Acknowledgements. The authors are grateful to the FSBI "Fund for the Promotion of the Development of Small Businesses in the Sphere of Science and Technology" for the financial support of the study.

For citation. A. V. Panfilov, A. R. Yusupov, A. A. Korotkiy, B. F. Ivanov. On the Control of the Technical Condition of Elevator Ropes Based on Artificial Intelligence and Computer Vision Technology. Advanced Engineering Research, 2022, vol. 22, no. 4, pp. 323–330. https://doi.org/10.23947/2687-1653-2022-22-4-323-330

Introduction. Increased attention is paid to safety issues during the operation of elevator equipment[1, 2, 3]. About 500 thousand passenger, hospital and freight elevators are being used in the Russian Federation. According to the statistics of elevator accidents, their prime causes are insufficient quality of elevators and components, as well as improper maintenance and repair.

Analysis of elevator accidents has shown that about 30 % of incidents are directly or indirectly related to the technical condition of the ropes [1]. Extremely dangerous are defects, whose growth causes elevator car fall. Passenger elevator accidents, especially tragedies with victims, are very resonant events. Administrative[4] and criminal[5] liability is provided for violation of safety requirements during operation of elevators.

Timely and high-quality control of the technical condition of steel ropes provides preventing dangerous incidents [2–5].

Damage to the ropes occurs due to their poor quality and errors during installation. The consequence of incorrectly performed work may be unacceptable interaction with elements of the elevator equipment, including electrical ones.

Steel ropes can be considered an indicator of the technical condition of elevator equipment. Their defects signal the pulley groove wear, rope slip on a pulley (including due to excessive lubrication), skewed winch mounts, backlash in the elements of the drive gears, etc. Possible malfunctions of the elements of the mechanical part of the elevator, depending on the defective parameters of the ropes, are presented in Table 1.

Table 1

Malfunctions of the mechanical equipment of the elevator related to the rejection indicators of ropes

No.	Rejection criteria	Possible malfunction indicator
1	Outer wire breaks	1. Pulley groove wear. 2. Skewing of the traction sheave during installation or maintenance. 3. Contact with external elements when moving in the shaft. 4. Unqualified supplied steel rope.
2	Surface wear of the rope	1. Pulley groove wear. 2. Skewing of the traction sheave during installation or maintenance.
3	Local increase or decrease in rope diameter	1. Unqualified supplied steel rope. 2. Defects in the installation or maintenance of balancing units and places for embedding steel ropes.
4	Undulation	1. Unqualified supplied steel rope. 2. Installation defects or improper maintenance of balancing units and places for embedding steel ropes.
5	Temperature effect (electrical arc discharge)	1. Exposure to electric current during installation, improper maintenance during operation.
6	Defects in balancing units and places for embedding steel ropes	1. Mounting defects. 2. Improper maintenance. 3. Installation of ropes from different batches.

[1] O poryadke obespecheniya bezopasnosti opasnykh ob"ektov v obshchestvennykh i zhilykh zdaniyakh: RF Government Decree of 24.06.2017, no. 743. URL: http://government.ru/docs/28241/ (accessed: 25.10.2022). (In Russ.)
[2] GOST R 55964-2014. Lifts. General Safety Requirements in Service. URL: https://docs.cntd.ru/document/1200109313 (accessed: 25.10.2022). (In Russ.)
[3] GOST R 54999-2012. Lifts. General Requirements for Maintenance Instruction. URL: https://docs.cntd.ru/document/1200096000 (accessed: 25.10.2022). (In Russ.)
[4] Narushenie trebovanii promyshlennoi bezopasnosti ili uslovii litsenzii na osushchestvlenie vidov deyatel'nosti v oblasti promyshlennoi bezopasnosti opasnykh proizvodstvennykh ob"ektov. 9.1.1 Article of RF Administrative Code. URL: http://www.consultant.ru/document/cons_doc_LAW_34661/6db72644d55f955ad23b924b678184a5d027d99f/ (accessed: 25.10.2022). (In Russ.)
[5] Proizvodstvo, khranenie, perevozka libo sbyt tovarov i produktsii, vypolnenie rabot ili okazanie uslug, ne otvechayushchikh trebovaniyam bezopasnosti. 238 Article of RF Criminal Code. URL: https://base.garant.ru/10108000/82fa894382554e9c56db483eff62c412/ (accessed: 25.10.2022). (In Russ.)

There is a significant difference in the rejection indicators and the standards for the rejection of ropes of various lifting structures [6, 7] and elevators. In the latter case, the criteria are included in the operating manual of the specific elevator. This approach reduces the number of defect indicators, which, specifically, does not contribute to improving operational safety. In [1], the criteria and norms of rejection are given.

Materials and Methods. Ropes are products of deep processing of steel. If their safety margin is reduced to a critical value, operation is unacceptable.

The control of ropes of lifting structures by magnaflux method is widely known. It is used in the diagnosis of passenger cable cars, cargo cranes, lifters. This approach makes it possible to recognize internal defects invisible to the eye, measure the loss of the cross-sectional area of the rope, and detect local inconsistencies. As a rule, the method is used to control steel ropes with a diameter of more than 20 mm.

The average service life of elevator ropes is regulated and does not exceed five years. During this time, loading cycles do not cause loss of cross-sectional area and fatigue damage to the wires of the inner layers. For this reason, magnetic flaw detection is not used for elevator installations.

The most common method of assessing the technical condition of elevator ropes is visual inspection control (VIC)[8]. It provides assessing the technical condition of the operated elevator ropes, which are evaluated according to the following standards of rejection:

- geometry change $P1(t)$;
- corrosion and wear $P2(t)$;
- wire breaks (fatigue) $P3(t)$;
- temperature effect $P4(t)$, etc.

Here, t — current operating time of the elevator.

The rejection rate is understood as the value of $Pi(t)$:

$$Pi(t) = Pio + Pi'(t). \quad (1)$$

Here, Pio — scleronomous part, it does not depend on t and is associated with a single application of loads; $Pi'(t)$ — rheonomic part, which accumulates in the process of elastoplastic cyclic deformation.

When assessing the technical condition of the rope during operation, the loss of its strength is calculated according to at least one of the rejection criteria:

$$Pi(t) \leq [Pi], \quad (2)$$

where $i = 1/12$.

Under the maintenance of passenger elevators, VIC of steel ropes is performed at intervals specified in the operations manual (as a rule, once a month).

VIC of steel ropes consists of two stages:

1) inspection of the rope and its attachment points with or without optics;

2) measurements of diameter, wear of outer wires, geometric out-of-straightness, electric shock, and attachment points.

[6] Ob utverzhdenii federal'nykh norm i pravil v oblasti promyshlennoi bezopasnosti “Pravila bezopasnosti opasnykh proizvodstvennykh ob"ektov, na kotorykh ispol'zuyutsya pod"emnye sooruzheniya”. Federal Service for Ecological, Technological and Atomic Inspection. URL: https://docs.cntd.ru/document/573275657 (accessed: 25.10.2022). (In Russ.)
[7] Ob utverzhdenii federal'nykh norm i pravil v oblasti promyshlennoi bezopasnosti “Pravila bezopasnosti passazhirskikh kanatnykh dorog i funikulerov”. Federal Service for Ecological, Technological and Atomic Inspection. URL: https://docs.cntd.ru/document/573191373 (accessed: 25.10.2022). (In Russ.)
[8] Possibilities to Improve Visual Wire Rope Inspection. O.I.T.A.F. Recommendations no. 30. International Organization for Transportation by Rope. URL: https://www.gosnadzor.gov.ru/industrial/equipment/cable%20cars%20and%20funiculars/method%20www.oitaf.org/ (accessed: 05.11.2022). (Transl. from Eng.)

The quality of VIC under maintenance of steel ropes is associated with the physiological capabilities of human visual perception [4–6]. The elevator can have from three to twelve parallel ropes with a complex balancing system. The quantity depends on the height and load capacity. Health assessment of ropes, balancing units and sealing off involves working at height, under difficult conditions, in tight working space, in low light[9]. The possibilities of human vision are limited. It is known that after watching a moving steel rope for more than ten minutes, the eyes get tired and perceive the numerous rejection indicators worse. High-quality, objective control of elevator ropes requires automation of the process. Analysis of literature sources, accidents and incidents, has shown that it is reasonable to use solutions based on computer vision and artificial intelligence technologies for automation [5–10].

The authors set a goal to create a program apparatus complex (PAC) of VIC for the practical implementation of visual and measurement control based on computer vision and artificial intelligence technologies[10].

Research Results. In elevators, defects in steel ropes and their attachments are automatically detected and identified using special means of photo and video recording. Machine vision and artificial intelligence process images of defects. An integral assessment of the types and parameters of the detected defects in the form of a color indication is transmitted to the mobile device. PAC VIC automates and combines two control methods: visual and instrumental.

The basic functions of the PAC VIC are listed below.

1. The solution based on a deep convolutional artificial neural network automatically detects and classifies the primary defects of ropes and their sealing off.

2. A set of cameras and an image scanning algorithm with distortion compensation give a three-dimensional image of the rope for the actual determination of the metric characteristics of defects.

3. On totality of the detected defects, an integral assessment of the technical condition of the rope is performed on the basis of risk analysis.

4. The integral assessment in the form of a color indicator is periodically transmitted to the user's mobile device.

The complex consists of three elements.

1. Hardware component. This is a housing with built-in video cameras that provide viewing the rope from all sides. A special module processes the video stream, and means of communication allow you to contact the server.

2. Software, created using a stack of Pytorch, TensorFlow, OpenCV technologies, searches for and classifies defects in steel ropes based on a deep convolutional artificial neural network.

3. Mobile application informs the user about the monitoring results.

Six IP cameras with a resolution of 640×480 are used to photograph sections of movable steel ropes. They are fixed in the housing installed in the elevator shaft. The number of cameras depends on the number of ropes on which the elevator car is suspended. The cameras are connected via a wired or wireless communication channel to a single-board computer that processes images and generates a batch message for forwarding to the server. A single-board computer generates a batch message. It is transmitted via an Ethernet cable or a wireless communication channel through a modem router to the server. The latter classifies defects, determines their number and metrological parameters, outputs an integral assessment of the technical condition of the rope, interprets it as a color indicator, and in this form transmits it to the user through a mobile application.

Figures 1–3 shows the PAC VIC modules for elevator installations, the functional diagram and the hardware component of the complex.

[9] Vallan A, Molinar F. A Vision-Based Technique for Lay Length Measurement of Metallic Wire Ropes. IEEE Transactions on Instrumentation and Measurement. 2009;5:1756–1762.
[10] Korotkiy AA, et al. Method of Visual and Dimensional Control of a Steel Cable. RF Patent no. 2775348, 2022.

Fig. 1. PAC VIC modules (the authors' figure)

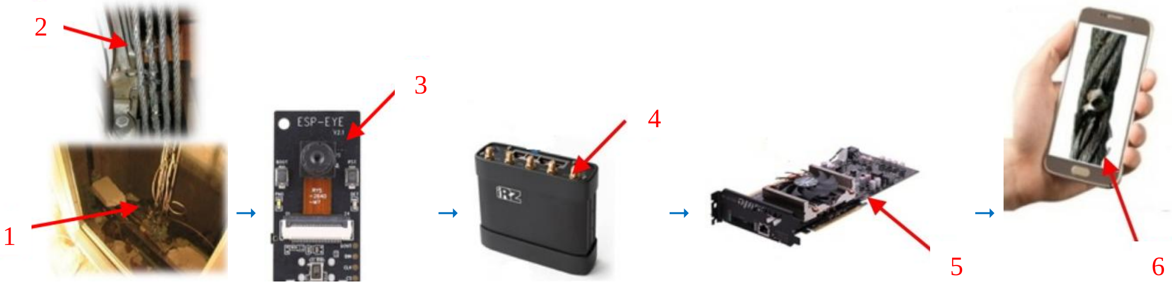

Fig. 2. PAC VIC functional diagram for detecting defects in steel ropes and balancing units based on computer vision and artificial intelligence technologies: 1 — balancing unit; 2 — rope defects; 3 — IP-camera; 4 — GSM-modem; 5 — neurocomputing device; 6 — image in a mobile device (the authors' figure)

a) *b*)

Fig. 3. Hardware component of PAC VIC: *a* — place in the elevator installation,
b — installation points of six IP cameras (the authors' photo)

PAC VIC identifies and classifies primary defects of steel ropes, elevator installations and balancing units using computer vision:

1) outer wire breaks;

2) surface wear of wires;

3) increase or decrease in rope diameter;

4) deformation in the form of undulation ("corkscrew");

5) electric arc damage;

6) balancing unit defects.

The database contains photo and video images of typical defects of steel ropes and balancing units. The complex periodically or on request outputs a remote integrated assessment of the rejection indicators of ropes and defects of balancing units and transmits it to the user's mobile application.

The computational tool is used for an integral assessment of the technical condition of the steel rope and interpretation of the result using color (red, yellow, green). This makes it possible to integrate with sensors installed in elevator control and dispatch communication systems, as well as with the "Elevator Monitoring"[11] online maintenance control program and the "Arpicon. Online"[12] cloud service automation platform.

The proposed solution was previously tested on a laboratory elevator installation with three ropes with an organic core. Their characteristics correspond to GOST 3077–80:

– double LK-O type rope;
– structure 6×19 (1 + 9 + 9) + 1 o. s.;
– diameter of 10 mm.

Testing has shown the feasibility of the method for determining the defects listed above using the PAC VIC. The reliability of detection and qualification of defects exceeded 80%. To improve the results, the investigation on deep learning of the system continues, i.e., algorithms are being improved, the number and quality of datasets of images of typical defects of steel ropes and balancing units are increasing.

Discussion and Conclusions. Defects in the steel ropes may cause the elevator cab to fall. When maintaining elevators, visual control is not enough to fully assess the actual risks of accidents and incidents.

It is established that computer vision and artificial intelligence technologies can be used for an integral assessment of the technical condition of steel ropes, and this significantly increases the level of safety during the operation of elevator installations.

The PAC VIC of elevator ropes eliminates the risks associated with the psychophysical state of the person who determines the state of the system. Thus, it is possible to increase safety of the elevator equipment operation.

Advantages of the developed PAC VIC of elevator ropes are as follows:

– functioning in automatic mode, directly in the operated elevator;
– contactless detection of rejection indicators using photo and video surveillance (machine vision);
– automatic evaluation of rejection indicators according to five criteria online (external wire breaks, surface wear, local increase or decrease in rope diameter, undulation, temperature exposure);
– transfer of color-coded rejection indicators to the user's mobile application;
– processing of images with defects of steel ropes by artificial intelligence.

Potential consumers of PAC VIC:

– operators — organizations responsible for the technical condition of elevators;
– home unit companies, homeowners' associations;
– manufacturers, buyers and sellers of passenger elevators.

References

1. Panfilov AV, Kolganov VP, Bahteev OA, et al. Reducing the Risk and the Severity of the Consequences of Accidents during Elevator Accidents. Scientific and Technical Journal of Bryansk State University. 2020;3:451–460. https://doi.org/10.22281/2413-9920-2020-06-03-451-460

2. Korotkiy AA, Khalfin MN, Ivanov BF, et al. RD ROSEK 012-97. Kanaty stal'nye. Kontrol' i normy brakovki. Novocherkassk: ROSEK; 1997. 50 p. (In Russ.)

3. Mouradi H, Barkany AE, Biyaali AE. Steel Wire Ropes Failure Analysis: Experimental Study. Engineering Failure Analysis. 2018;91:234–242. https://doi.org/10.1016/j.engfailanal.2018.04.019

[11] Rusanov SE. Computer program "Elevator Monitoring". URL: https://lmonitor.ru (accessed: 29.10.2022). (In Russ.)
[12] Arpicon. Online."Center" LLC. URL: https://lift.arpicon.ru (accessed: 29.10.2022). (In Russ.)

4. Deyst JP, Sounders M, Solomon OM. Bounds on Least-Squares Four-Parameter Sine-Fit Errors due to Harmonic Distortion and Noise. IEEE Transactions on Instrumentation and Measurement. 1995;44:637–642. 10.1109/19.387298

5. Soucup D, Huber-Mörk R. Convolutional Neural Networks for Steel Surface Defect Detection from Photometric Stereo Images. In: Advances in Visual Computing. ISVC 2014. Lecture Notes in Computer Science. 2014;8887:668–677. https://doi.org/10.1007/978-3-319-14249-4_64

6. Vallan AA, Molinar F. Vision-Based Technique for Lay Length Measurement of Metallic Wire Ropes. IEEE Transactions on Instrumentation and Measurement. 2009;58:1756–1762. 10.1109/TIM.2009.2012953

7. Platzer E-S, Süße H, Nägele J, et al. On the Suitability of Different Features for Anomaly Detection in Wire Ropes. In: Computer Vision, Imaging and Computer Graphics: Theory and Applications. Ranchordas A, et al. (eds.) VISIGRAPP 2009: Communications in Computer and Information Science. 2009;68:296–308. https://doi.org/10.1007/978-3-642-11840-1_22

8. Rodner E, Wacker E-S, Kemmler M, et al. One-Class Classification for Anomaly Detection in Wire Ropes with Gaussian Process in a Few Lines of Code. In: Proc. 12th IAPR Conference on Machine Vision Applications. URL: https://www.researchgate.net/publication/232805478_OneClass_Classification_for_Anomaly_Detection_in_Wire_Ropes_with_Gaussian_Processes_in_a_Few_Lines_of_Code (accessed: 29.09.2022).

9. Xinyuan Huang, Zhiliang Liu, Xinyu Zhang, et al. Surface Damage Detection for Steel Wire Ropes Using Deep Learning and Computer Vision Techniques. Measurement. 2020;161:107843. https://doi.org/10.1016/j.measurement.2020.107843

10. Xiangdong Chang, Yuxing Peng, Sheng-Yong Zou, et al. Evolution Properties of Tribological Parameters for Steel Wire Rope under Sliding Contact Conditions. Metals. 2018;8:743. 10.3390/met8100743

Received 31.10.2022.

Revised 18.11.2022.

Accepted 29.11.2022.

About the Authors:

Panfilov, Alexey V., associate professor of the Transport Systems Operation and Logistics Department, Don State Technical University (1, Gagarin sq., Rostov-on-Don, 344003, RF), Cand.Sci. (Eng.), ORCID, panfilov@ikcmysl.ru

Yusupov, Alexander R., senior lecturer of the Robotics and Mechatronics Department, Don State Technical University (1, Gagarin sq., Rostov-on-Don, 344003, RF), ORCID, temple_black@mail.ru

Korotkiy, Anatoly A., Head of the Transport Systems Operation and Logistics Department, Don State Technical University (1, Gagarin sq., Rostov-on-Don, 344003, RF), Dr.Sci. (Eng.), professor, ORCID, korot@novoch.ru

Ivanov, Boris F., leading researcher of the Centre for Scientific Competence, Don State Technical University (1, Gagarin sq., Rostov-on-Don, 344003, RF), Cand.Sci. (Eng.), associate professor, ORCID, ivanov@ikc-mysl.ru

Claimed contributorship:

A. V. Panfilov: basic concept formulation; research objectives and tasks; formulation of conclusions. A. A. Korotkiy: academic advising; analysis of the research results; the text revision; correction of the conclusions. B. F. Ivanov: accident and incident analysis; writing and editing the text. A. R. Yusupov: implementation of hardware and software parts; testing; processing of the results.

Conflict of interest statement

The authors do not have any conflict of interest.

All authors have read and approved the final manuscript.

Check for updates

UDC 620.179.17
https://doi.org/10.23947/2687-1653-2022-22-4-331-337

Original article

Acoustic Emission Method of Diagnostics of Structures Made of Composite Materials Based on Invariants

Alexey V. Popov ✉, Valentina Yu. Voloshina, Konstantin A. Zhuravsky, Maria A. Labina

Military Educational and Scientific Center of the Air Force "N.E. Zhukovsky and Y.A. Gagarin Air Force Academy", 54 a, Starykh Bol'shevikov St., Voronezh, Russian Federation

✉ avpnil@rambler.ru

Abstract

Introduction. Composite materials are the main way to reduce the weight of the aircraft structure and improve its flight performance. Methods of non-destructive testing enable to assess the technical condition of composite materials, as well as to determine stress concentrators in them to make a decision on the further operation of this control object. The paper presents an analysis of the use of composite materials in the aircraft design and ways to improve their flight performance through the application of composites. An acoustic-emission method for assessing crack resistance based on invariants was described. The study aimed at increasing the accuracy and efficiency of assessing the crack resistance of aircraft structures made of composite materials through the use of the acoustic emission method of non-destructive testing.

Materials and Methods. The nomenclature of composite materials used in aircraft was given, and their physical and mechanical properties were compared. The acoustic emission method of non-destructive testing of composite materials based on invariant ratios was used.

Results. A method for assessing the crack resistance of primary structural elements based on the invariants of acoustic emission processes, and a program apparatus complex based on it has been developed.

Discussion and Conclusions. The results obtained can be used to determine the strength characteristics of composite materials by the acoustic emission method of non-destructive testing to assess the technical condition of primary structural elements in mechanical engineering, shipbuilding, and aircraft construction. The paper is recommended to researchers involved in the development of aircraft.

Keywords: composite materials, aircraft, non-destructive testing, acoustic emission control.

Acknowledgments. The research was carried out with the support of the "UMNIK" program of the Russian Foundation for the Promotion of Innovation.

For citation. A. V. Popov, V. Yu. Voloshina, K. A. Zhuravsky, M. A. Labina. Acoustic Emission Method of Diagnostics of Structures Made of Composite Materials Based on Invariants. Advanced Engineering Research, 2022, vol. 22, no. 4, pp. 331–337. https://doi.org/10.23947/2687-1653-2022-22-4-331-337

Introduction. Improving aircraft performance characteristics (APC) and reducing the weight of aircraft structures while maintaining their sufficient strength and stiffness is a fundamental task in the aircraft industry [1, 2]. The introduction of composite materials (CM) partially solves this problem.

The developers of flying vehicles (FV) are constantly introducing new materials into aviation technology to increase the APC and reduce the weight of the structure. CM provide reducing the weight of the wing, fuselage and tail. High mechanical-and-physical properties of CM increase the stiffness and strength of the structure.

The major advantages of CM include high values of specific strength, stiffness (modulus of elasticity 130–140 GPa), wear resistance and fatigue strength[1,2] [3, 4]. The disadvantages of CM include hygroscopicity, significant cost, anisotropy of properties, low impact strength, low operational manufacturability.

The study aimed at increasing the accuracy and efficiency of assessing the crack resistance of composite structures through the use of acoustic emission (AE) control.

Materials and Methods. A wide range of CM is used in the aircraft industry [1, 4] (Fig. 1), due to which it is possible to lighten the weight of structures. This is achieved by replacing elements made of traditional materials (titanium and aluminum alloys, steel) with CM.

Aviation industry enterprises face two crucial tasks:

– to evaluate the processes of accumulation of damage and destruction of structures from CM in the entire range of alternating loads;

– to evaluate the quality of serial products from CM through strength testing.

Basically, the following CM destruction schemes are distinguished (Fig. 1):

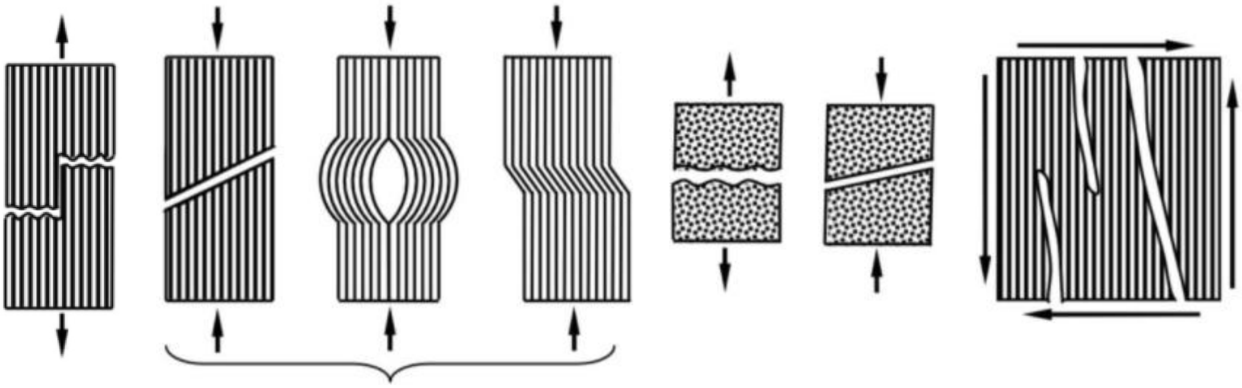

Fig. 1. Schemes of destruction of composite materials: *a* — when stretched along the fibers; *b* — when compressed along the fibers; *c* — when stretched across the fibers; *d* — caused by shear stresses when compressed across the fibers; *e* — delamination (the authors' figure)

Currently, the acoustic emission (AE) method of NDT is special among the methods of diagnosing high-duty structures.

The AE method is based on the registration of acoustic waves emitted under the destruction of CM. The major advantages of this method include [5–11]:

– complex nature of the CM study (fracture mechanics and acoustic diagnostics);

– registration of developing CM defects;

– high sensitivity to growing CM defects (sensitivity of AE equipment of the order of 1×10^{-6} mm^2 for a crack of CM with a length of 1 μm);

– using multiple converters;

– remote monitoring of objects at a considerable distance from the AE equipment.

AE in CM is a nonstationary random elastic wave emission process. Based on this, methods of static radio engineering can be used to treat and analyze such processes. Based on the Poisson distribution, a well-known equality between the mathematical expectation and the variance of the number of events in a random process is fulfilled:

$$m[x] = D[x] = \lambda, \tag{1}$$

where λ — intensity of the number of pulses at a given sampling interval.

This relation makes it possible to construct parametric invariants that are valid only for the Poisson process, and on this basis, to estimate the deviation of the analyzed process from the Poisson one [5, 6, 12, 13]:

$$I_1 = (m[x^3] - 3 \cdot m[x^2] \cdot m[x] + (m[x])^3) - m[x] = 0. \tag{2}$$

[1] Pravila organizatsii i provedeniya akustiko-emissionnogo kontrolya sosudov, apparatov, kotlov i tekhnologicheskikh truboprovodov. PB 03–593–03 RF Gostechnadzor. Moscow: PIO OBT; 2003. 102 p. URL: https://files.stroyinf.ru/Data2/1/4294816/4294816759.htm (accessed: 28.09.2022). (In Russ.)

[2] Ivanov VI, Vlasov IE. Metod akusticheskoi emissii. In: Nerazrushayushchii kontrol'. Spravochnik v 8 t. T. 7. Kn.1. Klyuev VV (ed.) Moscow: Mashinostroenie; 2006. 340 p. (In Russ.)

Expression (15) can be used as an invariant of the number of AE pulses to determine the degree of deviation of the AE pulse flow from the Poisson one when conducting AE tests of CM.

Based on (15), we obtain several more expressions to determine the degree of deviation of the AE pulse flow from the Poisson one:

$$I_2 = \frac{m[x]}{m[\dot{x}^3]} = 1; \quad (3)$$

$$I_3 = \frac{m[x]\left(1-2\cdot\left(m[x]^2\right)+3\cdot m[x^2]\right)}{m[x^3]} = 1. \quad (4)$$

When a macrodefect is formed, the characteristics of AE pulse flows become dependent, which destroys the Poisson flow hypothesis and causes a violation of equality (2–4).

This approach is implemented in the program apparatus complex (PAC) (Fig. 2), which provides identifying crack-like defects in various CM [12, 13].

PAC consists of the following components:

– broadband piezo sensors GT300, operating frequency range —100–800 kHz, resonant frequency 283 kHz;

– amplifier GT200A, gain factor — 1–200, limits of the permissible additional relative error of the charge conversion coefficient in the operating temperature range are from –40 ° to + 85 °C with an error of ± 1 %;

– ADC E20-10 is a high-speed ADC module with USB interface for connecting to a PC, which has four ADC channels 14 bit/10 MHz with multiplexing function, 16 channels of digital input and output compatible with TTL logic, as well as two channels of DAC 12 bit / ± 5 V;

– PC, HF cables.

Accuracy and reliability of the AE registration and processing is provided by the frequency parameters of piezotransducers and ADC, which are consistent with Kotelnikov theorem. It states that a continuous signal with a limited spectrum can be accurately reconstructed from its discrete samples if they were taken with a sampling frequency exceeding the maximum signal frequency by at least two times.

PAC uses software amplitude threshold filtering, as well as a method for smoothing the resonant amplitude of pulse attenuation based on a digital peak detector, which provides obtaining exponential smoothing of the shape of AE pulses to increase the accuracy of their registration.

A technique for evaluating multiparametric information based on combining ("convolution") informative parameters of AE by methods of the theory of operations research has been developed to perform a complex real-time analysis of a set of informative parameters of AE signals.

The developed software implementation of the technique has the following basic functional modes: setup; function check; input of restrictions and initial data; monitoring changes in loads, deformations and waveforms of AE pulses; a set of informative AE parameters and their "convolution" through registration channels; determining the location of defects; assessing the danger of defects and the possibility of further operation of the structure, storing the results.

Since AE is a passive method of non-destructive testing, one piezo sensor can register signals from a separate power element of the FV (Fig. 2 *b*).

The elastic wave attenuation, depending on the material, profile and thickness of the tested samples, determines the number of piezoelectric converters used and the distance between them. The attenuation of signals is determined experimentally using an AE signal simulator before testing samples and structural elements.

For fault isolation, the triangulation method[3,4] was taken as a basis, which provides determining the location of defects in the primary structural elements in real time with an accuracy of 0.1 m.

[3] PB 03–593–03. Pravila organizatsii i provedeniya akustiko-emissionnogo kontrolya sosudov, apparatov, kotlov i tekhnologicheskikh truboprovodov. RF Gostechnadzor. 2003. 102 p. (In Russ.)

[4] Nerazrushayushchii kontrol'. Spravochnik v 8 t. Klyuev VV (ed.) In Kn.1.: Ivanov VI, Vlasov IE. Metod akusticheskoi emissii. Kn. 2: Balitskiy FYa, Barkov AV, Barkova NA, et al. Vibrodiagnostika. 2-e izd., ispr. Moscow: Mashinostroenie; 2006. 829 p. (In Russ.)

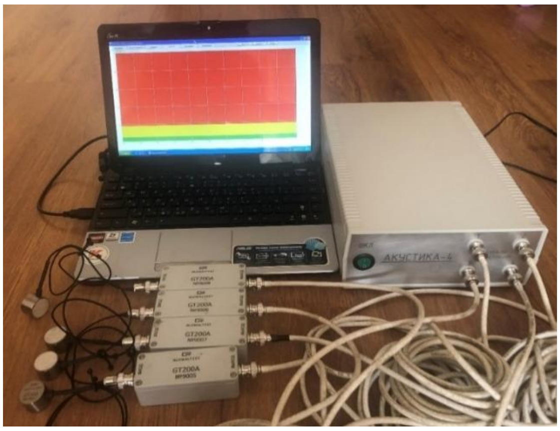

a)

b)

Fig. 2. Program apparatus complex of acoustic emission diagnostics: *a* — complete complex; *b* — placement of the complex sensor under testing of the aircraft aileron on the stand (the authors' photo)

Research Results. To assess the reliability of the proposed invariant method and the sensitivity of the PAC to the assessment of developing defects, strength tests of a series of KM KMU-1B samples were performed before destruction. The load was carried out by the RM-1 breaking machine. Before tensile tests, a piezoelectric sensor was installed on the surface of the sample through a layer of contact lubricant (Tsiatim) to improve acoustic contact. During the tests, acoustic pulses that occur in the structure of the OC when creating a load were recorded. Elastic AE waves were recorded by a piezo sensor, then the signal was amplified by a preamplifier, an analog-to-digital converter transformed the signal into an analog-to-digital form for subsequent processing on a PC. The results are shown in Figure 3:

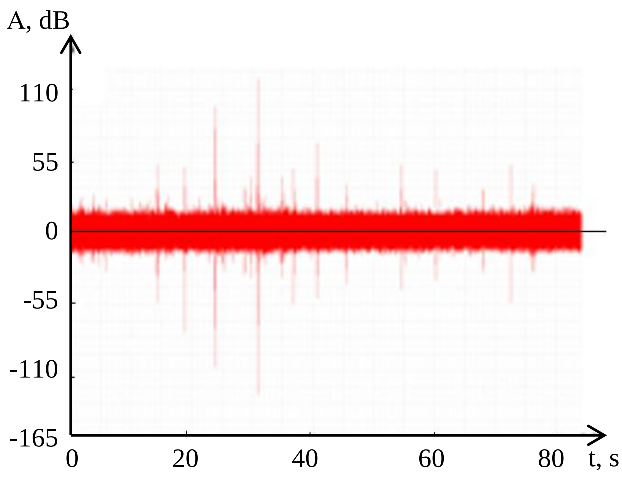

a)

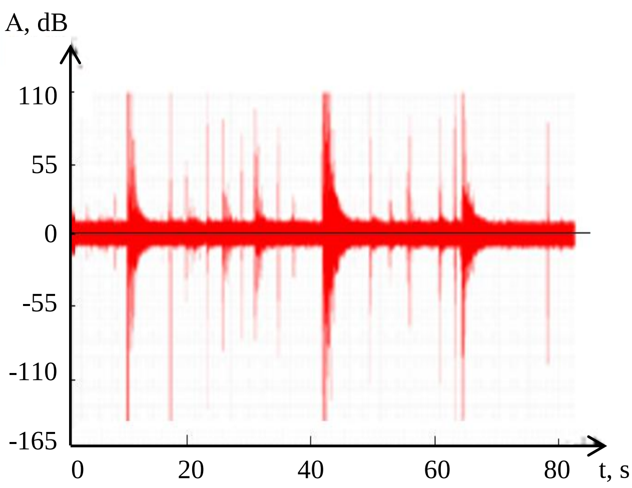

b)

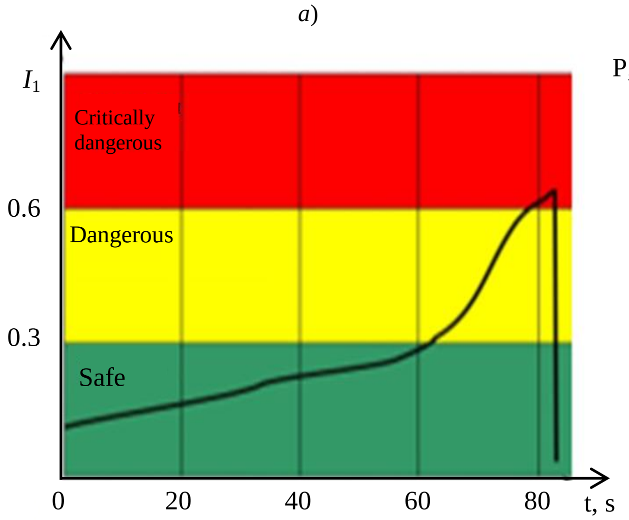

c)

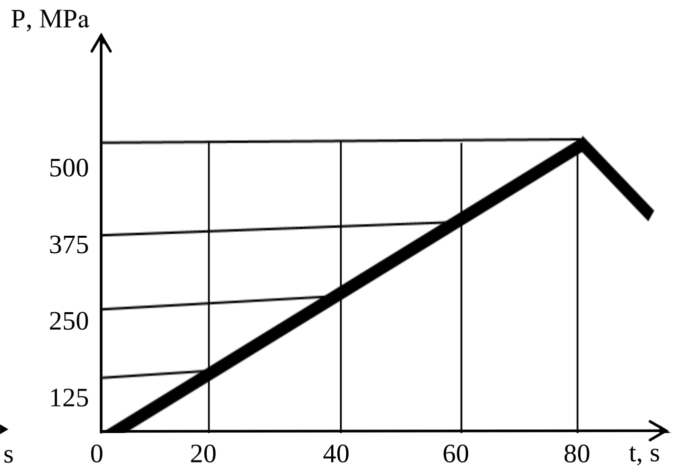

d)

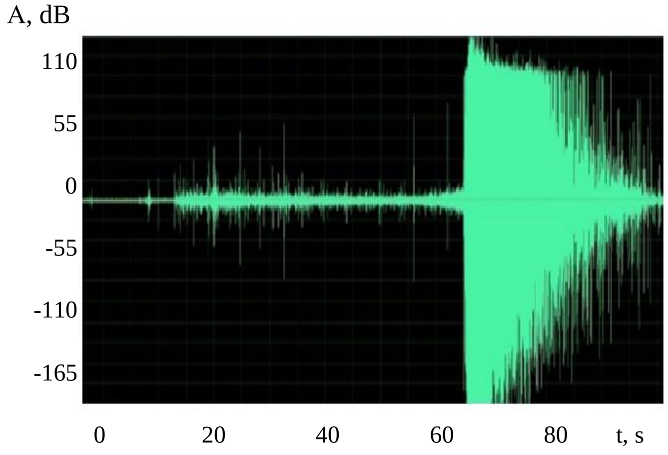

e)

Fig. 3. Experimental results before destruction of the samples: *a* — oscillogram of AE pulses during destruction of the composite material matrix; *b* — oscillogram of AE pulses under destruction of the composite material fibers; *c* — curve of invariant I_1; *d* — loading curve of the glider primary element from CM; *e* — oscillogram of the AE signal from the beginning of the load to the destruction of the sample (the authors' figure)

Figures 3 *a* and 3 *b* show the waveforms of AE pulses during the destruction of the matrix and fibers of the composite material, in which the maximum values of the AE signal amplitude correspond to the destruction of OC. At an amplitude of 55 dB, the CM matrix is destroyed, at 75 dB, the CM fibers are destroyed.

Figure 3 *c* shows the dependence of the invariant on time I_1 (load). The green zone is characterized by the absence of a defect in the primary element of the airframe. The yellow zone is characterized by an unfavorable loading environment of OC, the formation of developing defects (cracks, delamination). The red zone corresponds to the destruction of KMU-1V.

From the 60th second of loading at a load of 375 MPa, the formation of the main crack occurs (Fig. 3 *d*), which causes the exit of the invariant from the green (safe) zone. These conditions correspond to 75 % of the destructive load (350 MPa) of the samples. The reliability of the use of invariants is validated by a sharp increase in the amplitude and intensity of signals (Fig. 3 *e*), the results of optical control during tests.

At a load of P = 500 MPa, the destruction of CM occurs at a time equal to T = 80 s, which causes a decrease in the load and the amplitude of acoustic vibrations in the material of OC.

Discussion and Conclusions. This experiment reflects the acoustic emission control of samples (primary structural elements) from KMU-1V.

The developed PAC, based on the proposed invariant method, makes it possible to process multichannel and multiparametric information about changes in informative AE parameters on-the-fly (in real time), determine the location of defects in CM, assess the degree of danger of defects and the possibility of further operation of structures [12, 13].

In the future, it is proposed to introduce such automatic control systems to diagnose the design of aircraft in flight and during ground maintenance.

References

1. Kozlov DM. Proektirovanie uzlov aviatsionnykh konstruktsii. Komarov VA. (ed.) Samara: Izdatel'stvo Samarskogo universiteta; 2017. 96 p. (In Russ.)

2. Gishvarov AS. Analiz ekspluatatsionnykh razrushenii letatel'nykh apparatov i dvigatelei. Ufa: UGATU; 2003. 289 p. (In Russ.)

3. Makhutov NA, Ivanov VI, Musatov VV. Primenenie tekhnicheskoi diagnostiki dlya rascheta veroyatnosti razrusheniya tekhnicheskikh ustroistv i otsenki riska avarii. Occupational Safety in Industry. 2018;9:53–64. (In Russ.)

4. Andrievskiy RA, Ragulya AV. Nanostrukturnye materialy. Moscow: Akademiya; 2005. 192 p. (In Russ.)

5. Builo SI, Builo BI, Chebakov MI. Probabilistic-Informational Approach to Assessing the Reliability of the Results of the Acoustic-Emission Method of Control and Diagnostics. Russian Journal of Nondestructive Testing. 2021;5:37–44.

6. Builo SI. On the Information Value of the Method of Invariants of Acoustic-Emission Signals in the Diagnostics of Pre-Failure State in Materials. Russian Journal of Nondestructive Testing. 2018;54:18–23.

7. Zhang F, Wu G, Wang Z. Statistical Model and Analysis of AE Data from Aircraft. Insight: Non-Destructive Testing and Condition Monitoring. 2001;43:531–536.

8. Zheng GT, Backley M, Kister G. Blind Deconvolution of Acoustic Emission Signals for Damage Identification in Composites. AIAA Journal. 2001;39:1198–1205. https://doi.org/10.2514/2.1435

9. Skalskyi VR, Koval PM. Some Methodological Aspects of Application of Acoustic Emission. Lviv: Spolom; 2007. 336 p.

10. Maochen Ge. Analysis of Source Location Algorithms, Part I: Overview and Non-Iterative Methods. Journal of Acoustic Emission. 2003;21:14–28.

11. Barat V Borodin Y, Kuzmin A. Detection of AE Signals against Background Friction. Journal of Acoustic Emission. 2011;29:133–141.

12. Popov AV, Komlev AB, Samuylov AO, et al. Methods and Means of Acoustic Emission Diagnostics of Power Elements of the Airframe of Aircraft. NDT World. 2021;24:50–52. 10.12737/1609-3178-2021-52-54

13. Popov AV, Samuylov AO, Voloshina VYu, et al. Acoustic Emission Method of Diagnostics of Power Elements of an Aircraft Airframe Based on Invariants. Vestnik UGATU. 2021;25:50–55. 10.54708/19926502_2021_2539350

Received 19.09.2022.

Revised 16.10.2022.

Accepted 20.10.2022.

About the Authors:

Popov, Alexey V., professor of the **“**Restoration of Military Aviation Equipment” Department, Military Educational and Scientific Center of the Air Force “N.E. Zhukovsky and Y.A. Gagarin Air Force Academy” (54 a, Starykh Bol’shevikov St., Voronezh, 394956, RF), Dr.Sci. (Eng.), associate professor, ORCID, avpnil@rambler.ru

Voloshina, Valentina Yu., senior researcher, Military Educational and Scientific Center of the Air Force “N.E. Zhukovsky and Y.A. Gagarin Air Force Academy” (54 a, Starykh Bol’shevikov St., Voronezh, 394956, RF), Cand.Sci. (Economics), ORCID, tolkoradinauki@mail.ru

Zhuravsky, Konstantin A., service student of the **“**Restoration of Military Aviation Equipment” Department, Military Educational and Scientific Center of the Air Force “N.E. Zhukovsky and Y.A. Gagarin Air Force Academy” (54 a, Starykh Bol’shevikov St., Voronezh, 394956, RF), ORCID, tolkoradinauki@mail.ru

Labina, Maria A., engineer, “Synthesis of Technologies” LLC (54 a, Starykh Bol’shevikov St., Voronezh, 394956, RF), ORCID, Labina1310@rambler.ru

Claimed contributorship:

A. V. Popov: development of the invariant method; scientific management of research. V. Yu. Voloshina: conducting and analyzing research results; text layout. K. A. Zhuravsky: development and description of the hardware and software complex. M. A. Labina: analysis of composite materials and flight characteristics of aircraft.

Conflict of interest statement

The authors do not have any conflict of interest.

All authors have read and approved the final manuscript.

MACHINE BUILDING AND MACHINE SCIENCE

UDC 621.762.002
https://doi.org/10.23947/2687-1653-2022-22-4-338-345

Original article

Study on Processing Grinding Sludge Conglomerates in Devices with a Rotating Electromagnetic Field

Valeriy A. Lebedev, Andrey A. Schirin ✉, Nikolay S. Koval, Yuri M. Vernigorov
Don State Technical University, 1, Gagarin Sq., Rostov-on-Don, Russian Federation
✉ ANDREY.SHIRIN.94@yandex.ru

Abstract
Introduction. The key stages of sludge processing technology are the destruction of conglomerates into metal and non-metal components, as well as the grinding of component particles to obtain secondary raw materials of the required granulometric composition. The use of a rotating electromagnetic field for processing grinding sludge makes it possible to exclude the application of various means of destruction and grinding, avoiding contact interaction of agglomerates and the walls of the working chamber. Thus, the material consumption of technical means is reduced, and the efficiency of the destruction process is increased. The study aimed at establishing the features and basic patterns of sludge waste processing in devices with a rotating electromagnetic field.

Materials and Methods. For the research, grinding sludge was used, which was a collection of conglomerates of arbitrary shape, consisting of 80–85 % of metal chips. An induction method was applied based on establishing the connection of the EMF induced in an induction sensor and the magnetic induction of a rotating electromagnetic field. The influence of induction on the nature of interaction between sludge particles in a rotating electromagnetic field was evaluated by changing the relative EMF signal induced in an inductive sensor.

Results. As a result of experimental studies conducted using the induction method, it has been found that the dynamic characteristics of sludge waste conglomerates depend on the induction of a rotating field to a certain value. With an increase in the size of sludge conglomerates, with the same size of ferromagnetic particles entering it, the magnitude of the magnetic field induction required for their destruction decreased. With a decrease in the particle size of conglomerates, the field induction required for the destruction of conglomerate bonds increased. An increase in the number of particles in the conglomerate reduced the value of induction. The degree of destruction of the conglomerate and the grinding of its ferromagnetic particles depended on the duration of the rotating electromagnetic field induction.

Discussion and Conclusions. The proposed induction method makes it possible to investigate the influence of electromagnetic field parameters on the change in the state of the magnetic vibrating layer, as well as to evaluate the kinematic characteristics of ferromagnetic medium particles in the magnetic vibrating layer.

Keywords: grinding sludge, induction, magnetic vibrating layer, rotating electromagnetic field, conglomerate, ferromagnetic particles, destruction, grinding.

Funding information. The research is done with the financial support from RFFI within the framework of scientific project no. 20-38-90006.

Acknowledgements. The authors would like to thank the heads of enterprises of the Rostov region: PJSC "Beriev Aircraft", OAO "10-GPZ", for the samples of slurry waste of grinding production provided.

For citation. V. A. Lebedev, A. A. Schirin, N. S. Koval, Yu. M. Vernigorov. Study on Processing Grinding Sludge Conglomerates in Devices with a Rotating Electromagnetic Field. Advanced Engineering Research, 2022, vol. 22, no. 4, pp. 338–345. https://doi.org/10.23947/2687-1653-2022-22-4-338-345

Introduction. The technology of processing one of the most complex types of metal production waste — grinding sludge — to reuse its components in powder metallurgy and foundry production requires a number of successive stages: separation of process liquid (PL), drying, destruction of conglomerates, grinding, and separation of sludge solids [1–10]. The analysis has shown that the last two stages of sludge processing are the most labor-intensive, and the technical means and devices used for their implementation, despite their diversity, are ineffective in a number of technical-and-economic indices [1–15]. The latest achievements in the field of magnetism provide solving this problem on a qualitatively new level using a rotating electromagnetic field (Fig. 1).

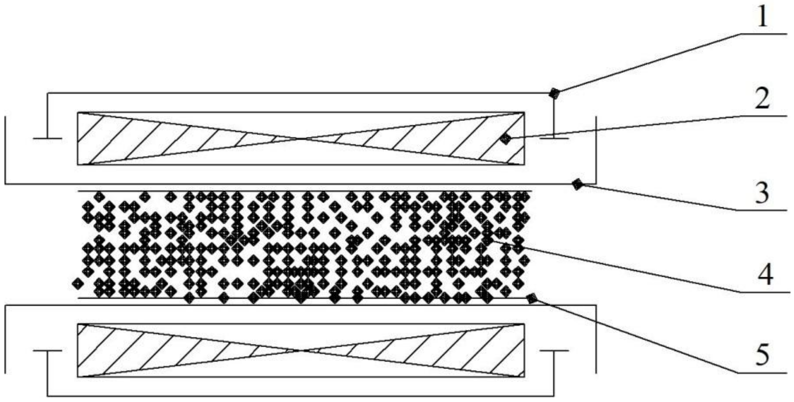

Fig. 1. Sludge processing scheme in a rotating electromagnetic field:
1 — housing; 2 — inductor; 3 — working area; 4 — sludge; 5 — replaceable sleeve (the authors' figure)

The use of a rotating electromagnetic field (REMF) for the processing of grinding sludge makes it possible to exclude the contact interaction of conglomerates with the working chamber walls and the use of metal beaters or other means of destruction and grinding. Thus, the material consumption of technical means is reduced, the efficiency of the processes of destruction of conglomerates and the grinding of metal particles of sludge is increased [16, 17].

A set of theoretical and experimental studies has been carried out to define the features and basic laws of sludge waste processing in devices with a rotating electromagnetic field. The results are presented in this paper.

Materials and Methods. The sludge to be destroyed and crushed is a collection of conglomerates of arbitrary shape, consisting of 80–85 % metal chips, which makes it possible to characterize the conglomerate as a solid with ferromagnetic properties [14].

When conglomerates are found in a rotating electromagnetic field characterized by induction B=Bv$cos\omega t$ and angular velocity ω, they perform a complex movement, bringing the system into a magneto-vibratory state. In this case, a magnetic vibrating layer (MVL) is formed, under which their contact interaction and, as a consequence, destruction and grinding occur.

The energy state of conglomerates in the MVL is described by the dependence in the form:

$$E = \frac{1}{2\pi}\frac{\rho_m{}^2}{\omega^2}\left[\frac{B_v^2}{I}+\frac{1}{m}\left(\frac{\partial B_v}{\partial y}\right)^2\right], \text{Дж}, \tag{1}$$

where p_m — magnetic moment, Am^2; $\frac{dB}{dy}$ — field gradient, A/m^2.

Based on equation (1), the energy conditions for the destruction of conglomerates are established:

$$\frac{\rho_m{}^2}{\pi\omega^2}\left[\frac{B_v^2}{I}+\frac{1}{m}\left(\frac{\partial B_v}{\partial y}\right)^2\right] = E_{\text{адг}}, \tag{2}$$

where $E_{\text{адг}}$ — adhesive strength of conglomerates, J.

Conditions for grinding ferromagnetic sludge particles with a degree of $Z_u = D_{\text{Н}}/D_{\text{К}}$ based on (1), has the form:

$$\frac{1}{2\pi}\frac{\rho_m{}^2}{\omega^2}\left[\frac{B_v^2}{I}+\frac{1}{m}\left(\frac{\partial B_v}{\partial y}\right)^2\right]+\frac{1}{2\pi}\frac{\rho_M{}^2}{\omega^2}\left[\frac{B_v^2}{I}+\frac{1}{M}\left(\frac{\partial B_v}{\partial y}\right)^2\right] = \frac{\pi\sigma^2 D_{\text{К}}^3}{12E}\left(Z_u^3-1\right), \tag{3}$$

where σ — ultimate strength at destruction of ferromagnetic particles, Pa; $D_и$ and $D_к$ — initial and final equivalent diameters of the particles, m; E — elastic modulus of the particle, Pa.

To study the influence of the electromagnetic field on the energy state of the MVL, an induction method was used (Fig. 2), based on establishing the connection of the EMF induced in the induction sensor with the magnetic induction of a rotating electromagnetic field.

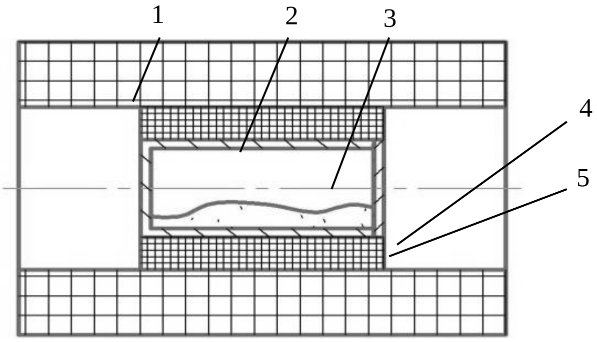

Fig. 2. Scheme for implementation of studies on the MVL state in a rotating electromagnetic field by induction method: 1 — inductor, 2 — inductive coil, 3 — cuvette, 4 — sludge, 5 — cuvette cover (the authors' figure)

An inductance coil is selected as the sensor. To create the coil, a frame with a width (H) of 25 mm and an outer radius (R_2) of 17.5 mm was made. Winding wire — PEL (GOST 2 773-78) with diameters: copper D_1 = 0.15 mm, insulated D = 0.18 mm. The cross-sectional area of the wire was S = 0.01767 mm^2. The measured resistance of the coil was 14.8 ohms. The inductance was 0.82 mH. The total number of turns was 139, the wire length was 15.27 m. The calculated resistance of the coil (1 m — 0.99 ohms) R = 15.27× 0.99 = 15.1 ohms.

The inductive sensor 2 and the cuvette 3 were placed in a cylindrical working area of the device with a rotating electromagnetic field (Fig. 1). The current in the circuit of the inductive sensor was controlled by a multimeter. Under various modes, it was 4.3–11.4 A. First, the induction EMF was measured without sludge waste particles, and then — with the studied samples of sludge waste at the selected parameters of the device with REMF.

Sludge waste conglomerates in a rotating electromagnetic field under the action of a moment tending to rotate them around the center of mass, perform, on the one hand, rotational motion, and on the other, translational motion in the direction of the external rotating electromagnetic field. Thus, the behavior of the magnetic moments of conglomerates under the action of ponderomotive forces can be characterized in the plane of the measuring coil of the XOY induction sensor as vibration-rotational and vibration-translational motion according to the harmonic law in a magnetic field (Fig. 3).

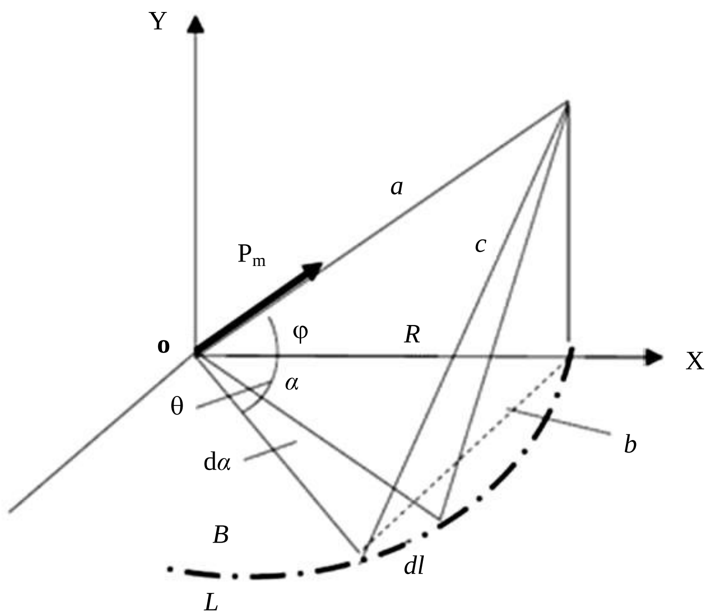

Fig. 3. Orientation of magnetic moment $\overrightarrow{p_m}$ in the induction converter space (the authors' figure)

The induced EMF, in accordance with the law of electromagnetic induction, is equal to:

$$\varepsilon = -\frac{d\psi}{dt}, \tag{4}$$

where $\psi = N\Phi$ — flux linkage; N — turn number of the measuring coil.

We express magnetic flux through the surface bounded by the contour of the coil of the induction converter L with radius *R*, in the following form:

$$\Phi = BS_{\text{к}}, \tag{5}$$

where $S_{\text{к}}$ — coil contour area; $S_{\text{к}} = \pi r^2$; r — middle radius of the coil contour, B — induction of a rotating electromagnetic field. In this case:

$$B = B_0. \tag{6}$$

The expression for calculating EMF of a multiturn induction converter is as follows

$$\varepsilon = \frac{2}{3} N B_0 \pi^2 R^2 f_1. \tag{7}$$

The influence of induction on the nature of the interaction between sludge particles in a rotating electromagnetic field was evaluated through changing the relative EMF signal induced in an inductive sensor, according to the ratio:

$$\frac{\Delta\varepsilon}{\varepsilon_0} = \frac{(\varepsilon - \varepsilon_0)}{\varepsilon_0}, \tag{8}$$

where ε and ε_0 — EMF in the sensor with and without medium, respectively.

Research Results. Figures 4, 5 show the results of an induction study of the effect of a rotating electromagnetic field on the energy state of sludge particles, and Figures 6–8 show the main technological patterns of the process of destruction of conglomerates in devices with a rotating electromagnetic field.

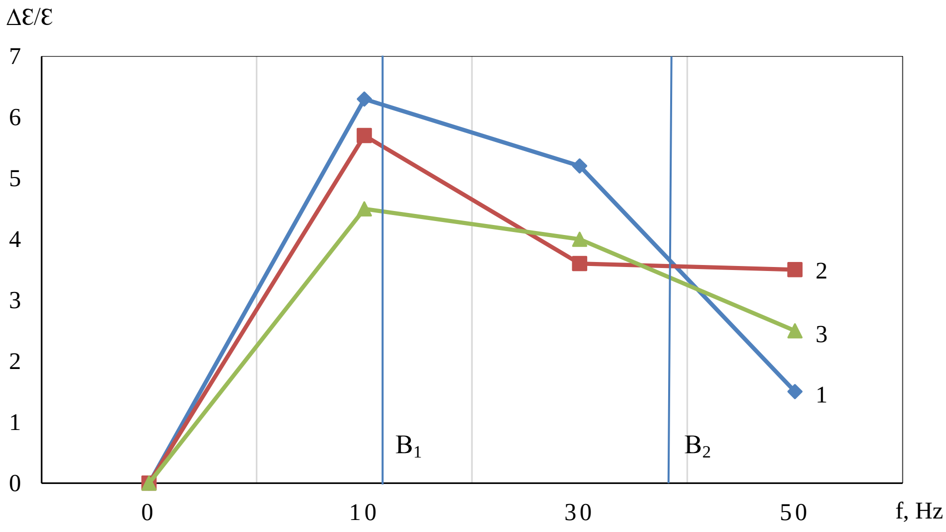

Fig. 4. Experimental dependence of relative signal $\Delta\varepsilon/\varepsilon$ on supply frequency (f), which determines induction of a rotational electromagnetic field at the level of loading of the working area of the device with a ferromagnetic medium: 1 — 0.3 %; 2 — 0.5 %; 3 — 0.75 % (the authors' figure)

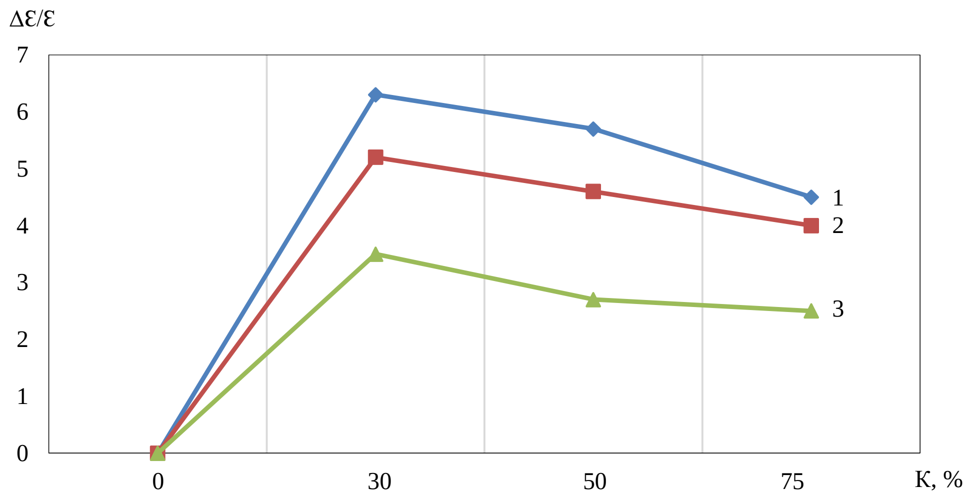

Fig. 5. Experimental dependence of relative signal Δε ⁄ε on the sludge loading factor in the working area of the device with a REMF determining induction of a rotational electromagnetic field: 1 — 10 Hz; 2 — 30 Hz; 3 — 50 Hz (the authors' figure)

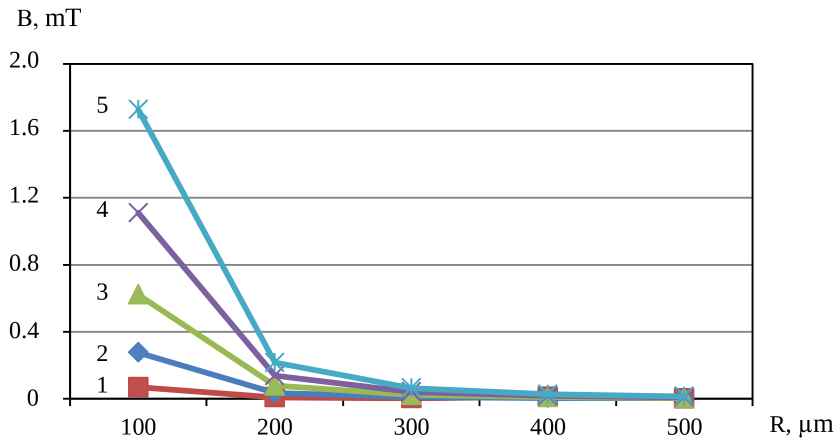

Fig. 6. Effect of the size of sludge conglomerates on the magnetic field induction value required for their destruction at the particle size r in the conglomerate: 1 — 50 µm; 2 — 40 µm; 3 — 30 µm; 4 — 20 µm; 5 — 10 µm (the authors' figure)

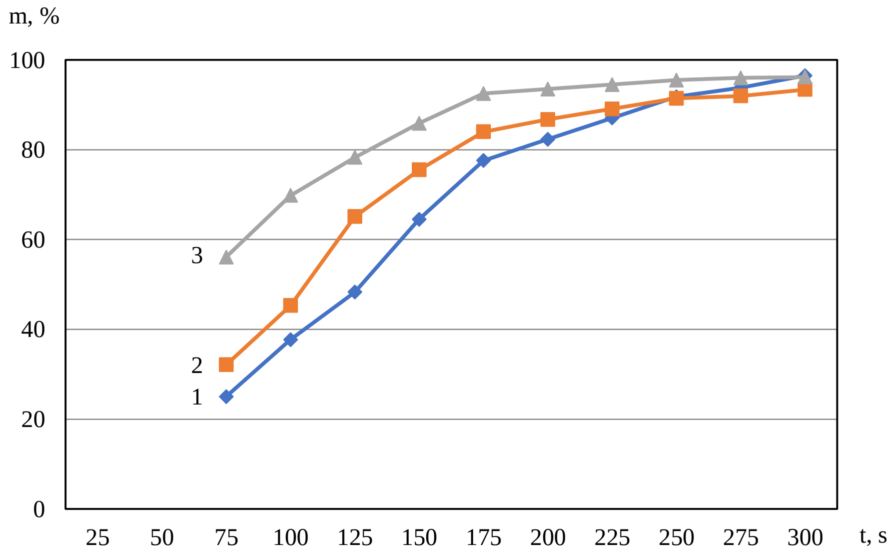

Fig. 7. Dependence of the separated abrasive on time at output current frequencies: 1 — 50 Hz; 2 — 30 Hz; 1 — 10 Hz (the authors' figure)

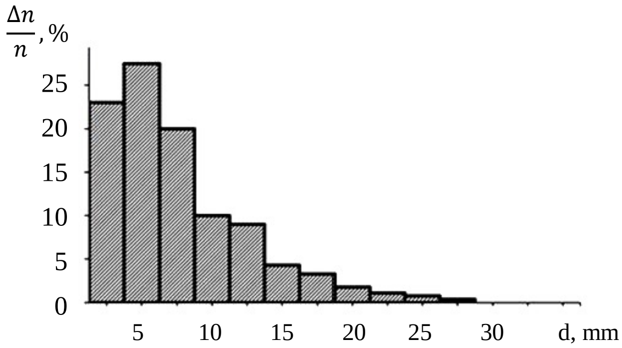

Fig. 8. Histogram of particle size distribution after 5 minutes of exposure to the magnetic vibrating layer (the authors' figure)

Discussion and Conclusions. Experimental studies conducted by the induction method have clearly shown that the dynamic characteristics of sludge waste conglomerates depend on the induction of a rotating field. As shown in Figure 4, a change in the field induction to value B_1 contributes to an increase in the energy activity of conglomerates in the magnetic vibrating layer. The processes that provide the technological effect of destruction of sludge waste conglomerates with a size of 10 μm proceed more intensively. A further increase in induction from B_1 to B_2 causes a decrease in the energy activity of conglomerates in the MVL, as shown by the induction method. This is due to the fact that with increasing induction, the degree of chaotization of conglomerates decreases, and chain complexes begin to form from them, creating so-called “magnetic strings”, whose vibration speed and amplitude are less than the vibration speed and amplitude of individual conglomerates. At $B > B_2$, “magnetic strings”, due to the growth of magnetostatic interaction, assume a stable character, significantly reducing the effect of magnetic vibration of sludge waste conglomerates, practically reducing it to zero at a high level of induction of a rotating electromagnetic field.

The study results presented in Figures 6–8 allowed us to draw the following conclusions:

– with an increase in the size of the sludge conglomerates, with the same size of the ferromagnetic particles entering it, the magnetic field induction value required for their destruction decreases, which is consistent with the model representations of the energy evaluation of the magnetic vibrating layer;

– with a decrease in the particle sizes of conglomerates, the field induction required for the destruction of conglomerate bonds increases; curve analysis suggests that for conglomerates consisting of particles with a radius of less than 3 μm, the induction exceeds 2–4 mT;

– the proposed model for estimating the energy state is valid for the destruction of less stable conglomerates;

– an increase in the number of particles in the conglomerate reduces the value of the induction that destroys it;

– the degree of destruction of conglomerates and grinding of its ferromagnetic particles depends on the duration of the induction of a rotating electromagnetic field.

References

1. Babichev AP, Vernigorov YM, Frolova NN. Operating Modes of the Device of the High Milling of the Powder $SmCo_5$. Fundamental and Applied Problems of Technics and Technology. 2012;296:64–70.

2. Bukin VI, Igumnov MS, Safonov ValVl, et al. Pererabotka proizvodstvennykh otkhodov i vtorichnykh syr'evykh resursov, soderzhashchikh redkie, blagorodnye i tsvetnye metally. Moscow: Delovaya stolitsa; 2002. P. 224. (In Russ.)

3. Komarov OS, Komarov DO, Urbanovich NI. Pererabotka i ispol'zovanie otkhodov, soderzhashchikh tsvetnye metally. Minsk: BNTU; 2018. 114 p. (In Russ.)

4. Reva VP, Moiseenko DV. High-Speed Powder Produced from Chip Wastes Ground in the Presence of High-Molecular Compounds. Russian Engineering Research. 2013;2:51–56.

5. Biktagirov FK, Shapovalov VA, Burnashev VR, et al. Pererabotka promyshlennykh otkhodov metalloproizvodstva. Electrometallurgy Today. 2013;1:40–44. (In Russ.)

6. Kayak G, Fomenko V, Andreev V. Recycling Technique for Grinding Sludge. FEFU: School of Engineering Bulletin. 2017;30:60–67. https://doi.org/10.5281/zenodo.399007

7. Djakonov OM. Slimes of Metal-Working Production. Part 1. Chemical Composition. Foundry and Metallurgy. 2010;54–55:154–159.

8. Povstyanoy AYu, Rud' VD. Ispol'zovanie otkhodov promyshlennogo proizvodstva dlya izgotovleniya materialov konstruktsionnogo naznacheniya. Sustainable Development: Science and Practice. 2014;1:159–164. (In Russ.)

9. Lebedev VA, Serga GV, Chaava MM. Method of Calculating the Machines Drive with Screw Working Bodies Mounted from Tetrahedral Hollows. In: Proceedings of the 6th International Conference on Industrial Engineering. 2021. P. 557–563. https://doi.org/10.1007/978-3-030-54814-8_64

10. Lebedev VA, Serga GV, Chaava MM, et al. The Study of Fine-Cleaning Treatment for Removal of Burrs in Screw Rotors. IOP Conference Series: Materials Science and Engineering. 2021;1029:012001. https://doi.org/10.1088/1757-899X/1029/1/012001

11. Tamarkin MA, Tishchenko EE, Kazakov DV, et al. Reliability of Centrifugal–Rotational Finishing by Steel Shot. Russian Engineering Research. 2017;37:326–329. https://doi.org/10.3103/S1068798X17040219

12. Motrenko DP, Babichev AP, Babichev UA, et al. Creation of Regular Microreliefs by Multicontact Shock Vibratory Tool. In: Proceeding of 2nd Asia - Pacific Forum on Precision Surface Finishing and Deburring Technology, July, 22‒24, 2002. Seoul, Korea; 2002. P. 246‒249.

13. Vernigorov YM, Leletko KK, Frolova NN. Simulation of Destruction of Ferromagnetic Materials Particles in Magneto-Vibrational Layer. World Science: Proceedings of Articles the International Scientific Conference. Czech Republic, Karlovy Vary – Russia, Moscow, June 29-30, 2017. P. 59–70.

14. Lebedev VA, Vernigorov YM, Shirin AA, et al. Improving the Efficiency of Metal Production Waste Processing in Electromagnetic Field. Materials Science Forum. 2021;1037:759–766. http://dx.doi.org/10.4028/www.scientific.net/MSF.1037.759

15. Kochubey AA, Lebedev VA, Vernigorov YuM, et al. Uprochnenie dlinnomernykh detalei vo vrashchayushchemsya ehlektromagnitnom pole. Rostov-on-Don: DSTU; 2018. 135 p. (In Russ.)

16. Lebedev V, Vernigorov Y, Prokopets G, et al. Quality Improvement of Powder Products by Means of Magneto-Vibrational Destruction of Aggregates. AIP Conference Proceedings. 2019;2188:020007. https://doi.org/10.1063/1.5138381

17. Lebedev VA, Kochubey AA, Kiricheck AV. The Use of the Rotating Electromagnetic Field for Hardening Treatment of Details. IOP Conference Series: Materials Science and Engineering. 2017;177:012126. https://doi.org/10.1088/1757-899X/177/1/012126

Received 10.10.2022.

Revised 03.11.2022.

Accepted 11.11.2022.

About the Authors:

Lebedev, Valeriy A., professor of the Mechanical Engineering Department, Don State Technical University (1, Gagarin sq., Rostov-on-Don, 344003, RF), Cand.Sci. (Eng.), professor, ScopusID, ORCID, va.lebidev@yandex.ru

Schirin, Andrey A., post-graduate student of the Mechanical Engineering Department, Don State Technical University (1, Gagarin sq., Rostov-on-Don, 344003, RF), ScopusID, ORCID, andrey.shirin.94@yandex.ru

Koval, Nikolay S., associate professor of the Tool Engineering and Biomedical Engineering Department, Don State Technical University (1, Gagarin sq., Rostov-on-Don, 344003, RF), Cand.Sci. (Eng.), ResearcherID, ORCID, koval-nc@mail.ru

Vernigorov, Yuri M., professor of the Physics Department, Don State Technical University (1, Gagarin sq., Rostov-on-Don, 344003, RF), Dr.Sci. (Eng.), professor, ORCID, jvernigorov@donstu.ru

Claimed contributorship:

V. A. Lebedev, Yu. M. Vernigorov: basic concept formulation; research objectives and tasks; academic advising; analysis of the research results; the text revision; correction of the conclusions. A. A. Schirin, N. S. Koval: computational analysis; text preparation; formulation of conclusions.

Conflict of interest statement

The authors do not have any conflict of interest.

All authors have read and approved the final manuscript.

MACHINE BUILDING AND MACHINE SCIENCE

UDC 621.865.8(075)
https://doi.org/10.23947/2687-1653-2022-22-4-346-352

Original article

Calculation of Angular Coordinates for the Control System of a Two-Link Industrial Robot Manipulator

Sergey P. Glushko
Kuban State Technological University, 2, Moskovskaya St., Krasnodar, Russian Federation
sputnik_s7@mail.ru

Abstract

Introduction. One of the tasks of two-link manipulators of industrial robots that move the end-effector along complex trajectories (e.g., robot welder) is associated with the need for careful programming of their movement. For these purposes, manual programming methods or training methods are used. These methods are quite labor-intensive, and they require highly qualified service personnel. A possible solution to the problem of programming the manipulator movements is the simulation of motion with the calculation of angular coordinates. This can help simplify the geometric adaptation of the manipulator in the process of debugging the control program. Therefore, this work aimed at calculating coordinates for programming the control system of a two-link manipulator operating in an angular coordinate system and moving the end-effector along a complex trajectory (e.g., when welding car bodies).

Materials and Methods. A two-link robot manipulator designed for cyclically repeating actions in an angular coordinate system was considered. The manipulator consisted of two rotating links: “arm” and “elbow”, which were fixed on the base. The base could rotate, which provided a third degree of freedom. This configuration increased the working area of the manipulator and minimized the area for its placement in production. The movement of the manipulator end-effector could be performed if the kinematics provided its positioning along three Cartesian and three angular coordinates. For software control of robots, including welding robots operating in an angular coordinate system and performing the movement of the end-effector along a complex trajectory, it was required to calculate the angular coordinates of the movement of the end-effector of a two-link articulated manipulator. The robot control system should determine the position of the tool in the angular coordinate system, converting it for user friendliness into x, y and z coordinates of the Cartesian coordinate system.

Results. The relations of angular and Cartesian coordinates have been obtained. They can be used for calculating when programming the control system of a two-link manipulator of an industrial robot and organizing the exchange of information between the user and the control system, as well as for checking the accuracy and debugging the movement of the end-effector of an industrial robot through feedback.

Discussion and Conclusion. The presented results can be used for software control of a welding robot operating in an angular coordinate system and performing a complex trajectory of the end-effector of a two-link articulated manipulator (gripper). A manipulator operating in an angular coordinate system can be used for contact spot welding when moving the end-effector along a complex trajectory using a positioning or contouring control system. These systems control the movement of the end-effector along a given trajectory with the help of technological commands.

Keywords: industrial robot, welding robot, manipulator, structural link, drive, movement, trajectory, program control.

Acknowledgements. The author would like to thank the editorial board of the journal and the reviewer for their critical analysis and assistance in correcting the article.

For citation. S. P. Glushko. Calculation of Angular Coordinates for the Control System of a Two-Link Industrial Robot Manipulator. Advanced Engineering Research, 2022, vol. 22, no. 4, pp. 346–352. https://doi.org/10.23947/2687-1653-2022-22-4-346-352

Introduction. Industrial robots are used for automated control of the spatial orientation of tools and labor objects in various manufacturing processes[1] [1–7]. An industrial robot, as a rule, includes a manipulator having several degrees of mobility, and a drive numerical control device. The manipulator is used to move a gripper or a tool along a given trajectory to specified points in the technological space[2] [1–3].

When developing programs for controlling the movements of a gripper or an industrial robot tool along complex trajectories (e.g., for welding robots), training methods that are complex in organization and technical equipment are used.

To simplify the programming of the control system of a two-link manipulator of an industrial robot that moves the end-effector along a complex trajectory (e.g., when welding car bodies), you can use modeling of its movements with the calculation of angular coordinates. This will simplify the geometric adaptation of the manipulator and the process of developing and debugging its control programs.

The study is aimed at calculating angular coordinates for programming the operation of the control system for a two-link manipulator, which functions in an angular coordinate system and moves the end-effector along a complex trajectory.

Materials and Methods. In practice, four main types of manipulators, which operate in cylindrical, spherical, rectangular or angular coordinate systems, are used.

Figure 1 shows the working zone of the robot manipulator operating in an angular coordinate system. The manipulator consists of two rotating links — "shoulder" and "elbow", which are fixed on the base. The base can rotate, which provides the third degree of freedom. This configuration increases the working zone of the manipulator and minimizes the area for its placement in production.

A manipulator operating in an angular coordinate system can be used for contact spot welding when moving the burner along a complex trajectory. To perform contact spot welding, robots with a positioning or contouring control system are most often used. These systems control the movement of the burner along a given trajectory at a specified orientation at a constant speed using technological commands.

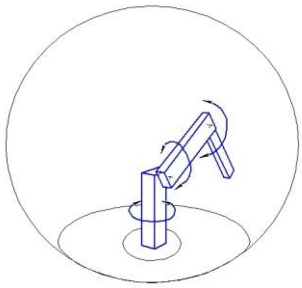

Fig. 1. Working zone of a manipulator operating in an angular coordinate system (the author's figure)

At that, the operation of the moving parts of the manipulator in the welding zone may be complicated by the influence of the heat generated. This problem is partially solved by the use of water cooling of burners with autonomous cooling devices. To completely eliminate this problem, you will need to additionally solve another task. Namely, a thermal problem with the simulation of a thermal process to determine and compensate for thermal expansion caused by heating by electric discharge or electric arc [8].

Research Results. To develop a control program for a robot that operates in an angular coordinate system (Fig. 1), it is required to calculate the angular coordinates of the movement of the end-effector of the manipulator (gripper) [1–4, 6, 7]. Figure 2 shows its scheme, consisting of two rods 1 and 2, which are connected by a

[1] Kozyrev YuG. Promyshlennye roboty: osnovnye tipy i tekhnicheskie kharakteristiki. Moscow: KNORUS; 2015. 560 p. (in Russ.)
[2] Ibid.

ball-and-socket joint 3 and a flat joint 4. The whole structure is installed on the base 5. The manipulator rods have lengths l_1 and l_2. Joint 3 can rotate in the horizontal plane (angle α) and in the vertical plane (angle β). Joint 4 rotates in a vertical plane (angle γ).

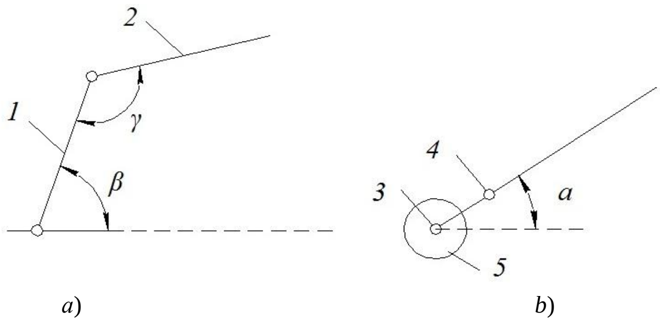

Fig. 2. Design of a two-link articulated manipulator: *a* — main view; *b* — top view (the author's figure)

Figure 3 shows a diagram of a two-link articulated manipulator in the form of a hemisphere with radius $R = l_1 + l_2$ and with a cut-out hemisphere with radius r, which is determined empirically when debugging the manipulator.

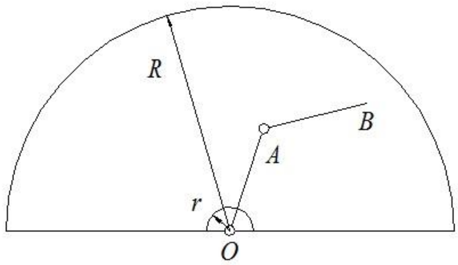

Fig. 3. Diagram of a two-link articulated manipulator (the author's figure)

The manipulator control system should set the position of the tool in the angular coordinate system and, for the convenience of the user, convert it into the parameters of the Cartesian coordinate system.

We take the base of the structure (point O) as the Cartesian coordinate system origin and arrange its axes as shown in Figure 4.

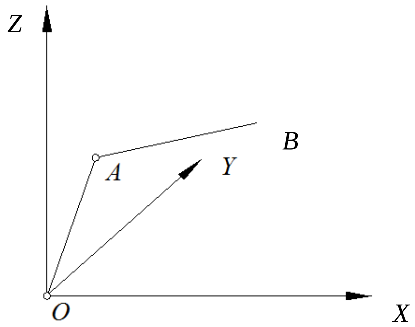

Fig. 4. Rectangular coordinate system centered at point O (the author's figure)

Angle α of the projection of the segment OB on plane XOY is shown in Figure 5.

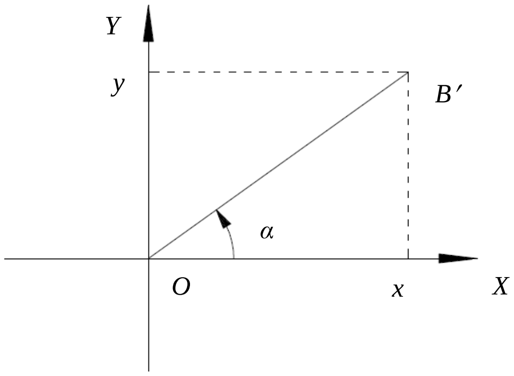

Fig. 5. Determination of the projection angle of segment OB on plane XOY (the author's figure)

Angle α is determined from the formula:

$$\alpha = \pm arccos \frac{x}{\sqrt{x^2 + y^2}},$$

where x and y — coordinates of point B.

The sign "+" should be put if y is greater than or equal to zero, and the sign "–", when y is less than zero.

Angles of plane ZOB' β_1, β_2 and γ between the coordinate axes and levers l_1 and l_2 are shown in Figure 6.

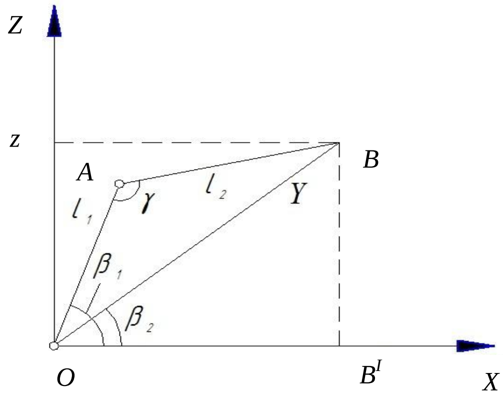

Fig. 6. Determination of angles β_1, β_2 and γ (the author's figure)

We find formulas for determining angles β_1, β_2 and γ using the cosine theorem:

$$\beta_1 = arccos\left[\frac{l_1^2 + z^2 + x^2 + y^2 - l_2^2}{2 \cdot l_1 \cdot \sqrt{z^2 + x^2 + y^2}}\right];$$

$$\beta_2 = arcsin\left[\frac{z}{\sqrt{z^2 + x^2 + y^2}}\right];$$

$$\gamma = arccos\left[\frac{l_1^2 + l_2^2 - z^2 - x^2 - y^2}{2 \cdot l_1 \cdot l_2}\right],$$

where x, y and z — coordinates of point B.

The ratios obtained can be used to calculate angular coordinates when developing control programs for a two-link manipulator of an industrial robot, solving problems of positioning or contouring control using feedback sensors for continuous monitoring and correction of intermediate points of the manipulator trajectory[3] and drive motor control [5, 6].

Dynamic systems of robots, including two-link manipulators operating in an angular coordinate system, are characterized by nonlinearities and are subject to disturbances. Therefore, to eliminate errors when reproducing the movement trajectory of the manipulator end-effector, the proposed calculation of angular coordinates can be supplemented with solutions using the following methods:

[3] Glushko SP, Chastikov AP, Kornienko VG, et al. Software System for Testing and Debugging Control Programs for a Robotic Complex. Certificate of Software State Registration No. 2011611987, 2011. (In Russ,)

– neural network modeling [9];

– simulation study of the robotic arm system for fault detection and evaluation [10];

– equivalent principle of variable sliding mode structure for accurate recovery of arbitrary nonlinear faults [11];

– genetic algorithm for solving the trajectory planning problem [12];

– joint trajectory generation for robotic arms with collision avoidance capability [13].

To control a two-link articulated manipulator with complex trajectories of its movement, it is promising to use the adaptive control with feedback sensors. Its signals are processed, and, based on the results of processing, decisions on further actions are made.

The structure of the proposed control system hardware (Fig. 7) includes drives of the manipulator links, sensors of the angular position of the manipulator links, temperature sensors of the burner mounting unit, a programmable logic controller that performs manipulator control functions.

Industrial robots use electric, hydraulic and pneumatic drives with translational and rotational motion. An electric drive, which is distinguished by a wide range of engine capacities, ease of speed control, and ease of automating control processes, is the most widespread in robotics.

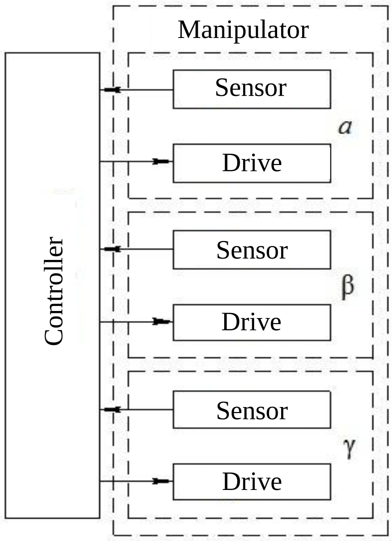

Fig. 7. Structure of hardware of the multilink articulated manipulator control system (the author's figure)

To control angular movements in multilink articulated mechanisms of manipulators with adaptive control systems performing complex trajectories, it is recommended to use angular position sensors — encoders. They provide measuring the movement parameters of the tool or the object being processed, the angles of their rotation, the direction of movement, the rotation speed of the shaft of the electric motor or gearbox, the angular position in relation to the zero mark, the direction of rotation.

Incremental and absolute encoders can be used in adaptive control systems. Incremental encoders are characterized by simplicity, reliability, and relatively low cost. Absolute encoders are more complicated and more expensive, but they provide determining the rotation angles of the axes of the links at any time immediately after turning on the power, and even in the stationary state of the links. Absolute encoders also enable to determine the rotation angles of the axes of the links when disconnecting and then restoring power, and do not require the device to return to its initial position. Moreover, the signals of absolute encoders are not affected by interference and vibration. In recent developments of adaptive control systems, inertial sensors with a number of improvements to compensate for errors in the manipulator movement control system have appeared [14].

Discussion and Conclusions. The calculation of angular coordinates for programming the operation of the control system of a two-link manipulator performing in an angular coordinate system and moving the working body along a complex trajectory was carried out. The relations of angular and Cartesian coordinates obtained in the work can be used to calculate and control angular displacements and to program control systems for two-link manipulators of industrial robots that move end-effectors along complex trajectories.

The calculation of angular coordinates for controlling a two-link manipulator of an industrial robot is presented in this paper as a solution to a geometric positioning problem. It can be used when modeling a similar manipulation device or when building a control system for such a manipulator and organizing the exchange of information between the user and the control system. It is also designed to check the accuracy and debug the movement of the end-effector of an industrial robot using feedback.

References

1. Goritov AN. Production Cycle Interruptible Industrial Robots Programming. Proceedings of TUSUR University. 2009;1(1):61–64.

2. Goritov AN, Kolotaev IV. Operated Mechanical Devices Synthesis with Application of Expert System. Proceedings of TUSUR University. 2009;1(1):72–76.

3. Goritov AN, Alferov SM. Smoothing of Movement Pattern of Robot Manipulator. Bulletin of the TPU. Geo Assets Engineering. 2006;309:176—179.

4. Goritov AN, Korikov AM. Modelirovanie adaptivnykh mekhatronnykh sistem. Tomsk: V-Spektr; 2007. 350 p. (in Russ.)

5. Bosinzon MA. Avtomatizirovannye mekhatronnye moduli lineinykh i vrashchatel'nykh peremeshchenii metalloobrabatyvayushchikh stankov. Privodnaya tekhnika. 2002;1:10–19. (in Russ.)

6. Bukreev VG, Gusev NV. Algorithm of Programming Mechanical Trajectory of Multi-Coordinate Servo Electric Drive. Russian Electromechanics. 2003;3:16–20.

7. Gusev NV. Algoritmicheskoe obespechenie sistem upravleniya sledyashchimi ehlektroprivodami. Russian Electromechanics. 2006;3:57–60. (in Russ.)

8. Glushko SP, Beda KS, Chichua NA. Analytical Solution of the Heat Problem of the Process of Centrifugal Bimetallizing with Electric Arc Heating. Svarochnoe Proizvodstvo. 2009;6:30–35.

9. Uglev VA, Suchinin DI. Automated Education: Tendency for Scientific Approaches Convergence. In: Proc. 2nd International Conference on Applied Social Science Research (ICASSR2 014). 2014. P. 20–23. 10.2991/icassr-14.2014.6

10. Xing-Gang Yan, Edwards, Ch. Nonlinear Robust Fault Reconstruction and Estimation Using Sliding Mode Observers. Automatica. 2007;43:1605-1614. https://doi.org/10.1016/j.automatica.2007.02.008

11. Jing He, Changfan Zhang. Fault Reconstruction Based on Sliding Mode Observer for Nonlinear Systems. Mathematical Problems in Engineering. 2012;2012:451863. https://doi.org/10.1155/2012/451843

12. Abu-Dakka FJ, Valero FJ, Suñer JL, et al. A Direct Approach to Solving Trajectory Planning Problems Using Genetic Algorithms with Dynamics in Complex Environments. Robotica. 2015;33:669-683. 10.1017/S0263574714000393

13. Kivelä T, Mattila J, Puura J, et al. On-Line Path Planning with Collision Avoidance for Coordinate-Controlled Robotic Manipulators. In: Proc. ASME/BATH 2017 Symposium on Fluid Power and Motion Control. 2017. P. 1–10. 10.1115/FPMC2017-4297

14. Titterton, D. H. Strapdown Inertial Navigation Technology, 2nd ed. / D. H. Titterton, J. L. Weston // MPG Books Ltd.: Bodmin, Cornwall, UK; 2004. — 558 p.

Received 19.09.2022.

Revised 14.10.2022.

Accepted 20.10.2022.

About the Author:

Glushko, Sergey P., associate professor of the Department "Engineering of Control Systems, Materials and Technologies in Mechanical Engineering", Kuban State Technological University (2, Moskovskaya St., Krasnodar, 350000, RF), Cand.Sci. (Eng.), associate professor, ORCID, sputnik_s7@mail.ru

Conflict of interest statement

The author does not have any conflict of interest.

The author has read and approved the final manuscript.

UDC 62-529.4
https://doi.org/10.23947/2687-1653-2022-22-4-353-364

Original article

Study on the Relevance of Robotics Technology

Marina V. Yadrovskaya, Ilya V. Gurin ✉
Don State Technical University, 1, Gagarin Sq., Rostov-on-Don, Russian Federation
✉ midwai61rus@gmail.com

Abstract

Introduction. Robotic technologies serve as an important indicator of the technological and economic state of the country, they also affect the lives of individuals. Their development is a promising and urgent task affecting many aspects of the life of modern society. Currently, robotics is going through another stage of development, which has its own characteristics, new directions. The work aims at analyzing the situation and ways of development of this industry in the world and in our country, as well as the attitude of people to the use of robotic systems and their willingness to improve them. The topic under consideration is understudied.

Materials and Methods. In the presented work, the historical aspects of the formation of unique robotic technologies are defined, the ratio of the number of manufacturers and consumers of robotic products in the world is specified, the areas of the robotic technology application are named. The central place in the research is given to the results of an online survey conducted by the authors. Its statistical analysis made it possible to study, using specific data, the factors that influence the spread of robotic systems and robotic technologies and contribute to them.

Results. The survey results, on the one hand, showed a high assessment of the prospects of robotic systems given by the respondents, and confirmed that young people have an interest in robot-making technologies. On the other hand, they allowed us to note the high level of knowledge in the field of robotic technologies among engineering students and the presence of more than elementary knowledge of these technologies among representatives of other special fields. In the opinion of the authors, there are all prerequisites for the further successful development of these technologies.

Discussion and Conclusions. The analysis of the use of robotics in the world and in our country, as well as the results of the survey conducted by the authors, enable to conclude that these technologies are developing and will continue to develop actively, and the interest of current students in this, confirmed by the answers to the questionnaire, will contribute to the wider introduction of robots into the lives of future generations.

Keywords: robotic technology, robotics, industrial robots, robotic systems, research, Internet survey, statistical analysis.

Acknowledgements. The authors would like to thank the staff and students of the Robotics and Mechatronics Department, Don State Technical University, for their assistance in data collection. Appreciation is expressed to anonymous reviewers.

For citation. M. V. Yadrovskaya, I. V. Gurin. Study on the Relevance of Robotics Technology. Advanced Engineering Research, 2022, vol. 22, no. 4, pp. 353–364. https://doi.org/10.23947/2687-1653-2022-22-4-353-364

Introduction. Robots are automatic devices capable of performing monotonous and complex work. They appeared in a person's life, changing over time. Over the past decade, they have transformed into mechanisms capable of effectively interacting with people, understanding their gestures and emotions. This was made possible thanks to the development of robotics. The rapid development of intelligent control and information processing technologies against the background of scientific discoveries in the field of energy, mechanical engineering, microprocessor technology and telecommunication systems determines a new stage in the production and application of robotic systems (RS) [1–3].

Robotics is an industry that widely applies modern information technologies in engineering applications, contributing to the involvement of technical means to obtain and use information to create control systems for complex objects. According to experts, robotic systems that are used in machine, automobile and shipbuilding, aviation, astronautics, medicine, textile industry, etc., contribute to an increase in the level of automation of production, which causes a reduction of 15 to 90 % of costs, depending on the area of application[1].

The history of the phenomenon of robotic systems for lay persons is connected with the thoughts of science fiction writers, for experts — with the development of the first industrial robot manipulators. In fact, the concept of automated mechanisms that can independently perform the required operations appeared earlier and has gone a long way of development. In fact, the concept of automated mechanisms that can independently perform the required operations appeared earlier and has gone a long way of development. The history of the creation of robots is connected with the development of mechanics. In many countries, even B.C., the first automatic devices were designed. The principles of their creation and functioning were formulated in Ancient Greece, which can be considered the birthplace of robotics. At the final stage of the era of the Ancient World, many types of gears and engines were discovered, the basic laws of classical mechanics were formulated. With the beginning of the Renaissance, automatic mechanisms were worked out, spring and pendulum winding mechanisms were developed, which allowed skilled craftsmen to create incredible devices that were able to automatically perform certain actions. At first, these devices were entertaining and aesthetic. The technology of creating such devices has become widespread in Europe and throughout the world, it has developed and expanded the scope of application. Later on, the development of electricity technology became crucial. Electric current has become a power source, a means of receiving, transmitting and processing information. In consequence of the accumulated achievements in the 1920s and 1930s, mechanisms were developed that met the requirements of robotic systems and demonstrated scientific findings. After the end of the Second World War, the use of robotics in industry started, the functionality and control systems of robots introduced into industrial production were continuously improved [1, 4].

Traditionally, industrial and service robotics is distinguished. Today, robotics is experiencing a new round of development. Mobile industrial robotics (IR), collaborative robotics (robotique collaborative), appeared, which allowed humans and robots to solve complex tasks together [5]. Two areas are developing most actively. The first is connected with remote control of robotic systems, which can be carried out by a person or a computer. The second involves the use of mechanical manipulator systems such as “arm” or “leg” for operating objects [1].

Currently, the development of robotics is based on the cooperation of independent experts, scientific organizations and companies [1]. The state plays a leading role in the development of innovative robotic technologies: implementation of national development strategies, grant financing, placement of defense orders[2]. The largest number of innovative robotics companies are located in Canada, Denmark, Finland, Italy, Israel, the Netherlands, Norway, Russia, Spain, Great Britain, Sweden and Switzerland [1].

Let us analyze the current state of production and consumption of robotic systems. The key manufacturers of IR are Northern and Western Europe, the USA, Southeast Asia. The following top manufacturers of robotic devices are: Japanese FANUC, Yaskawa, Kawasaki, Nachi, Denso, Mitsubishi, Epson, Omron, Swedish-Swiss ABB. New companies are also emerging. Specifically, the robotics company Universal Robotics announced itself in 2005 as a small university startup to create a compact robot[2].

[1] Analiticheskii obzor mirovogo rynka robototekhniki. 2019. URL: https://adindex.ru/files2/access/2019_07/273895_sberbank_robotics_review_2019_17.07.2019_m.pdf (accessed: 15.10.2021). (In Russ.)

[2] Analiticheskii obzor mirovogo rynka robototekhniki. 2019. (In Russ.)

In 2018, 74 % of the global IR market was occupied by China, Japan, South Korea, the USA and Germany. Japan is in the first place in the world in the production and export of industrial robots: in 2018, it accounted for 52 % of the world trade in industrial robots. In 2018, the production of robotics in the USA amounted to 40.3 ths. IR, which is 22 % more than it was in 2017. Germany is the fifth country in the world and the first in Europe in terms of the IR market. It is followed by Italy and France [6].

The Asian region is considered the largest producer of IR. It should be noted that in the Republic of Korea, since February 2018, the third program "Development Strategy for the Production of Smart Robots" has been implemented. Its tasks are to popularize collaborative and service robots, increase the innovative potential of robotics, expand the robotics market, increase government support measures, and strengthen public awareness in the field of robotics[3]. In 2018, the production of IR in China and South Korea decreased, while in Japan it increased. Overall, the growth in the Asian region was 1 %.

The second important producer is the European region. It demonstrates a constant increase in the growth rate of IR (from 2017 to 2018, the increase was 14 %).

In 2012, the European Commission initiated the Robolaw project, aimed at solving the problems of terminology, legal and ethical standards related to robots [5]. The results of this work formed the basis of the resolution of the European Parliament of 16.02.2017 No. 2015/2103 (INL) "Norms of Civil Law on Robotics", as well as the initiative to create the European Agency for Robotics and Artificial Intelligence and the introduction of the status of "digital persona" for robots[4].

It should be noted that in Russia, legal conditions for the development of robots within the framework of "regulatory sandboxes" have also been created. Robotics is included in the list of technologies used in the framework of experimental legal regimes in the field of digital innovation due to the decree of the Government of the Russian Federation No. 1750 dated 28.10.2020[5].

In recent years, a record production growth of IR has been observed in North and South America (Fig. 1) [6].

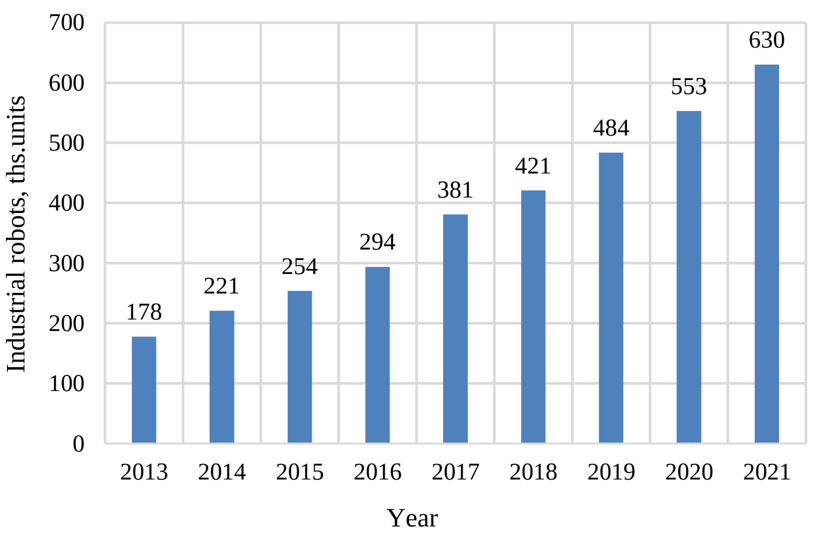

Fig. 1. Growth dynamics of the global market of industrial robots, ths. units. (the authors' figure)

China is the largest consumer of industrial robots with a share of 36 % of the total number of manufactured IR (154 ths.) with a total value of 5.4 billion dollars, which is more than the number of robots operating in Europe and America. In South Korea, the number of IR put into operation has increased by 12 % annually since 2013.

[3] Kim Sang-mo. Policy Directions for S. Korea's Robot Industry. Business Korea. Special Report on Korea's Robot Industry. 2018. URL: http://www.businesskorea.co.kr/news/articleView.html?idxno=24394 (accessed: 20.10.2021).

[4] European Parliament resolution of 16 February 2017 with recommendations to the Commission on Civil Law Rules on Robotics (2015/2103(INL)). URL: https://www.europarl.europa.eu/doceo/document/TA-8-2017-0051_EN.pdf (accessed: 22.10.2021).

[5] Ob utverzhdenii perechnya tekhnologii, primenyaemykh v ramkakh eksperimental'nykh pravovykh rezhimov v sfere tsifrovykh innovatsii: postanovlenie pravitel'stva Rossiiskoi Federatsii ot 28.10.2020 No. 1750. URL: http://static.government.ru/media/files/o8LH12RcKX2aDbzOOyGYp78LPATZqQu7.pdf (accessed: 23.10.2021) (In Russ.)

The chief user of IR in the world with a share of 30 % of the total supply is the automotive industry. The major consumer countries of such robots are China, Japan, Germany, the USA, South Korea [1].

Unfortunately, Russia is not among the top-ranking countries in terms of the use of industrial robots. The introduction of robotics is carried out at a low pace, therefore, in recent years there has not been a high growth in demand for industrial robots observed in the period from 2005 to 2010. Although interest in technologies using industrial robots is growing in our country every year, and the number of integrator companies that are technological conductors between manufacturers and end customers is also increasing [7]. The Government of the Russian Federation, within the framework of the "Strategy for the development of the information technology industry in the Russian Federation for 2014–2020 and for the future until 2025", has included the development of robotics in the list of priority areas of technological development. According to experts, the key task of the state should be support of the R&D associated with the development of robotics, formation of an order, and stimulation of demand for products being created for various industries, including industrial production, the military industry, communications, and energy [8].

Currently, the electronics industry accounts for about a third (32 %) of robot deliveries in the world [1]. The main consumer countries of IR in the electrical/electronic industry are China, South Korea, Japan [6]. Plastics production and chemical industry use 5 % of IR supplies; food and beverage production — 3 %.

An important indicator of the industrial robotization is the number of IR per 10 thousand employees. In the manufacturing industry, this indicator is as follows: in Europe — 114 units, in the North and South America — 99; in Asia and Australia — 91. From 2013 to 2018, the average annual growth rate of the number of robots used in Asia was 16 %, in America — 9 %, in Europe — 6 %. According to this indicator, Singapore has been in first place over many years (831 IR per 10 thousand employees in 2018), South Korea (774 IR) is in second place, and Germany (338 IR) is in third place [6]. The average robotization density in Russia is twenty times lower than in the world. Unlike the West, in our country, it did not take place non-stop due to a number of socioeconomic shocks[6].

Collaborative robots (cobots) are included with the IR used to perform tasks together with employees. They can complement and improve human activity without creating threats to it. They are characterized by security, relatively low price, short payback period, flexibility, multitasking. They are easily reconfigured to perform various scenarios, and they can be created by transformation from industrial robots[7]. These robots are most widely used in medicine, pharmaceuticals, and the automotive industry. Much attention is paid to cobots by the mass media. The market for these robots is small. In 2018, about fourteen thousand units were sold, which is 3.24 % of 422 ths. IR supplied by the customer [6].

Currently, two groups of service robots can be distinguished: professional (to benefit from the provision of services) (PSR) and personal (for use in everyday life) [6]. The market for personal robots is increasing all the time. According to forecasts, 61.1 million units (worth $11.5 billion) can be sold in 2022 [6].

European and American companies are the largest producers of PSR. Americans are leading in the segment of logistics systems, while Europeans are leading in the field of medical robotics. European and Asian companies produce 45 % of agricultural robots [6].

In 2018, the total sales of the PSR amounted to $9.2 billion. 41 % of the PSR sold were logistics systems, 39 % were PSR for inspection and repair work [3]. In 2017, a total of 6,055 robots were sold for agriculture; 300 — for mining; 1,000 — for the nuclear industry, shipbuilding and aircraft construction. It is these industries that are traditionally

[6] Tekhnologicheskie tendentsii razvitiya promyshlennykh robotov. Gosudarstvo. Biznes. Tekhnologii. Obzor "Rossiiskii rynok promyshlennoi robototekhniki. 2021" URL: https://www.tadviser.ru/index.php/Статья:Технологические_тенденции_развития_промышленных_роботов (accessed: 07.10.2021) (In Russ.)

[7] Tekhnologicheskie tendentsii razvitiya promyshlennykh robotov. Gosudarstvo. Biznes. Tekhnologii. Tadviser. 2020. (In Russ.)

strong in Russia. Experts are counting on the development of robotic systems in these industries[8]. In 2018, 106 thousand control and maintenance systems were sold, 5.8 thousand milking robots, 5.1 thousand medical robots, which are the most expensive of service robots. Their average price is 548 thousand dollars, including accessories and services. There is also a constantly growing demand for ancillary work for the elderly in Europe and Asia [6].

The production of powered human exoskeletons capable of maintaining the ergonomics of work and reducing the burden on the employee has increased, it amounted to 7.3 thousand pieces in 2018 [6].

The distinction between industrial and service robotics is gradually eliminating due to the development of industrial use of service robotics, i.e., there is a “convergence of industrial and service robotic technologies” [1]. In the near future, the division of robots into industrial and service robots will lose its meaning, since the same robot will be able to solve tasks both in the workshop and in the service environment[9].

Significant factors in the spread of robots include the high demand for robotic products, a significant increase in investment in the robot-making, an increase in the number of patents for robotic developments, and the increasingly widespread introduction of artificial intelligence (AI) systems [1]. Experts denote the trend in the development of AI robots, bearing in mind the fact that every controlled robot has AI elements [10].

The increase in demand for robots is accompanied by a decrease in their cost. The average price of one industrial robot fell from $45,500 in 2016 to $44,000 in 2017, and the share of “inexpensive” robots grew.

In future, the use of robotic systems will grow, and the development of robots will be carried out in the following areas: improvement of mechanisms, drives, algorithms; development of self-learning control systems using weak artificial intelligence; development of human-computer interfaces, speech recognition, etc. [8–10]. Experts denote the need to pay special attention to cybersecurity when creating and implementing industrial robots. At the same time, cybersecurity should be understood not only as the security of human and robot collaboration, but more broadly — security of the production complex as a whole, setting up the security policy for remote robot control, commercial and industrial secrets, intellectual property protection[11].

According to experts, the manufacturing industry remains the most important robotics market for the coming decade. A special contribution to robotics will be made by the digitalization of production and the development of autonomous vehicles that promote mobility. Logistics, “smart” agriculture, and healthcare, in which surgical and medical telepresence robots will acquire advantage, will also be developed [6].

Materials and Research Methods. To study the attitude to robotic technologies, a questionnaire[12] was posted on social networks, and an online survey was conducted. The study aimed at the application of statistical methods to processing and generalizing the data obtained. The study does not claim to be fundamental, but allows us to form an up-to-date opinion about the attitude to robotic systems in society and about the current state of robotics.

Let us characterize the group of respondents. The number of respondents was 116 people. They included undergraduate and graduate students of the technical university who initiated the survey, people familiar and close to them, university lecturers. Most of the respondents were people not related to robotics. The average age of participants was 24 years. The maximum age was 67 years, the minimum — 12 years (Fig. 2). The majority of those who answered the questions were males (70 %) (Fig. 3). 58.7 % of respondents had or were receiving higher education (Fig. 4). 73.3 % majored in engineering, information technology and technical sciences (Fig. 3).

[8] Analiticheskii obzor mirovogo rynka robototekhniki. 2019. (In Russ.)
[9] Ibid.
[10] Tekhnologicheskie tendentsii razvitiya promyshlennykh robotov. Gosudarstvo. Biznes. Tekhnologii. Tadviser. 2020. (In Russ.)
[11] Ibid.

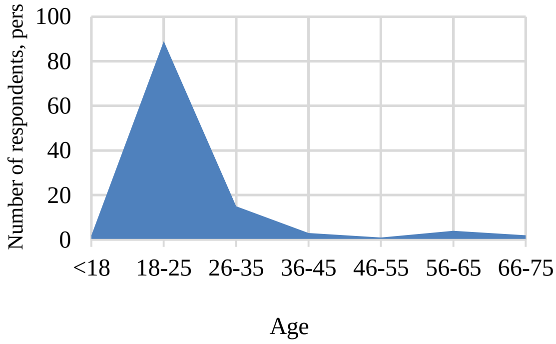

Fig. 2. Number of respondents by age (the authors' figure)

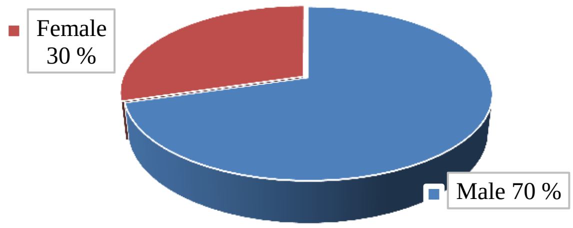

Fig. 3. Gender of respondents, % (the authors' figure)

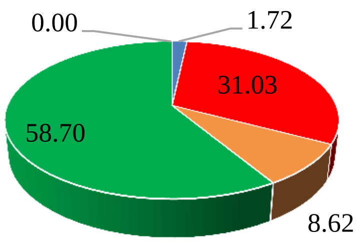

Fig. 4. Number of respondents by education, % (the authors' figure):

- basic general education (grades 5–9);
- general secondary education (grades 10–11);
- secondary vocational education;
- higher education.

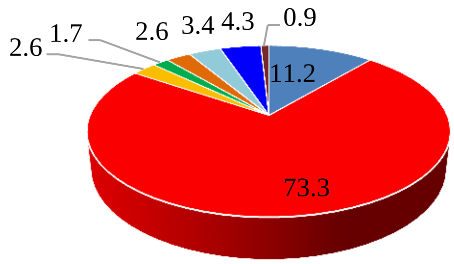

Fig. 5. Number of respondents by special fields, % (the authors' figure):

- mathematical and natural sciences;
- engineering, information technology and technical sciences;
- healthcare and medicine;
- agriculture and agricultural sciences;
- social sciences;
- education and pedagogical sciences.

Respondents identified their hobbies as follows: programming (including microcontrollers), engineering, electronics, robotics, computer games, decorative welding, assembly of radio devices, poker-painting, writing, English, information technology, sports, reading, art, drawing, music lessons, flower-growing. As can be noted, the range of hobbies is very wide. At that, the respondents' main interests are programming, engineering, electronics, robotics, computer games and information technology, which can be proved by the specialty of the majority of respondents (Fig. 6). This fact is important for the objectivity of the results obtained.

96 % of respondents are Russian nationals. The remaining four percent of respondents do not live in Russia (Fig. 7–9).

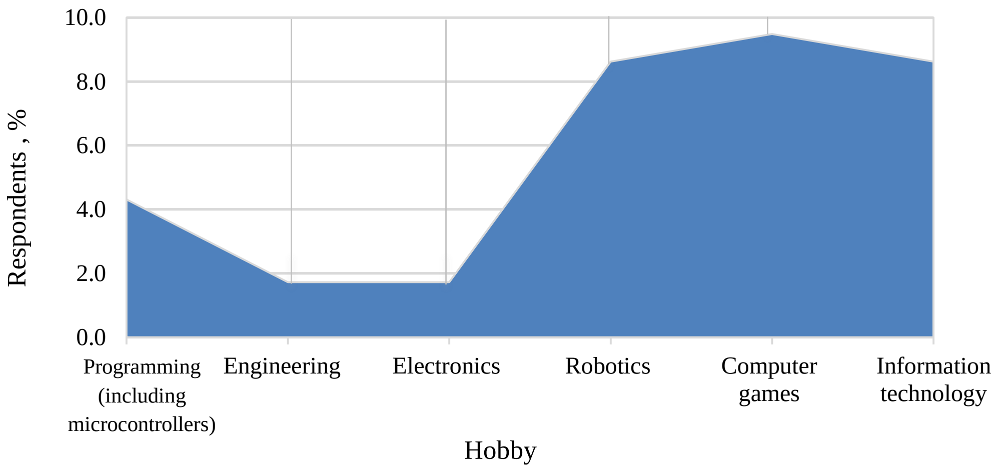

Fig. 6. Number of respondents by hobbies, % (the authors' figure)

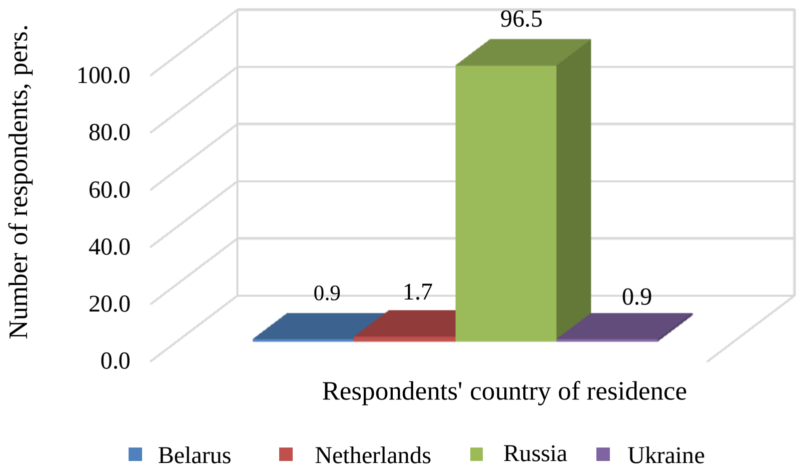

Fig. 7. Number of respondents by place of residence (country), % (the authors' figure)

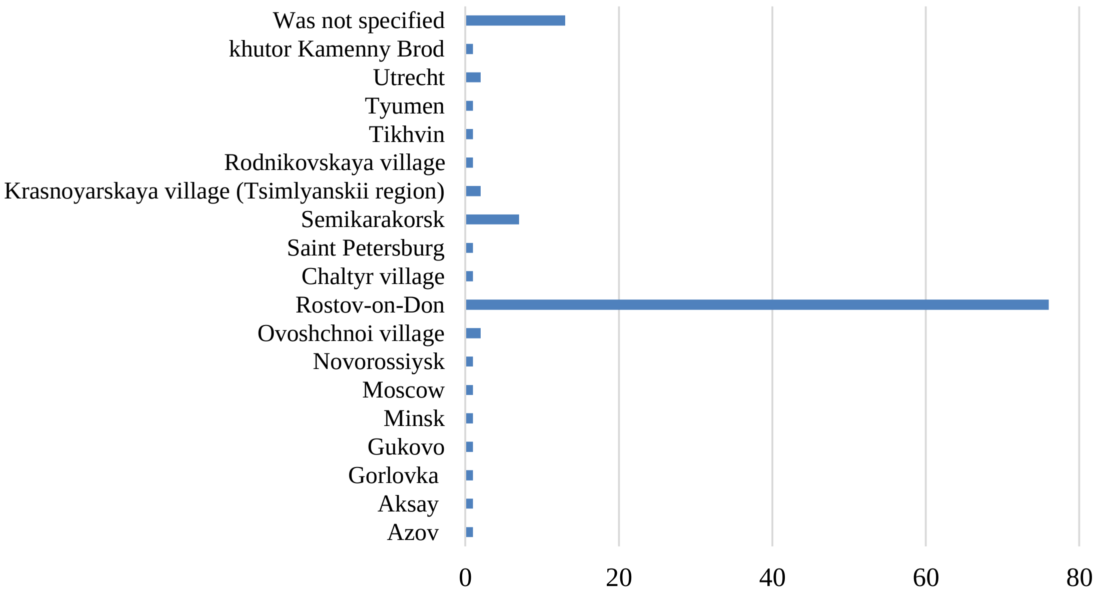

Fig. 8. Number of respondents by place of residence (settlement), pers. (the authors' figure)

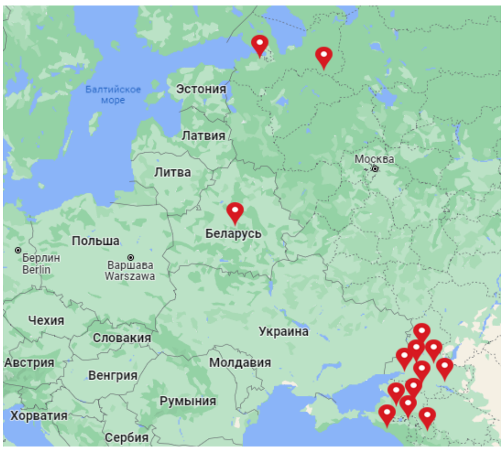

Fig. 9. Map showing respondents' placeof residence

Research Results. Let us look at the key data of the survey. 65 % of those who answered the questionnaire gave the highest rating to the prospects of robotic systems (Fig. 10). It should be noted that the hypothesis was confirmed that the opinion about the prospects of robots does not depend on the specialty of respondents. At the same time, the hypothesis is true that the opinion about the prospects of robots does not affect the definition of the field of the widest application of robotics today.

The hypothesis was also confirmed that the opinion about the most promising field of application of robots does not depend on the specialty of respondents. 48 % of respondents consider the construction sector the most promising, 33 % — industry (Fig. 11).

Residents of other countries took part in the survey. Due to the small number of foreign respondents, the question of the influence of the country of residence on determining the most promising field of application of robots could not affect the results of the survey.

The areas of the most widespread use of robots today, according to respondents, are industry (65 % of respondents think so), construction (19 %), everyday life (9 %) (Fig. 12).

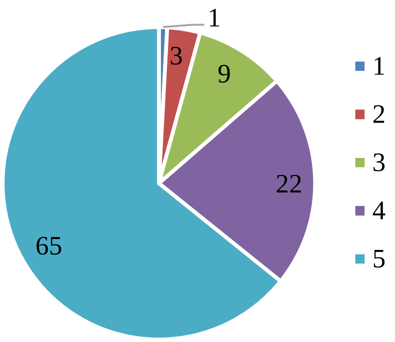

Fig. 10. Respondents' estimates (1–5 points) about the prospects of robots, % (the authors' figure)

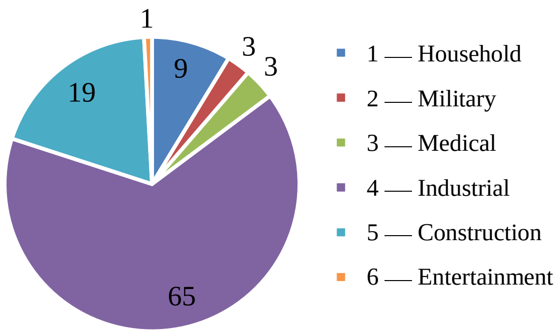

Fig. 11. The most promising areas of application of robots, according to respondents, %) (the authors' figure)

The hypothesis was confirmed that the desire to create robots and the opinion about the prospects of robots were dependent. 40 % of respondents expressed the desire to create robots, the same number considered it possible to create robots, and only 20 % of respondents did not want to do this (Fig. 13). It should be noted that the desire to create robots depended on gender, on the specialty and on the age of the respondents. At the same time, respondents were on the point of realizing the desire to create robots within their specialty.

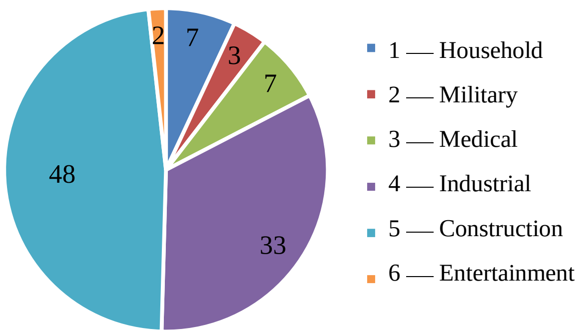

Fig. 12. Areas of the most widespread use of robots today, according to respondents, % (the authors' figure)

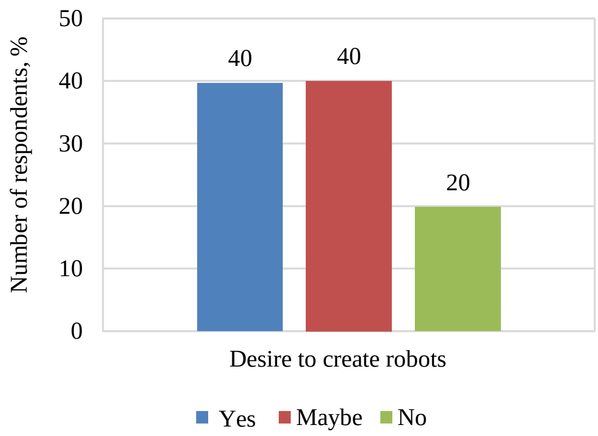

Fig. 13. Number of people willing to create robots, % (the authors' figure)

27 % of respondents gave maximum points to the desire of making robots as a hobby (Fig. 14). The same number of respondents (28 %) gave maximum points to the desire of making robots within the specialty (Fig. 15). The number of respondents who wanted to make robots as part of a hobby and as part of a specialty was in close agreement. It should be noted that the desire to make robots within the specialty depends on the specialty, on the level of knowledge in the field of robotics and on the respondents' belief in the prospects of robots, but does not depend on education.

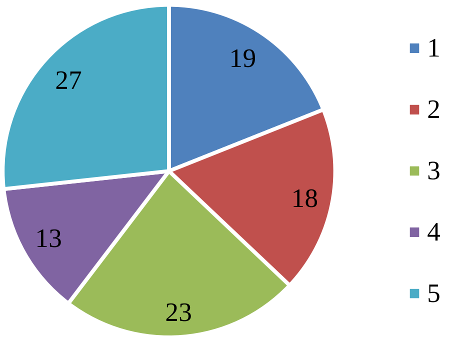

Fig. 14. Number of respondents who wanted to make robots as a hobby (1–5 points), % (the authors' figure)

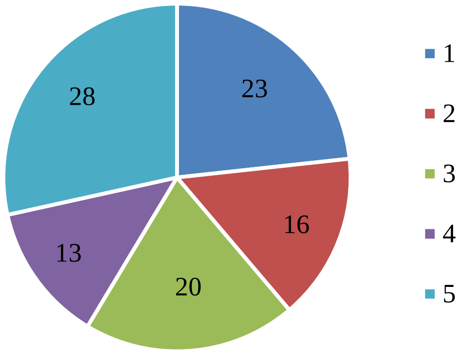

Fig. 15. Number of respondents who wanted to make robots within the specialty (1–5 points), % (the authors' figure)

29 % of respondents gave maximum points (1 point out of 5) to their level of knowledge in the field of robotics, and 5 % — the maximum (Fig. 16). 16 % of respondents gave minimum points (1 point out of 10) to knowledge of how robots are arranged and work, and 10 % — the maximum (Fig. 17).

Note that the number of respondents of all specialties decreases as their level of knowledge in the field of robotics increases (starting from the 3rd level). At the same time, the number of respondents with knowledge level 2 for all specialties turns out to be more than with level 1 (minimum level). This can be explained by the presence of certain knowledge of robotics (not only elementary) among all respondents due to their interest in this area.

No correlation was found between the level of knowledge in the field of robotics and the age of respondents, as well as their place of residence. These conclusions may become a reason for further research in the field of the quality of training of robotics experts, which is undoubtedly a challenge at the moment, taking into account global trends.

The following conclusion, which was made due to the survey, confirmed the already existing hypothesis: the level of knowledge in the field of robotics depends on gender. Indeed, more interest in this topic was shown by males. This is supported by the ratio of girls and boys majoring in the robotics at universities.

The next question concerned the influence of the specialty on the knowledge of how robots are arranged and work. Only 26 % of non-engineering respondents rated themselves for having this knowledge below level 5 (10 levels in total). Among the respondents with engineering specialties, there were respondents with a high level of knowledge of how robots are arranged and work. It is hoped that it is not just the teachers who participated in the survey. It is also important to emphasize that the inquiry revealed a very small number of respondents with engineering specialties with a low level of knowledge of robots (up to level 4). This is less than could be expected. And, conversely, there were more respondents with a high level of knowledge of robots than expected.

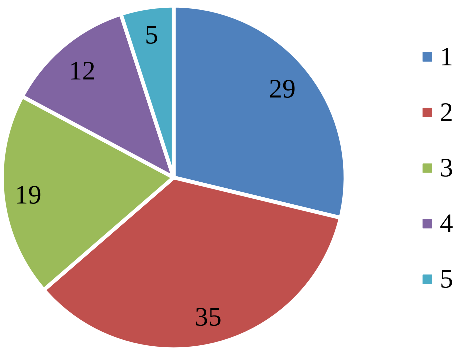

Fig. 16. Number of respondents by level of knowledge (1–5 points) in robotics, % (the authors' figure)

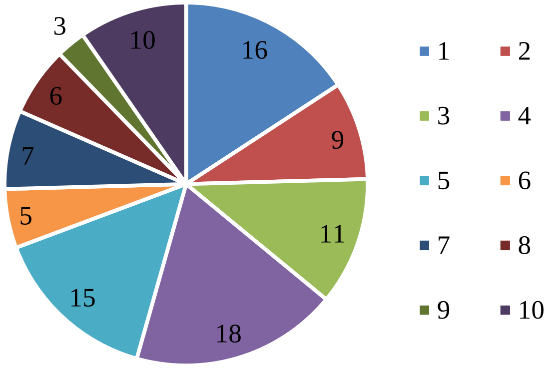

Fig. 17. Number of respondents assessing knowledge (1–5 points) of how robots are arranged and work, % (the authors' figure)

5 % of respondents believe that due to the widespread use of robotic systems, a rise of the machines is possible, 29 % doubt this possibility, and 56 % think it is impossible (Fig. 18). The opinion about the possibility of a rise of the machines depends neither on the knowledge of the device of robots, nor on the age of the respondents.

41 % of respondents are convinced that robots can displace people from jobs, 40 % consider it possible, and only 19 % do not believe in it (Fig. 19). The opinion that robots will displace a person from jobs does not depend on education, specialty, country of residence and on the level of knowledge of respondents in the field of robotics.

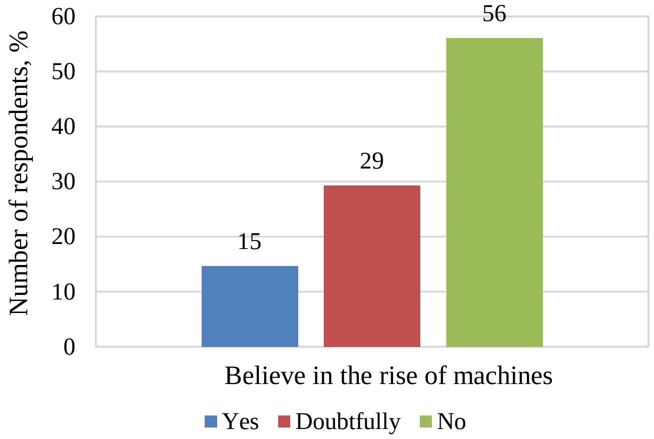

Fig. 18. Number of respondents who believe that the rise of machines is possible, % (the authors' figure)

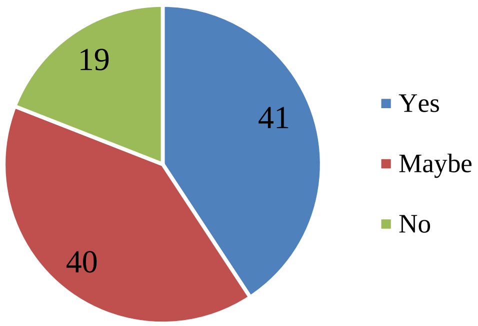

Fig. 19. Number of respondents who believe that robots can displace people from jobs, % (the authors' figure)

41 % — the maximum assessment (Fig. 20). Many people are wary of human-like robots. The gender characteristics of the respondents affected the concerns associated with man-like robots. The presence of fears associated with human-like robots does not depend on the respondent's specialty. The hypothesis that if the respondents have concerns about human-like, then they believe in the possibility of a machine rise has not been confirmed.

The majority of respondents do not have robots, except for a robot vacuum (18 % of respondents have) and some household appliances, which can partly be attributed to robotic systems (Fig. 21).

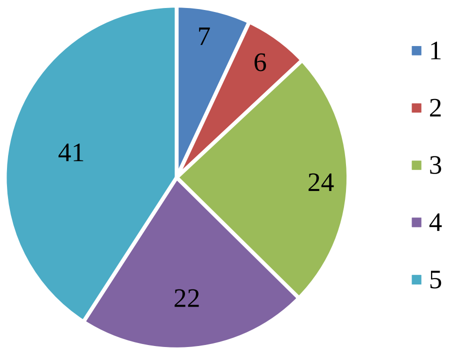

Fig. 20. Number of respondents who are afraid of human-like robots (1–5 points), % (the authors' figure)

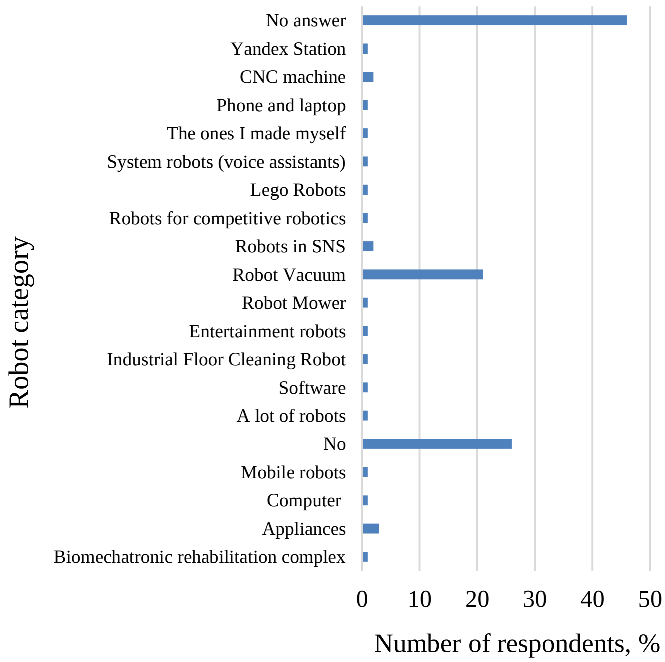

Fig. 21. Number of respondents with robots of various purposes, % (the authors' figure)

Discussion and Conclusions. The analysis of robotic technology, the study of people's opinions about the use of robotic systems allowed us to obtain the following results.

Despite the fact that the development of robotics in our country is currently being carried out at a low pace, interest in robotic technology is growing every year, separate innovative approaches to its implementation are being performed, challenging developments are emerging, and their implementation is taking place in various spheres of life.

The results of the survey have confirmed that young people show an increased interest in creating robotic systems. 80 % of respondents wish to make robots, both as a hobby and as part of their specialty, if they see the prospect of such activity. At the same time, 65 % of respondents gave a high assessment of the prospects for the development of robotic systems. Due to the fact that there were few roboticists among the respondents, the dependence of the respondents' level of knowledge on their specialty was not statistically revealed. But the hypothesis about the influence of the specialty on the knowledge of how robots are arranged and work has been confirmed. Only 26 % of respondents of non-engineering specialties gave themselves low marks for having this knowledge. Among the respondents with engineering specialties, those with a high level of knowledge of how robots are arranged and function are noted. It is hoped that it is not just the teachers who participated in the survey. It is also important to emphasize that among the respondents with engineering specialties, there were fewer people with a low level of knowledge of robots (up to the 4th level of knowledge) than could be expected. And, conversely, there were more respondents with a high level of knowledge of robots than expected.

The low level of knowledge in the robotic technology, which respondents generally noted, on the one hand, is not an obstacle to the further development of this technology due to the high degree of motivation of respondents to study and create robots, as well as due to the availability of experts. On the other hand, it is the increase in the level of knowledge that can contribute to the elimination of wariness about human-like robots, and fears associated with the idea of the possibility of robots displacing a person from his workplace.

To solve social problems related to the spread of robots in Russia, the following measures are being implemented: legal conditions are being created for the development of robots within the framework of “regulatory sandboxes”, robotics is included in the list of technologies used within the framework of experimental legal regimes in the field of digital innovation. All this, along with the efforts of universities that train students majoring in the robotic systems, allows us to hope that such technologies will be further developed, and their introduction into production and everyday life will go faster.

References

1. Keisner A, Raffo J, Wunsch-Vincent S. Robotics: Breakthrough Technologies, Innovation, Intellectual Property. Foresight and STI Governance. 2016;10:7–27. — URL: https://cyberleninka.ru/article/n/robototehnika-proryvnye-tehnologii-innovatsii-intellektualnaya-sobstvennost (accessed: 10.10.2021).

2. Lektorskiy VA, Pruzhinin BI, Alekseeva IYu, et al. Konvergentsiya biologicheskikh, informatsionnykh, nano- i kognitivnykh tekhnologii: vyzov filosofii. Problems of Philosophy. 2012;12:3–23. (In Russ.)

3. Manko SV, Lokhin VM, Romanov MP. The Concept of Multi-Agent Robotic Systems. Russian Technological Journal. 2015;.3–1:156–165.

4. Kolpakov SG, Myachikov AD. Klassifikatsiya robotov po ispol'zovaniyu, peredvizheniyu i komponentam. Young Scientist. 2017;137:241–244. URL: https://moluch.ru/archive/137/36438/ (accessed: 10.10.2022). (In Russ.)

5. Palmerini E, Bertolini A, Battaglia F, et al. RoboLaw: Towards a European Framework for Robotics Regulation. Robotics and Autonomous Systems. 2016;86:78–85 URL: https://www.researchgate.net/publication/308131616_RoboLaw_Towards_a_European_framework_for_robotics_regulation (accessed: 10.10.2021). 10.1016/j.robot.2016.08.026

6. Zhilina IYu. Mirovoi rynok robototekhniki: sostoyanie i perspektivy. Sotsial'nye i gumanitarnye nauki: Otechestvennaya i zarubezhnaya literature. Seriya 2: Ekonomika. 2020;1:118–126. URL: https://cyberleninka.ru/article/n/mirovoy-rynok-robototehniki-sostoyanie-i-perspektiv (accessed: 14.10.2021). (In Russ.)

7. Sinyakov DK, Achkasov OR. The Pace of Development of Robotics in Russia. Actual Problems of Aviation and Astronautics. 2016;12: 33–55. URL: https://cyberleninka.ru/article/n/tempy-razvitiya-robototehniki-v-rossii (accessed: 24.10.2021).

8. Paraskevov AV, Levchenko AV. Modern Robotics in Russia: Reality and Future. Scientific Journal of KubSAU. 2014;104:1680–1701. URL: https://cyberleninka.ru/article/n/sovremennaya-robototehnika-v-rossii-realii-i-perspektivy-obzor (accessed: 07.11.2021).

9. Komissina IN. Current State and Future Prospects for Robotics Technology in China. Problems of National Strategy. 2020;58:123–145. URL: https://riss.ru/documents/852/f26f688f72f144138a9f4eb5e28cf729.pdf (accessed: 11.11.2021).

10. Diane Seku AK. Intellectual Robots and Multi-Agent Robotic Systems: Perspectives of Social Integration. Philosophical Problems of IT and Cyberspace. 2016;12:74–83. URL: https://cyberleninka.ru/article/n/intellektualnye-roboty-i-mnogoagentnye-robototehnicheskie-sistemy-perspektivy-sotsialnoy-integratsii (accessed: 25.11.2021).

Received 30.09.2022.
Revised 20.10.2022.
Accepted 28.10.2022.

About the Authors:

Yadrovskaya, Marina V., associate professor of the Robotics and Mechatronics Department, Don State Technical University (1, Gagarin Sq., Rostov-on-Don, 344003, RF), Cand.Sci. (Phys.-Math.), associate professor, ORCID, marinayadrovskaia@rambler.ru

Gurin, Ilya V., graduate student of the Robotics and Mechatronics Department, Don State Technical University (1, Gagarin Sq., Rostov-on-Don, 344003, RF), ORCID, GurinIV86@yadex.ru

Claimed contributorship:

M. V. Yadrovskaya: basic concept formulation; research objectives and tasks; computational analysis; analysis of the research results; text preparation; correction of the conclusions. I. V. Gurin: computational analysis; work with literature; text preparation; text preparation.

Conflict of interest statement

The authors declare that they have no competing interests.

All authors have read and approved the final manuscript.

MACHINE BUILDING AND MACHINE SCIENCE

UDC 621.822.17
https://doi.org/10.23947/2687-1653-2022-22-4-365-372

Original article

Investigation of the Wear Resistance of a Journal Bearing with Polymer-Coated Grooved Support Ring

Vladimir V. Vasilenko, Victoria I. Kirishchieva, Murman A. Mukutadze ✉, Valentina E. Shvedova
Rostov State Transport University, 2, Rostovskogo Strelkovogo Polka Narodnogo Opolcheniya Sq., Rostov-on-Don, Russian Federation
✉ murman1963@yandex.ru

Abstract

Introduction. In modern heavy-loaded friction units, metallopolymer coated bearings operating in the boundary friction mode are widely used. Their successful application is provided by the viscoelastic deformation of these coatings under load. To pass from boundary friction to liquid friction, it is required to create a bearing hydrodynamic wedge. Currently, the use of journal bearings with polymer-coated grooved support ring is hindered by the lack of a methodology for their calculation. This work analyzes a model of movement of a micropolar lubricant in the operating clearance of a journal bearing with a nonstandard support profile having a PTFE composite coating with a groove on the bearing surface. The study aims at establishing the dependence of the stable hydrodynamic regime on the width of the groove on the surface of the bearing profile.

Materials and Methods. Tribological tests of journal bearings with a nonstandard bearing profile having a polymer coating with a groove on the surface were carried out on samples in the form of partial bushes (blocks). Using the equation of movement of a lubricant with micropolar rheological properties, as well as the continuity equation, new mathematical models were obtained that took into account the width of the groove, polymer coating, and nonstandard bearing profile.

Results. A significant expansion of the applicability of design models of journal bearings with structural changes has been achieved. Polymer-coated bearings with a groove provided a hydrodynamic lubrication mode. The results obtained allowed us to evaluate the operational characteristics of the bearing: hydrodynamic pressure value, load capacity, and coefficient of friction.

Discussion and Conclusions. The design of polymer coated journal bearing and a groove 3 mm wide on the surface of the liner provided a stable ascent of the shaft on the hydrodynamic wedge, which was validated experimentally. The experiments were carried out for journal bearings with a diameter of 40 mm with a groove 1–8 mm wide, at a sliding speed of 0.3–3 m/s and a load of 4.8–24 MPa.

Keywords: journal bearing, increased wear resistance, antifriction polymer composite coating, groove, hydrodynamic mode, verification, micropolar lubricant, nonstandard bearing profile.

Acknowledgements. The authors would like to thank Vladimir I. Kolesnikov, Head of the laboratory of the Theoretical Mechanics Department, Don State Technical University, Academician of the Russian Academy of Sciences, for his assistance in conducting experimental research.

For citation. V. V. Vasilenko, V. I. Kirishchieva, M. A. Mukutadze, V. E. Shvedova. Investigation of the Wear Resistance of a Journal Bearing with Polymer-Coated Grooved Support Ring. Advanced Engineering Research, 2022, vol. 22, no. 4, pp. 365–372. https://doi.org/10.23947/2687-1653-2022-22-4-365-372

Introduction. The issues of providing the reliability of machines and mechanisms are among the major ones in modern industry. New technologies and calculation methods are being developed and existing ones are being improved to increase the resource of technical devices, their wear resistance, economic and operational characteristics.

It is known that the most common cause of failures of friction units are wear and malfunction, and the proportion of failures reaches 80 %. Investigations conducted in the field of friction units suggest the use of new antifriction coatings, modern varieties of materials, original design features of friction units.

Primarily, during calculations and design, the qualities of friction units are underpinned, while modeling methodologies are constantly being developed and improved [1–5]. The parameters affecting the friction units keep changing in accordance with their working conditions and the materials used to obtain a protective coating on the contact surfaces [6–10]. At the same time, there is a need for new methods for adequate modeling and experimental verification of the models obtained.

It follows from the basic results of [11–15] that the formation of secondary structures of frictional transfer of tribological processes in the system “railway track — rolling stock” during the implementation of metal cladding technologies provides reducing the coefficient of friction and wear, and improving vibration-absorbing properties. It has been found that the transverse deformation of a solid body is reduced by 1.5 % and enables to reduce the wear of wheel sets and rails in indirect sections, as well as to increase the traction power of the locomotive. At that, the longitudinal deformation of the solid increases by 60.6 %.

The research results [16, 17] are devoted to the development of a mathematical model of journal bearings of finite length and dampers with porous structural elements on the surface of the bearing bush. The obtained study results enable to increase the bearing capacity by 20–22 % and reduce the transmission coefficient of the damper by 15–17 %, and the coefficient of friction by 13–15 %.

The paper[1] shows that the use of a low-melting coating on the surface of the bearing bush as an additional lubricant, taking into account its rheological properties and the melt coating having truly viscous rheological properties, increases the operating time of bearings in the hydrodynamic friction mode by 10–12 % and prevents an emergency shortage of lubricant.

In [19–21], computational models were developed that provided the most effective hydrodynamic lubrication mode both in normal and emergency mode during “lubricant starvation”. They were designed to establish a balanced combination of the composition of metal alloys for coatings of movable and fixed contact surfaces of tribo-nodes and the type of lubricant. As a result, it was found that the degree of improvement for the load capacity was 26.2 %, for the coefficient of friction — 12.8 %.

Based on the above, it can be concluded that it is required to develop new design models of bearings, or improve the accuracy of existing ones. A property of the computational models of journal bearings obtained by the authors is the generalization of a whole complex of additional factors previously considered only individually in a single block.

The study aims at establishing the regularities for a stable hydrodynamic regime due to the width of the groove on the bearing profile surface through applying a polymer coating.

Problem Statement. The laminar flow of a micropolar fluid in the journal bearing clearance between a trunnion and a nonstandard bearing profile on which a polymer coating with a groove is located, is studied. In this case, the speed of rotation of the trunnion is equal to Ω, and the speed of the bushing is zero under the conditions of an adiabatic process.

[1] Lagunov EO, Mukutadze MA. The Radial Bearings of Sliding Caused by Fusion. In: Proc. IV Int. Science and Technology Conf. “PROM-ENGINEERING”. Chelyabinsk: South Ural State University; 2018. P. 56–62.

The micropolar lubricant flow is given by the well-known equation in the approximation “for a thin layer” and the continuity equation:

$$\left(2\mu'+\kappa'\right)\left(\frac{\partial^2 v_{\theta_i}}{\partial r'^2}+\frac{1}{r'}\frac{\partial v_{\theta_i}}{\partial r'}\right)=\frac{1}{r'}\frac{dp_i'}{d\theta}-\kappa'\frac{\partial' v_{r_i'}}{\partial r'};$$

$$\gamma'\left(\frac{\partial^2 \upsilon_i'}{\partial r'^2}+\frac{1}{r'}\frac{\partial \upsilon_i'}{\partial r'}\right)=\kappa'\upsilon_i'+\kappa'\frac{\partial v_{\theta_i}}{\partial r'},\qquad \frac{\partial v_{r_i'}'}{\partial r'}+\frac{v_{r_i'}}{r'}+\frac{1}{r'}\frac{\partial v_{\theta_i}}{\partial \theta}=0. \tag{1}$$

In the polar coordinate system (Fig. 1) with a pole in the center of the bushing, the equation of the trunnion contour, the bushing with a noncircular profile of the bearing surface and the bushing with a nonstandard bearing profile, on which the polymer coating is located, is given as:

$$r'=r_0\left(1+H\right);\quad r'=r_1-a'\sin\omega\theta;\quad r'=r_1-\tilde{h}-a'\sin\omega\theta. \tag{2}$$

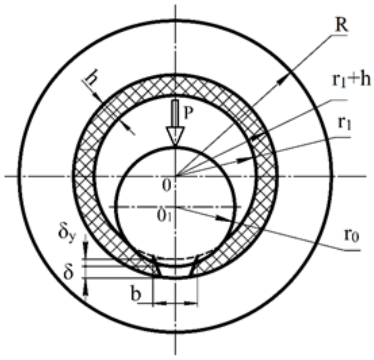

Fig. 1. Journal bearing having a polymer coating with a groove on the bearing surface (the authors' figure)

Generally accepted boundary conditions up to terms $O\left(\varepsilon^2\right)$:

$$v_\theta=0;\quad v_{r'}=0\quad at\quad r'=r_1-a'\sin\omega\theta;\quad \theta_1<\theta<\theta_2;$$

$$v_\theta=0,\quad v_{r'}=0\qquad at\quad r'=r_1-\tilde{h}-a'\sin\omega\theta;\quad 0\le\theta\le\theta_1\quad and\quad \theta_2\le\theta\le 2\pi;$$

$$v_\theta=r_0\Omega;\ v_{r'}'=-\Omega e\sin\theta\quad at\quad r'=r_0+e\cos\theta;$$

$$p(0)=p(\theta)=p_g. \tag{3}$$

To make the solution simpler, let us pass on to dimensionless quantities:

$$r'=r_1-\delta r;\quad \delta=r_1-r_0;\quad r'=\left(r_1-\tilde{h}\right)-\delta r;$$

$$\delta=\left(r_1-\tilde{h}\right)-r_0;\quad v_{\theta_i}=\Omega r_0 v_i;\quad v_{r_i'}=\Omega\delta u;$$

$$p'=p^*p;\quad p^*=\frac{(2\mu+\kappa)\Omega r_0^2}{2\delta^2};\quad \upsilon'=\upsilon;\quad \mu'=\mu;\quad \kappa'=\kappa;\quad \gamma'=\gamma;$$

$$N^2=\frac{\kappa}{2\mu+\kappa};\quad N_1=\frac{2\mu l^2}{\delta^2\kappa};\quad l^2=\frac{\gamma}{4\mu}. \tag{4}$$

Taking into account (4), equations (1) and (3) are transformed into a system of dimensionless equations with the corresponding boundary conditions, but the condition of constant lubricant consumption should be considered:

$$\frac{\partial^2 u_i}{\partial r^2}+N^2\frac{\partial \upsilon_i}{\partial r}=e^{-\alpha p}\frac{dp_i}{d\theta};\qquad \frac{\partial^2\upsilon_i}{\partial r^2}=\frac{\upsilon_i}{N_1}+\frac{1}{N_1}\frac{du_i}{dr};\qquad \frac{\partial u_i}{\partial\theta}+\frac{\partial v_i}{\partial r}=0; \tag{5}$$

$$v=1;\quad u=-\eta\sin\theta;\quad \upsilon=0\ \ at\ \ r=1-\eta\cos\theta;$$

$$v=0;\quad u=0;\quad \upsilon=0\ \ at\ \ r=\eta_1\sin\omega\theta;\quad \theta_1\le\theta\le\theta_2;$$

$$v=v^*(\theta);\quad u=u^*(\theta);\quad \upsilon=0\ \ at\quad r=\eta_2+\eta_1\sin\omega\theta;\quad 0\le\theta\le\theta_1\ \ \text{и}\ \ \theta_2\le\theta\le 2\pi;$$

$$p(0)=p(\theta_1)=p(\theta_2)=p(2\pi)=\frac{p_g}{p^*}, \tag{6}$$

where $\eta=\dfrac{e}{\delta}$; $\eta_1=\dfrac{a'}{\delta}$; $\eta_2=\dfrac{\tilde{h}}{\delta}$.

The solution to problem (5), taking into account boundary conditions (6), is sought by the well-known method [20, 21] in the form of:

$$v_i=\frac{\partial\psi_i}{\partial r}+V_i(r,\theta);\quad u_i=-\frac{\partial\psi_i}{\partial\theta}+U_i(r,\theta);$$
$$\psi_i(r,\theta)=\tilde{\psi}(\xi_i);\quad \xi_2=\frac{r}{h(\theta)}\ \text{at}\ \theta_1\le\theta\le\theta_2;$$
$$V_i(r,\theta)=\tilde{v}_i(\xi_i);\quad U_i(r,\theta)=-\tilde{u}_i(\xi_i)\cdot h'(\theta);$$
$$\xi_{1,3}=\frac{r-\eta_2}{h(\theta)-\eta_2}\ \text{at}\ 0\le\theta\le\theta_1\ \text{и}\ \theta_2\le\theta\le 2\pi, \tag{7}$$

where $h(\theta)=1-\eta\cos\theta-\eta_1\sin\omega\theta$.

For hydrodynamic pressure and velocity field, we obtain the following analytical expressions:

$$\tilde{\psi}_i'(\xi_i)=a_1\frac{\xi_i}{2}(\xi_1-1),\quad \tilde{u}_i(\xi_i)=b_1\frac{\xi_i^2}{2}-\frac{N^2}{2N_1}\left(\frac{\xi_1^3}{3}-\frac{\xi_1^2}{2}\right)-\left(\frac{N^2}{12N_1}+\frac{b_1}{2}+1\right)\xi_1;$$

$$p_1=\frac{p_g}{p^*}+6\left(1+\alpha\frac{p_g}{p^*}-\frac{\alpha^2}{2}\left(\frac{p_g}{p^*}\right)^2\right)\left(-\tilde{\eta}\sin\theta+\frac{\tilde{\eta}_1}{\omega}(\cos\omega\theta-1)+\frac{\tilde{\eta}_1\theta}{2\pi\omega}(\cos 2\pi\omega-1)\right);$$

$$\tilde{\psi}_2'(\xi_2)=a_2\frac{\xi_2}{2}(\xi_2-1),\quad \tilde{u}_2(\xi_2)=b_2\frac{\xi_2^2}{2}-\frac{N^2}{2N_1}\left(\frac{\xi_2^3}{3}-\frac{\xi_2^2}{2}\right)-\left(\frac{N^2}{12N_1}+\frac{b_2}{2}+1\right)\xi_2+1;$$

$$p_2=\frac{p_g}{p^*}+6\left(1+\alpha\frac{p_g}{p^*}-\frac{\alpha^2}{2}\left(\frac{p_g}{p^*}\right)^2\right)\left[(\theta-\theta_1)\left(\frac{\theta_1^2}{4\pi^2}-\left(1-\frac{5\theta_1}{2\pi}\right)\left(\frac{\eta_1}{2\pi\omega}(\cos 2\pi\omega-\cos\omega\theta_1)+\right.\right.\right.$$
$$\left.\left.\left.+\frac{\eta}{2\pi}\sin\theta_1\right)\right)+\left(1-\frac{3\theta_1^2}{4\pi^2}\right)\left(\frac{\eta_1}{\omega}(\cos\omega\theta-\cos\omega\theta_1)+\eta(\sin\theta-\sin\theta_1)\right)\right];$$

$$\tilde{\psi}_3'(\xi_3)=a_3\frac{\xi_3}{2}(\xi_3-1),\quad \tilde{u}_3(\xi_3)=b_3\frac{\xi_3^2}{2}-\frac{N^2}{2N_1}\left(\frac{\xi_3^3}{3}-\frac{\xi_3^2}{2}\right)-\left(\frac{N^2}{12N_1}+\frac{b_3}{2}+1\right)\xi_3+1;$$

$$p_3=\frac{p_g}{p^*}+6\left(1+\alpha\frac{p_g}{p^*}-\frac{\alpha^2}{2}\left(\frac{p_g}{p^*}\right)^2\right)\left[(\theta-\theta_2)\left(\frac{\theta_2^2}{4\pi^2}-\left(1-\frac{5\theta_2}{2\pi}\right)\left(\frac{\tilde{\eta}_1}{2\pi\omega}(\cos 2\pi\omega-\cos\omega\theta_2)-\right.\right.\right.$$
$$\left.\left.\left.-\frac{\tilde{\eta}}{2\pi}\sin\theta_2\right)\right)+\left(1-\frac{3\theta_2^2}{4\pi^2}\right)\left(\frac{\tilde{\eta}_1}{\omega}(\cos\omega\theta-\cos\omega\theta_2)+\tilde{\eta}(\sin\theta-\sin\theta_2)\right)\right]. \tag{8}$$

Determining the bearing capacity and friction force, we use the following formulas:

$$R_x=\frac{6(\mu+\kappa)\omega r_0^3}{2\delta^2}\left[\int_0^{\theta_1}p_1\cos\theta d\theta+\int_{\theta_1}^{\theta_2}p_2\cos\theta d\theta+\int_{\theta_2}^{2\pi}p_3\cos\theta d\theta\right].$$

$$R_y=\frac{6(\mu+\kappa)\omega r_0^3}{2\delta^2}\left[\int_0^{\theta_1}p_1\sin\theta d\theta+\int_{\theta_1}^{\theta_2}p_2\sin\theta d\theta+\int_{\theta_2}^{2\pi}p_3\sin\theta d\theta\right].$$

$$L_{\text{тр}}=(\mu+\kappa)\Omega r_0^2\left[\int_0^{\theta_1}\left(\frac{\tilde{\psi}_1''(0)}{(h(0)-\eta_2)^2}+\frac{\tilde{v}_1'(0)}{(h(0)-\eta_2)}\right)d\theta+\int_{\theta_1}^{\theta_2}\left(\frac{\tilde{\psi}_2''(0)}{h^2(0)}+\frac{\tilde{v}_2'(0)}{h(0)}\right)d\theta+\right.$$

$$+\int_{\theta_2}^{2\pi}\left(\frac{\tilde{\psi}_3''(0)}{\left(h(0)-\eta_2\right)^2}+\frac{\tilde{v}_3'(0)}{\left(h(0)-\eta_2\right)}\right)d\theta\Bigg]. \tag{9}$$

Numerical analysis (9) was performed for the following ranges of values: $(\theta_2 - \theta_1) = 5.74–22.92$ (groove width), $d = 40$ mm; $V = 0.3–3$ m/s; $\sigma = 4.8–24$ MPa; $\mu_0 = 0.0707–0.0076$ N·s/m^2 (oil MS-20).

Experimental Procedure. The experimental study consists of:

1) verification of the developed calculation model;

2) a set of experimental investigations of a bearing with a newly developed design of the bearing surface of the bushing.

The experiment was carried out on an upgraded AI 5018 friction machine using samples in the form of partial bushes. The blocks were cut from the annular blank at a central angle equal to 60 °. Polymer coatings and grooves along the tribocoupling axis to the coating depth were applied to their working surfaces. In addition, the blocks had holes for thermocouples.

Research Results. As a result of theoretical research, it has been found that the bearing capacity of a journal bearing with a polymer coating of the bushing surface containing a groove, as well as a profile of the bearing surface adapted to friction conditions, was increased by 8–9 %, and the coefficient of friction was reduced by 7–8 % (Table 1).

Table 1

Results of theoretical study on the surface of the support ring with fluoroplastic-containing composite polymer coating

No.	σ, MPa	Friction ratio				
		1	2	3	4	5
1	4.8	0.00815	0.01982	0.01781	0.01056	0.00363
2	9.6	0.00614	0.01493	0.01342	0.007958	0.0027354
3	14.4	0.00413	0.01005	0.00903	0.005356	0.0018408
4	19.2	0.00212	0.00516	0.00464	0.002754	0.0009462
5	24	0.00011	0.000281	0.000253	0.0001497	0.0000516

As a result of the experimental study, a stable hydrodynamic regime was obtained after two minutes of processing. The load increased five times with the same interval (Table 2).

Table 2

Results of experimental study on the surface of the support ring with fluoroplastic-containing composite polymer coating

No.	Mode		Results of theoretical research		Results of experimental study		Error rate, %	
	σ, MPa	*V*, m/s	Polymer coating	Grooved coating	Polymer coating	Grooved coating		
1	4.8	0.3	0.0160	0.0142	0.0184	0.0159	5–12	6–13
2	9.6	0.3	0.0105	0.0088	0.0119	0.0064		
3	14.4	0.3	0.0085	0.0066	0.0098	0.0078		
4	19.2	0.3	0.00100	0.0076	0.0122	0.0097		
5	24	0.3	0.0140	0.0109	0.0152	0.0123		

The study results validate the effectiveness of the developed theoretical models and prove the advantage of the investigated journal bearings over existing ones by increasing the load capacity and reducing the friction ratio.

Discussion and Conclusions. Theoretical research determined the required cross section of the oil-supporting grooves to enter the hydrodynamic lubrication mode at a given load. Then, after setting the parameters of the grooves, a computational model was developed describing the operation of the journal bearing in the hydrodynamic mode for a micropolar lubricant, taking into account the bearing profile adapted to the friction conditions.

In the studied design, when the shaft rotates in the groove, a circulating movement of the lubricant occurs. The resulting force lifts the shaft, and a hydrodynamic wedge is formed in the resulting gap.

In accordance with the target goal, the general experimental technique is validated both according to classical single-factor and full-factorial designs.

Conclusions:

1. As a result of the study, a significant expansion of the possibilities of applying in practice computational models of a grooved journal bearing with a polymer coating has been achieved. They provide an assessment of operational characteristics, i.e., the magnitude of hydrodynamic pressure, load capacity, and coefficient of friction.

2. The use of the studied journal bearings with a groove width of 3 mm significantly increases their load capacity (by 8–9 %) and reduces the friction ratio (by 7–8 %).

3. The design of a polymer-coated journal bearing with a 3 mm wide groove provides stable ascent of the shaft on a hydrodynamic wedge.

Reference designation

$v_{r_i'}$, v_{θ_i} — components of the velocity vector of the lubricating medium; υ_i' — particle velocity in the micropolar medium; $H = \varepsilon\cos\theta - \frac{1}{2}\varepsilon^2\sin^2\theta + ...$, $\varepsilon = \frac{e}{r_0}$, r_0 — shaft radius; r_1 — bushing radius; $\tilde{h}$ — groove height; e — eccentricity; ε — relative eccentricity; $\eta = \frac{e}{\delta}$ — bearing design parameter with standard bearing profile; $\eta_1 = \frac{a'}{\delta}$ — bearing design parameter with adapted profile; $\eta_2 = \frac{\tilde{h}}{\delta}$ — design parameter characterizing the groove; p_g — pressure at the ends of the interval; θ_1 and θ_2 — the angular coordinates of the groove, respectively; $u^*(\theta)$ and $v^*(\theta)$ — known functions due to the presence of a polymer coating on the surface of the bearing sleeve.

References

1. Polyakov R, Savin L. The Method of Long-Life Calculation for a Friction Couple “Rotor – Hybrid Bearing”. In: Proc. 7th Int. Conf. on Coupled Problems in Science and Engineering, Coupled Problems. Rhodes Island: International Center for Numerical Methods in Engineering; 2017. P. 433–440.

2. Polyakov RN, Savin LA, Vnukov AV. Mathematical Model of the Non-Contacting Finger Seal with Active Management of the Clearance. Fundamental and Applied Problems of Technics and Technology. 2018;327:66–71.

3. Polyakov R, Majorov S, Kudryavcev I, et al. Predictive Analysis of Rotor Machines Fluid-Film Bearings Operability. Vibroengineering PROCEDIA. 2020;30:61–67. http://dx.doi.org/10.21595/vp.2020.21379

4. Negmatov SS, Abed NS, Saidakhmedov RKh, et al. Research of Viscoplastic and Adhesion-Strength Property and Development of Effective Vibration Absorbing Composite Polymeric Materials and Coatings of Mechanical Engineering Purpose. Plasticheskie massy. 2020;7–8:32–36. https://doi.org/10.35164/0554-2901-2020-7-8-32-36

5. Kornaeva EP, Kornaev AV, Kazakov YUN, et al. Application of Artificial Neural Networks to Diagnostics of Fluid-Film Bearing Lubrication. IOP Conference Series: Materials Science and Engineering. 2020;73:012154. http://dx.doi.org/10.1088/1757-899X/734/1/012154

6. Shutin DV, Polyakov RN. Active Hybrid Bearings as Mean for Improving Stability and Diagnostics of Heavy Rotors of Power Generating Machinery. IOP Conference Series: Materials Science and Engineering. 2020;862:032098. 10.1088/1757-899X/862/3/032098

7. Zinoviev VE, Kharlamov PV, Zinoviev NV, et al. Analysis of Factors Affecting the Strength of Fixed Bonds Assembled Using Metal-Polymer Compositions. IOP Conference Series: Materials Science and Engineering. 2020;900:012009. 10.1088/1757-899X/900/1/012009

8. Kharlamov PV. Monitoring Measurements in Elastic-Dissipative Characteristics for Solving Tasks on Studying Tribological Processes in the “Railway – Rolling Stock” System. Vestnik RGUPS. 2021;81:122–129. https://doi.org/10.46973/0201-727X_2021_1_122

9. Glushko SP. Investigation of the Electrospark Coating, Alloying and Strengthening Technology. Advanced Engineering Research. 2021;21:253–259. https://doi.org/10.23947/2687-1653-2021-21-3-253-259

10. Tamarkin MA, Tishchenko EhEh, Verchenko AV, et al. Formation of Surface Layer Quality under Abrasive Treatment of Polymer-Composite Materials. Advanced Engineering Research. 2020;20:235–242. https://doi.org/10.23947/2687-1653-2020-20-3-235-242

11. Kharlamov PV. Application of the Physico-Chemical Approach to Study the Mechanism of Formation of Secondary Frictional Transfer Structures on the Control Surface. Vestnik RGUPS. 2021;83:37–45. https://doi.org/10.46973/0201-727X_2021_3_37

12. Kharlamov PV. Study of Formation of Secondary Structures of Frictional Transfer on Surface of Steel Samples in Implementation of Metal-Plating Technology. Assembling in Mechanical Engineering and Instrument-Making. 2021;12:556–560. https://doi.org/10.36652/0202-3350-2021-22-12-556-560

13. Shapovalov VV, Migal YuF, Ozyabkin AL, et al. Metal-Plating of Friction Surfaces of the Pair "Wheel – Rail". Journal of Friction and Wear. 202;41:464–474. 10.32864/0202-4977-2020-41-4-464-474

14. Shapovalov VV, Shcherbak PN, Bogdanov VM, et al. Improving the Efficiency of the "Wheel – Rail" Friction System. Russian Railway Science Journal. 2019;7:177–182. https://doi.org/10.21780/2223-9731-2019-78-3-177-182

15. Shapovalov VV, Kolesnikov VI, Kharlamov PV, et al. Improving the Efficiency of the Path-Rolling Stock System Based on the Implementation of Anisotropic Frictional Bonds. IOP Conference Series: Materials Science and Engineering. 2020;900:012011. 10.1088/1757-899X/900/1/012011

16. Kolesnikov IV, Mukutadze AM, Avilov VV. Ways of Increasing Wear Resistance and Damping Properties of Radial Bearings with Forced Lubricant Supply: ICIE 2018. In: Proc. 4th Int. Conf. on Industrial Engineering; 2019. P. 1049–1062. 10.1007/978-3-319-95630-5_110

17. Akhverdiev KS, Mukutadze AM, Zadorozhnaya NS, et al. Damper with a Porous Element for Bearing Arrangements. Journal of Friction and Wear. 2016;37:502–509.

18. Akhverdiev KS, Mukutadze MA, Lagunova EO, et al. Hydrodynamic Calculation of the Radial Bearing with Lubricated Melt Fusible Coating in the Presence of Lubricant. Vestnik RGUPS. 2017;2:129–135.

19. Khasyanova DU, Mukutadze MA, Mukutadze AM, et al. Mathematical Model for a Lubricant in a Sliding Bearing with a Fusible Coating in Terms of Viscosity Depending on Pressure under an Incomplete Filling of a Working Gap. Journal of Machinery Manufacture and Reliability. 2021;50:405–411. 10.3103/S1052618821050083

20. Mukutadze MA, Lagunova EO. Mathematical Model of a Lubricant in a Bearing with a Fusible Coating on the Pilot and Irregular Slider Profile. In: Proc. 7th Int. Conf. on Industrial Engineering (ICIE 2021). 2022. P. 834–840. https://doi.org/10.1007/978-3-030-85233-7_97

21. Khasyanova DU, Mukutadze MA. Improvement of Wear Resistance of a Journal Bearing Lubricated with Micropolar Lubricants and a Molten Metallic Coating. Journal of Machinery Manufacture and Reliability. 2022;51:322–328. https://doi.org/10.31857/S0235711922040101

Received 10.10.2022.
Revised 03.11.2022.
Accepted 09.11.2022.

About the Authors:

Vasilenko, Vladimir V., Head of the Training Unit, Deputy Head of the Military Training Center, Lecturer of the Department of Railway Troops, Rostov State Transport University (2, Rostovskogo Strelkovogo Polka Narodnogo Opolchenia sq., Rostov-on-Don, 344038, RF), ORCID, vvv_voen@rgups.ru

Kirishchieva, Victoria I., postgraduate student of the Higher Mathematics Department, Rostov State Transport University (2, Rostovskogo Strelkovogo Polka Narodnogo Opolchenia sq., Rostov-on-Don, 344038, RF), ORCID, Milaya_vika@list.ru

Mukutadze, Murman A., Head of the Higher Mathematics Department, Rostov State Transport University (2, Rostovskogo Strelkovogo Polka Narodnogo Opolchenia sq., Rostov-on-Don, 344038, RF), Dr.Sci. (Eng.), professor, ScopusID, ResearcherID, ORCID, murman1963@yandex.ru

Shvedova, Valentina E., postgraduate student of the Higher Mathematics Department, Rostov State Transport University (2, Rostovskogo Strelkovogo Polka Narodnogo Opolchenia sq., Rostov-on-Don, 344038, RF), ORCID, Shvedovavalya@yandex.ru

Claimed contributorship:

V. V. Vasilenko: basic concept formulation; research objectives and tasks. V. I. Kirishchieva: conducting the experiment; formulation of conclusions. M. A. Mukutadze: academic advising; analysis of the research results; the text revision; correction of the conclusions. V. E. Shvedova: calculation analysis; text preparation.

Conflict of interest statement

The authors do not have any conflict of interest.

All authors have read and approved the final manuscript.

INFORMATION TECHNOLOGY, COMPUTER SCIENCE, AND MANAGEMENT

UDC 004.11.6
https://doi.org/10.23947/2687-1653-2022-22-4-373-383

Original article

Determinants Factors in Predicting Life Expectancy Using Machine Learning

Brou Kouame Amos, Ivan Smirnov
Peoples' Friendship University of Russia (RUDN), 6, Miklikho-Maklaya St., Moscow, Russian Federation
✉ broukouameamos9@gmail.com

Abstract
Introduction. Life expectancy is, by definition, the average number of years a person can expect to live from birth to death. It is therefore the best indicator for assessing the health of human beings, but also a comprehensive index for assessing the level of economic development, education and health systems. From our extensive research, we have found that most existing studies contain qualitative analyses of one or a few factors. There is a lack of quantitative analyses of multiple factors, which leads to a situation where the predominant factor influencing life expectancy cannot be identified with precision. However, with the existence of various conditions and complications witnessed in society today, several factors need to be taken into consideration to predict life expectancy. Therefore, various machine learning models have been developed to predict life expectancy. The aim of this article is to identify the factors that determine life expectancy.

***Materials and Methods*.** Our research uses the Pearson correlation coefficient to assess correlations between indicators, and we use multiple linear regression models, Ridge regression, and Lasso regression to measure the impact of each indicator on life expectancy. For model selection, the Akaike information criterion, the coefficient of variation and the mean square error were used. R^2 and the mean square error were used.

Results. Based on these criteria, multiple linear regression was selected for the development of the life expectancy prediction model, as this model obtained the smallest Akaike information criterion of 6109.07, an adjusted coefficient of 85 % and an RMSE of 3.85.

Conclusion and Discussion. At the end of our study, we concluded that the variables that best explain life expectancy are adult mortality, infant mortality, percentage of expenditure, measles, under-five mortality, polio, total expenditure, diphtheria, HIV/AIDS, GDP, longevity of 1.19 years, resource composition, and schooling.

The results of this analysis can be used by the World Health Organization and the health sectors to improve society.

Keywords: life expectancy, machine learning, machine learning models.

Acknowledgments. This paper has been supported by the RUDN University Strategic Academic Leadership Program.

For citation. Brou Kouame Amos, I. Smirnov. Determinants Factors in Predicting Life Expectancy Using Machine Learning. Advanced Engineering Research, 2022, vol. 22, no. 4, pp. 373–383. https://doi.org/10.23947/2687-1653-2022-22-4-373-383

Introduction

Human life expectancy can be understood as a statistic used in demography to estimate the average age at which people in a given region and at a given time can be expected to live under current conditions [1]. Life expectancy is not only a statistical indicator of human health, but also a means of assessing the degree of economic, educational, health [2] and environmental development. It should be noted that the World Health Organization (WHO) considers life expectancy to be a key, if not the most important, indicator of health, reflecting the instruments of human existence [3–6]. In the majority of the world countries, life expectancy has in fact increased. Global life expectancy increased from 67.2 years in 2005 to 70.8 years in 2015[1]. The United Nations and individual national governments now have the optimization of human life expectancy, health and well-being as their main objective [7–8]. The UN has been a strong promoter of human health by providing sanitary remedies, which greatly improves the urban environment and helps developing countries[2]. In the African region of the World Health Organization, life expectancy is 61.2 years, while in the European region, it is 77.5 years, giving a ratio of 1.3 between the two regions [9]. Analysis of the disparities in life expectancy between developed and developing countries will enable the United Nations to improve its health promotion and humanitarian assistance activities. It will also enable governments of different nations to establish more effective policies to increase life expectancy and improve living standards. States would be able to significantly increase the life expectancy of their population by investing more in the health care system [7]. According to [10], the increase in life expectancy in the United States as a function of per capita income is substantially related to the increase in income level. According to some researchers, the relevant factors affecting life expectancy are mainly environmental, social and economic factors. These vary according to location and involve economic development, medical and health requirements. Existing research has given rise to debates about the factor that determines life expectancy. In [11], the author analysed life expectancy in Tibet, China, and found the main factors determining life expectancy. The author in [12], thought that social economy played an important role in determining life expectancy in the early stages of development. However, it was replaced by diet and lifestyle when economic development reached a certain level. The article [13] considered that the determining factor in the evolution of life expectancy in Eastern Europe was lifestyle.

In the end, several studies have identified numerous factors influencing life expectancy. However, few studies compared economic development with environmental factors to analyse the intensity of their impact on life expectancy. Several studies are trying to find out the determining factor of life expectancy. It must be said that there are several. Epidemiological studies in developed countries reveal large differences in life expectancy that are often highly complex. A current study in the United States suggests that 10 to 38 % of the differences in life expectancy can be explained by work-related stress. Life expectancy depends on many factors such as economic status, regional changes in education, gender disparities, physical and mental illnesses, alcohol consumption, GDP, health care spending, and many other demographic factors. Life expectancy has actually increased during the 20th and 21st centuries in industrialized countries [14–20]. The improvement in life expectancy in Europe is followed by a population growth in the over-50 age group. There were 179 million people aged 50 or over in all EU Member States in 2008, and 195 million in 2014, with women accounting for about 55 % of the total [21–24].

According to some sources, the level of economic development has a significant effect on life expectancy. Indeed, studies have shown that people who are financially well off and those from wealthy families tend to have a higher life expectancy [25, 26]. For some researchers, other economic development variables such as GDP per capita [27, 28], urbanisation rate [29] and level may affect life expectancy to different degrees. Some studies show that environmental

[1] United Nations Statistical Yearbook, 2017 edition. United Nations, New York; 2017.
[2] United Nations Economic and Development website: https://www.un.org/chinese/esa/health.htm (accessed: 9 February, 2021)

factors are determinants of life expectancy [29]. Indeed, according to [29, 30], most environmental factors, such as ecological resilience and environmental sustainability, are positively correlated with life expectancy, while some factors, including biodiversity, are negatively correlated with life expectancy. In [31], current environmental conditions influence the life expectancy of the population at birth, while cumulative changes in circumstances continue to influence the remaining life expectancy of the population at different ages over time. J. O. Anderson in [32] thought that people living in an environment with high levels of particulate pollutants over a long period of time had higher cardiovascular morbidity, and that there was some degree of dose dependence. Other researchers have studied the impact of different environmental variables on life expectancy. A. Wuffle [33] compared the average temperature of all US states. The results showed that the lower the average temperature in November, the higher the life expectancy of the population in those states [34–36].

Therefore, through machine learning, we will determine the factors that influence life expectancy. Machine learning (ML) can be understood as a discipline that lies at the intersection of mathematics, statistics and computer science. Machine learning has played an important role in the development of artificial intelligence (AI). Thus, artificial intelligence, through machine learning, helps companies to prevent problems and increase profits. In the field of health, machine learning is still surprising researchers. It is now the most widely used tool for prediction and forecasting. Machine learning, which represents a cutting-edge technology due to its predictive accuracy in several problems, is widely used to increase life expectancy by reducing the mortality rate [17]. Indeed, given that several elements impact on life expectancy, the multiple regression model is of paramount importance and corresponds to the exploration of the specific relationship and level of impact between several factors and life expectancy.

This paper uses multiple linear regression models and Pearson's correlation coefficient to examine the relationship between several variables on life expectancy and provide more help for future research on both sides. These models are also used as a basis for suggestions to states for improving life expectancy in order to achieve a development of human society.

Materials and Methods

The World Health Organization (WHO) Global Health Observatory (GHO) data repository tracks health status and many other related factors for all countries. The datasets are made available to the public for analysis of health data. Data on life expectancy and health factors for 193 countries were collected on the same WHO website and the corresponding economic data were collected on the UN website. From all categories of health-related factors, only the most representative critical factors were selected. It has been observed that in the last 15 years, the health sector has undergone enormous development, resulting in improved human mortality rates, especially in developing countries, compared to the last 30 years. Therefore, in this project, we considered data from the year 2000 to 2015 for 193 countries for further analysis. The individual data files were merged into a single dataset. Initial visual inspection of the data revealed some missing values. As the datasets were from WHO, we did not find any obvious errors.

Our dataset had missing data, and the missing data were for population, hepatitis B and GDP. Imputation of missing data using the *mice* function in the R package of the same name.

Each variable is associated with an imputation model, conditional on the other variables in the data set: if we have X_k variables, the missing data for the variable X_i will be replaced by the predictions of a model created from the other variables.

The final file is composed of 22 attributes, the target variable "life expectancy" and various other social factors, such as total expenditure on life, population, education and health factors, such as BMI, measles, etc. These data are available on Kaggle [18]. All predictors were then divided into several broad categories: vaccination-related factors, mortality factors, economic factors, and social factors.

Data mining

The objective of this section is to gain a better understanding of the data by extracting information from the data. We mainly want to determine the relationship between the variables.

The correlation matrix, visualized using a heat map (as shown in Figure 1), is one of the best ways to understand the correlation between variables. It is plotted using the R library “Reshape2” and shows us the strength of the linear relationships between the variables. The linear relationship between the outcome and the characteristics can be estimated by a correlation matrix. In multivariate analysis, it plays an important role, as it elaborates the relationship between the different components [19]. Looking at Figure 1, we can see that:

the target variable Life expectancy is strongly correlated (positively or negatively) with:

– Adult mortality (-0.70);

– HIV/AIDS (-0.56);

– Composition of income resources (0.72);

– Schooling (0.75).

There is also a very low correlation between the target variable Life Expectancy and Population (-0.02) or no correlation at all.

The child deaths variable is extremely positively correlated with deaths under five years of age (1.00).

The GDP variable and the percentage of expenditure are positively correlated (0.90).

The Hepatitis B variable is moderately positively correlated with Polio and Diphtheria (0.49) and (0.61).

The variables diphtheria and polio are strongly positively correlated (0.67).

The HIV/AIDS variable is negatively correlated with resource composition (-0.25).

The thinness variable 10 ... 19 years is very strongly positively correlated with the thinness variable 5 ... 9 years (0.94).

The variable Schooling and the income composition of resources are very strongly correlated (0.8).

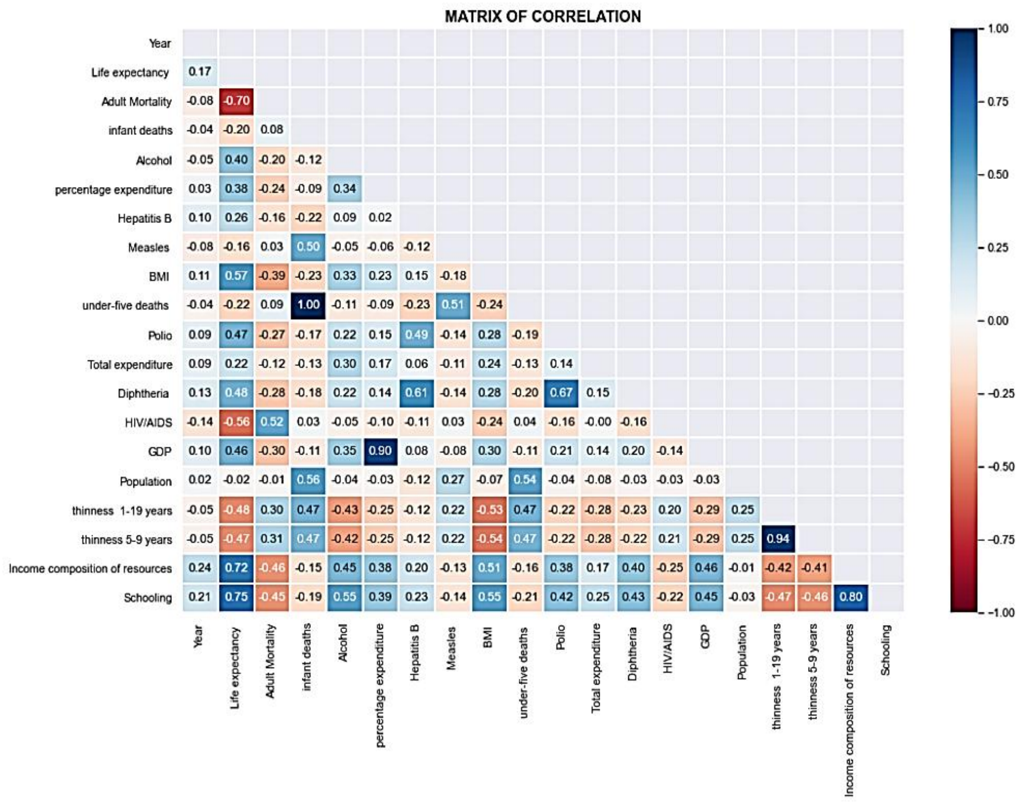

Fig. 1. Visualisation of the correlation matrix by heat map (the authors' figure)

By examining the correlation coefficients in Figure 1, we detect potential predictors of life expectancy. For each numerical variable that is potentially predictive of life expectancy, we will run a simple linear regression between it and the life expectancy variable, display the Pearson correlation coefficient and its P

y = a$x + b$. y is the dependent variable and x is the independent variable. a and b are the model parameters (a is the slope of the fitted line and b is the intercept).

From the result of this exploratory analysis on our data, we concluded that adult mortality, HIV/AIDS, BMI, income composition, and education are the most important factors in predicting life expectancy. This selection was made on the basis of the Pearson correlation coefficient and p-value (as shown in Figures 2, 3, 4, 5, 6).

– The correlation between the variable infant mortality, GDP, alcohol, percentage of expenditure, hepatitis B, measles, under-five deaths, polio, total expenditure, diphtheria, population, age 1–19, age 5–9, and life expectancy is statistically significant as their p-values are less than 0.001, but the linear relationship between these variables is weak with a Pearson correlation coefficient of less than 0.5. Under these conditions, the variables child deaths, GDP, alcohol, percentage of expenditure, hepatitis B, measles, under-five deaths, polio, total expenditure, diphtheria, population, leanness 1–19 years, leanness 5–9 years, cannot be considered as a predictor of life expectancy.

– There is a strong negative correlation between the variables Adult Mortality and Life Expectancy with a Pearson correlation coefficient of –0.7 and statistically significant since the p-value is less than 0.001. In other words, as adult mortality increases, life expectancy decreases. Under these conditions, the adult mortality variable can be considered a predictor of life expectancy.

– There is a negative correlation between the variables HIV/AIDS and life expectancy with a Pearson correlation coefficient of -0.56 and statistically significant since the p-value is less than 0.001. As the number of people affected by HIV/AIDS increases, life expectancy decreases. Under these conditions, the HIV/AIDS variable can be considered a predictor of life expectancy.

– There is a positive correlation between the BMI and life expectancy variables with a Pearson correlation coefficient of 0.56 and statistical significance since the p-value is less than 0.001. Under these conditions, the BMI variable can be considered a predictor of life expectancy.

– There is a strong positive correlation between the variables Income composition of resources and life expectancy with the Pearson correlation coefficient of 0.69 and statistically significant as the p-value is less than 0.001. The graph shows that as the composition of income increases, life expectancy increases. Under these conditions, the variable Income composition of resources can be considered as a predictor of life expectancy.

– There is a strong positive correlation between the variables Education and Life Expectancy with a Pearson correlation coefficient of 0.72 and statistically significant as the p-value is less than 0.001. The graph shows that the higher the education, the higher the life expectancy. Under these conditions, the education variable can be considered a predictor of life expectancy.

Fig. 2. Correlation between life expectancy and HIV/AIDS variable (the authors' figure)

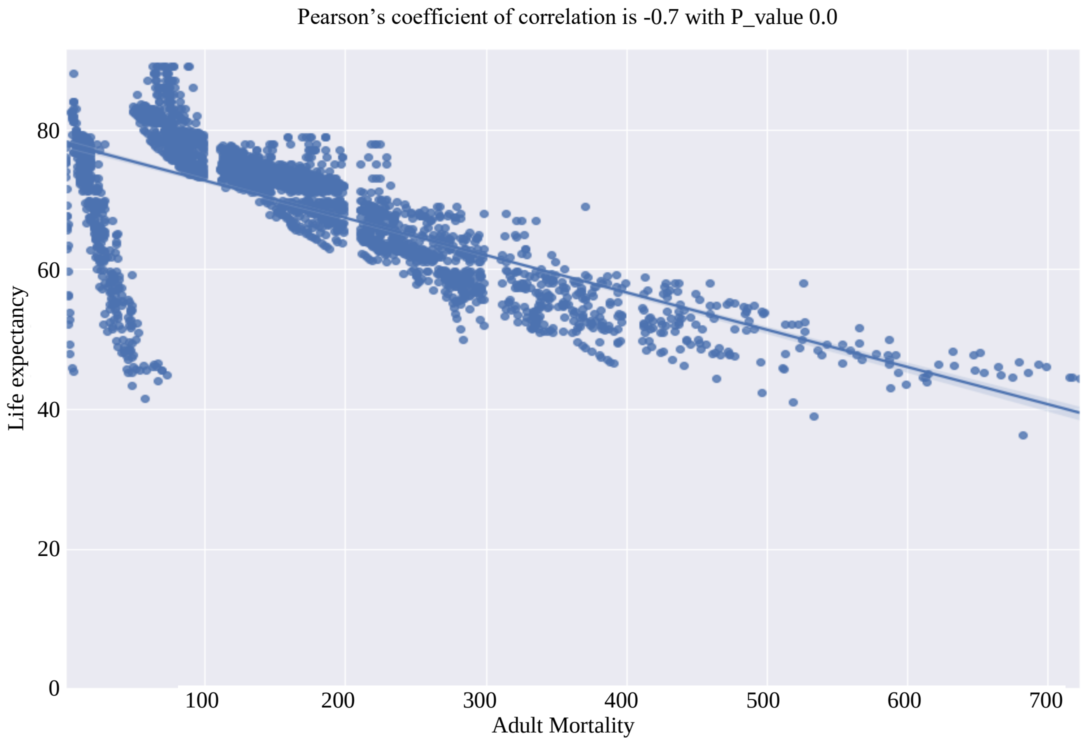

Fig. 3. Correlation between life expectancy and the adult mortality variable (the authors' figure)

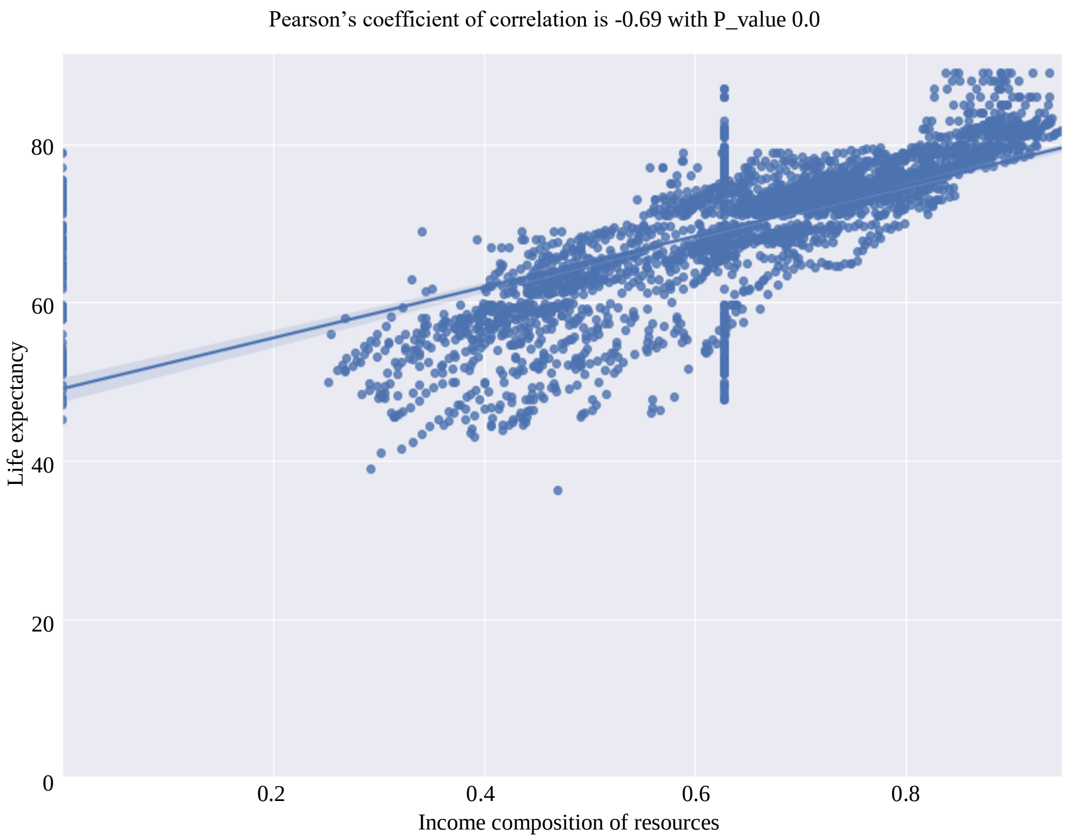

Fig. 4. Correlation between life expectancy and the income composition variable (the authors' figure)

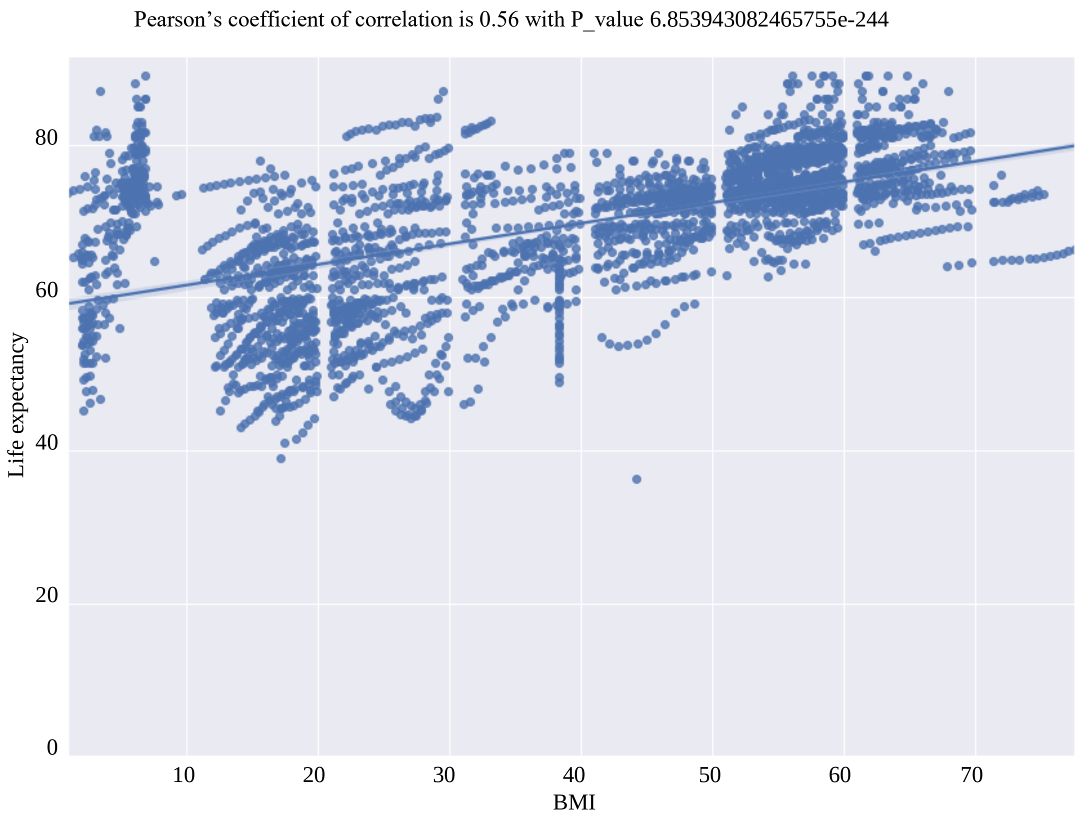

Fig. 5. Correlation between life expectancy and the BMI variable (the authors' figure)

Fig. 6. Correlation between life expectancy and the education variable (the authors' figure)

Based on the results of the Pearson correlation, we detect the variables that have an influence on life expectancy. However, the Pearson correlation is not sufficient to determine the predictors of life expectancy. For this purpose, we will run several regression models to select the one with the smallest AIC, the highest fit, and the smallest mean square error, R^2 and the smallest root mean square error (RMSE).

Methodology

In order to determine the variables that predict life expectancy, different regression models are used, namely, multiple linear regression, rigid regression and lasso regression. We will then examine the criteria for selecting (p – 1) explanatory variables from the k available explanatory variables. These criteria are: Mallows' Cp criterion, the coefficient of determination, R^2 The Bayesian information criterion (BIC), the Akaike information criterion (AIC).

Multiple linear regression

Multiple linear regression is an immediate generalization of simple linear regression. In multiple linear regression, the function F that we want to estimate no longer depends on a single variable, but on several. If we have n pairs of the form (X_i = ($x_{i,1}$, $x_{i,2}$, ..., $x_{i,m}$) ϵR^m, y_i ϵ R^m), with y_i the result obtained for the observation X_i = ($x_{i,1}$, $x_{i,2}$, ..., $x_{i,m}$), then the function we wish to estimate will be of the general form below :

$$F\ (X_i = (x_{i,1}, x_{i,2}, ..., x_{i,m}) = a_1x_{i,1} + a_2x_{i,2} + ...+ a_mx_{i,m} + a_0. \quad (1)$$

The objective is to estimate the vector A = a_1, a_2 , ..., a_m, a_0 so that the function F is as close as possible to y_i .

As with simple linear regression, the least squares method can be used to find the vector A, and the function to be minimized will be defined as follows:

$$E = \sum_{i=1}^{n}[\ y_i - F\ (x_{i,1}, x_{i,2}, ..., x_{i,m})]^2. \quad (2)$$

One of the most difficult aspects of abundant regression algorithms is to determine how to converge to the configurations (a_1, a_2 , ..., a_m, a_0) that yield errors Ɛ = $\hat{y}_i - y_i$ and avoid the trap of over-learning.

The best-known approach to minimizing the error calculation function E while avoiding over-learning is the introduction of the concept of regularization.

There are two regularizations widely used with regression models: the Lasso regularization and the Ridge regularization.

Lasso and Ridge regression

Lasso regression is a regression model in which the selection and regulation of variables take place simultaneously. This method uses a penalty that affects the value of the regression coefficients. With Lasso regularization, the error function to be minimized becomes:

$$E_{Lasso} = \sum_{i=1}^{n}[\ y_i - F\ (x_{i,1}, x_{i,2}, ..., x_{i,m})]^2 + λ\sum_{i=0}^{m} |\ a_i|. \quad (3)$$

The difference between E and E_{Lasso} is that in E_{Lasso} we have added the term λ$\sum_{i=0}^{m} |\ a_i|^2$ to further sanction solutions with values of (a_1, a_2 , ..., a_m, a_0).

Ridge regression is a regularised regression algorithm that performs an L2 regularisation by adding an L2 penalty, which is equal to the square of the magnitude of the coefficients. With Ridge regularization, large values of (a_1, a_2 , ..., a_m, a_0) are more protected, and the error function to be minimized becomes:

$$E_{Ridge} = \sum_{i=1}^{n}[\ y_i - F\ (x_{i,1}, x_{i,2}, ..., x_{i,m})]^2 + λ\sum_{i}^{m} a_i^2. \quad (4)$$

We note that in both the Lasso and Ridge regularization cases, when the value λ is set to 0, then E = E_{Lasso} = E_{Ridge}.

Mallows' Cp criterion

Mallows' Cp is a selection criterion between several regression models. It compares the accuracy and bias of the full model with those of models containing a subset of predictors. Mallows' Cp criterion is defined from the following formula:

$$C_p = \frac{SC_{res}}{\hat{\delta}^2} - (n - 2p). \quad (5)$$

But the problem is that we can no longer estimate δ^2 by $s^2 = \frac{SC_{res}}{n-p}$ because C_p would always be equal to p and then it would no longer be interesting [9]. So, in practice, we estimate δ^2 by the s^2 of the model that involves all k explanatory variables of the available model, then we choose among the models the one for which Mallows' Cp criterion is closest to p.

The coefficient of determination R^2

The website R^2 is the simplest to use. However, with the introduction of new variables, it increases monotonically even if they are weakly correlated with the explained variable. It is therefore advisable to turn to the use of other criteria such as the adjusted R^2adjusted criterion, Mallows' Cp, the AIC and AICc criteria, the BIC criterion.

The adjusted coefficient of determination R^2 is the evolved version of the coefficient of determination R^2.

The adjusted R^2 determines the amount of variance of the dependent variable, which can be explained by the independent variable. On the basis of the fitted value R^2 value, one can judge whether the data in the regression equation are appropriate. The higher the R^2 the higher the fitted value, the better the regression equation because it implies that the independent variable is chosen to determine the dependent variable.

The Bayesian information criterion BIC

The Bayesian Information Criterion (BIC) is derived from the Akaike Information Criterion (AIC) and is defined by : BIC = -2 log (L) + k log (n). It is more parsimonious than the AIC criterion because it penalises the number of variables present in the model more. According to [9], the AIC was introduced to retain the variables relevant to the forecast, whereas the BIC criterion aims at selecting the statistically significant variables in the model.

The Akaike Information Criterion (AIC)

The Akaike Information Criterion (AIC) is a mathematical method that is applied to models estimated by a maximum likelihood method to assess how well a model fits the data from which it was generated. AIC is applied to analysis of variance, multiple linear regression, logistic regression and Poisson regression. The AIC criterion is defined by :

$$AIC = 2K - 2Log\,(L), \tag{6}$$

where L is the maximised likelihood and k is the number of model parameters. With this criterion, the deviance of the model -2 log (L) is penalised by two times the number of parameters.

Therefore, the AIC represents a compromise between bias, which decreases with the number of parameters, and parsimony, the desire to describe the data with as few parameters as possible.

The rigour would dictate that all models compared should derive from the same 'complete' model included in the list of models compared.

The best model is the one with the lowest AIC. When the number of parameters k is large compared to the number of observations n, i.e., if N/k < 40, it is recommended to use the corrected AIC. The corrected Akaike information criterion, AICc, is defined by:

$$AICc = AIC + \frac{2K(K+1)}{n-K-1}. \tag{7}$$

Results

Our analysis has shown that life expectancy increases over the years, and that it is on average higher in developed countries than in developing countries.

This study has also led us to the conclusion that the model chosen for the selection of life expectancy predictors is multiple linear regression (Table 1), as this model obtained the lowest Akaike information criterion of 6109.07, an adjusted coefficient of 85% and an RMSE of 3.85. R^2 of 85 % and an RMSE of 3.85.

These measures were better than those of the Lasso and Ridge regression models. According to this model and following the p-value of less than $2.2e^{-16}$, all variables are significant, except for: Alcohol, Hepatitis B, Measles, Population, Slimness.1.19, Slimness.5.9. This means that we can do without these variables to explain life expectancy. However, applying the Akaike information criterion to the multiple linear regression model, the variables that best explain life expectancy are: adult mortality, infant deaths, percentage of expenditure, measles, under-five deaths, polio, total expenditure, diphtheria, HIV/AIDS, GDP, thinness. 1.19 years, income composition, and school enrolment.

Table 1

Models	Adjusted R^2	RMSE
Multiple Linear Regression	**0.85**	**3.85**
Lasso Regression	0.82	3.85
Ridge Regression	0.82	3.91

Conclusion

Before analysing this data set, we had the impression that life expectancy could be increased if we had more money. This is because it takes money to be healthy and to receive appropriate medical treatment. Moreover, if a country is economically developed (GDP), all its citizens can afford appropriate medical treatment. This would mean that life expectancy depends largely on economic factors. However, after analysing this dataset, we have concluded that life expectancy is mainly affected by adult mortality, infant mortality, percentage of expenditure, measles, under-five mortality, polio, total expenditure, diphtheria, HIV/AIDS, GDP, wasting. 1.19 years, income composition, and schooling. This makes sense because if a person is educated enough to recognize health problems, they can make appropriate lifestyle changes, including but not limited to diet and exercise, which would ideally extend their life expectancy. Education can change a person's perception and help them understand the benefits of being fit and its impact on health. In addition, a higher level of education could be linked to a higher income, and a higher income would mean higher spending on health and fitness. Thus, education is directly or indirectly a good predictor of life expectancy. Various machine learning models have been used for training. Among these models, the multiple linear model has proven to be very effective in determining both the coefficient of determination and the errors. This model can therefore be used for the prediction of life expectancy.

References

1. Arias E. United States Life Tables, 2009. National Vital Statistics Reports. 2014; 62:1–63.

2. Yafei Wu, Ke Hu, Yaofeng Han, et al. Spatial Characteristics of Life Expectancy and Geographical Detection of Its Influencing Factors in China. International Journal of Environmental Research and Public Health. 2020;17:906. https://doi.org/10.3390/ijerph17030906

3. Ming Wen, Danan Gu. Air Pollution Shortens Life Expectancy and Health Expectancy for Older Adults: The Case of China. The Journals of Gerontology: Series A. 2012;67:1219–1229. https://doi.org/10.1093/gerona/gls094

4. Cervantes PAM, López NR, Rambaud SC. The Relative Importance of Globalization and Public Expenditure on Life Expectancy in Europe: An Approach Based on MARS Methodology. International Journal of Environmental Research and Public Health. 2020;17:8614. http://dx.doi.org/10.3390/ijerph17228614

5. Reynolds MM, Avendano M. Social Policy Expenditures and Life Expectancy in High-Income Countries. American Journal of Preventive Medicine. 2018;54:72–79. https://doi.org/10.1016/j.amepre.2017.09.001

6. Sede IP, Ohemeng W. Socio-economic determinants of life expectancy in Nigeria (1980–2011). Health Economics Review. 2015;5:1–11.

7. Daquan Huang, Shuimiao Yang, Tao Liu. Life Expectancy in Chinese Cities: Spatially Varied Role of Socioeconomic Development, Population Structure, and Natural Conditions. International Journal of Environmental Research and Public Health. 2020;17:6597. http://dx.doi.org/10.3390/ijerph17186597

8. Okamoto, K. Life Expectancy at Age 65 and Environmental Factors: An Ecological Study in Japan. Archives of Gerontology and Geriatrics. 2006;43:85–91. http://dx.doi.org/10.1016/j.archger.2005.09.005

9. WHO. Ambient Air Pollution: A Global Assessment of Exposure and Burden of Disease. World Health Organization, 2016. 121 p. https://apps.who.int/iris/handle/10665/250141

10. Xinjie Zha, Yuan Tian, Xing Gao, et al. Quantitatively Evaluate the Environmental Impact Factors of the Life Expectancy in Tibet, China. Environmental Geochemistry and Health. 2019;41:1507–1520. https://link.springer.com/article/10.1007/s10653-018-0211-z

11. Nkalu CN, Edeme RK. Environmental Hazards and Life Expectancy in Africa: Evidence from GARCH Model. *SAGE* Open; 2019, 9. https://doi.org/10.1177/2158244019830500

12. Inglehart Ronald, Christian Welzel. How Development Leads to Democracy What We Know About Modernization. Foreign Affairs. 2009;88:33–48.

13. Cockerham WC. The Social Determinants of the Decline of Life Expectancy in Russia and Eastern Europe: A Lifestyle Explanation. Journal of Health and Social Behavior. 1997;38:117–130.

14. Jessica Y Ho, Arun S Hendi. Recent Trends in Life Expectancy across High Income Countries: Retrospective Observational Study. BMJ. 2018;362:k2562. https://doi.org/10.1136/bmj.k2562

15. Penuelas J, Krisztin T, Obersteiner M, et al. Country-Level Relationships of the Human Intake of N and P, Animal and Vegetable Food, and Alcoholic Beverages with Cancer and Life Expectancy. International Journal of Environmental Research and Public Health. 2020;17:7240. https://doi.org/10.3390/ijerph17197240

16. Sidey-Gibbons JAM, Sidey-Gibbons CJ. Machine Learning in Medicine: A Practical Introduction. BMC Medical Research Methodology. 2019;19:1–18. https://bmcmedresmethodol.biomedcentral.com/ articles/10.1186/s12874-019-0681-4

17. Malpe V, Tugaonkar P. Machine Learning Trends in Medical Sciences. In: Proc. 2nd International Conference on I-SMAC (IoT in Social, Mobile, Analytics and Cloud), August 2018. P. 495–499.

18. KumarRajarshi. WHO. Life Expectancy. Statistical Analysis on Factors Influencing Life Expectancy. https://www.kaggle.com/datasets/kumarajarshi/life-expectancy-who

19. Thu Pham-Gia, Vartan Choulakian. Distribution of the Sample Correlation Matrix and Applications. Open Journal of Statistics. 2014;4:48571. 10.4236/ojs.2014.45033

20. Svensson K. Predicting Life Expectancy Using Machine Learning. 2018. https://www.semanticscholar.org/paper/Predicting-Life-Expectancy-Using-Machine-Learning-Svensson/984adbb5aee 16d38a6686895dda2afd3087b2261

21. Müller AC, Guido S. Introduction to Machine Learning with Python.,1st ed. O'Reilly Media, Inc.; 2016.

22. Ki-Young Lee, Kyu-Ho Kom, Jeong-Jin Kang, et al. Comparison and Analysis of Linear Regression and Artificial Neural Network. International Journal of Applied Engineering Research. 2017;12:9820–9825.

23. Paranjape RS, Challacombe SJ. HIV/AIDS in India: An Overview of the Indian Epidemic. Oral Diseases. 2016;22:10–14. http://dx.doi.org/10.1111/odi.12457

24. Haebong Woo. Patterns and Evolution of Life Span Inequality Using the Gini Coefficient. Pogŏn Sahoe Yŏn'gu. 2013;33:419–451. 10.15709/hswr.2013.33.4.419. https://www.researchgate.net/publication/275246163_Patterns_and_Evolution_of_Life_Span_Inequality_Using_the_Gini_Coefficient

25. Chen Wu. Human Capital, Life Expectancy, and the Environment. Journal of International Trade and Economic Development. 2017;26:885–906.

26. Carolina Cosculluela-Martínez, Raquel Ibar Alonso, Geoffrey JD Hewings. Life Expectancy Index: Age Structure of the Population and Environmental Change. Social Indicators Research. 2019;142:507–522.

27. Muhamad Haroon Shah, Nianyong Wang, Irfan Ullah, et al. Does Environment Quality and Public Spending on Environment Promote Life Expectancy in China? Evidence from a Nonlinear Autoregressive Distributed Lag Approach. International Journal of Health Planning and Management. 2021;36:545–560. http://dx.doi.org/10.1002/hpm.3100

28. Mariani F, Pérez-Barahona A, Raffin, N. Life Expectancy and the Environment. Journal of Economic Dynamics and Control. 2010;34:798–815.

29. Tuljapurkar Sh, Horvitz CC. From Stage to Age in Variable Environments: Life Expectancy and Survivorship. Ecology. 2006;87:1497–1509. http://dx.doi.org/10.1890/0012-9658(2006)87[1497:FSTAIV]2.0.CO;2

30. Kampa M, Castanas E. Human Health Effects of Air Pollution. Environmental Pollution. 2008;151:362–367. http://dx.doi.org/10.1016/j.envpol.2007.06.012

31. Tagaris E, Kuo-Jen Liao, DeLucia AJ, et al. Potential Impact of Climate Change on Air Pollution-Related Human Health Effects. Environmental Science and Technology. 2009;43:4979–4988.

32. Anderson JO, Thundiyil JG, Stolbach, A. Clearing the Air: A Review of the Effects of Particulate Matter Air Pollution on Human Health. Journal of Medical Toxicology. 2012;8:166–175. http://dx.doi.org/10.1007/s13181-011-0203-1

33. Wuffle A, Brians CL, Coulter K. Taking the Temperature: Implications for the Adoption of Election Day Registration, State level Voter Turnout, and Life Expectancy. PS: Political Science & Politics**.** 2012;45:78–82.

34. Brunner E, Maruyama K. SP4-32 Health and Sustainability: An International Ecological Study of Carbon Dioxide Emissions and Life Expectancy. Journal of Epidemiology and Community Health. 2011;65:A442–A443.

35. Clootens N. Public Debt, Life Expectancy, and the Environment. Environmental Modeling & Assessment. 2017;22:267–278.

36. Tetzlaff F, Epping J, Sperlich S, et al. Widening Income Inequalities in Life Expectancy? Time Trend Analysis Using German Health Insurance Data. Journal of Epidemiology and Community Health. 2020;74:592–597. 10.1136/jech-2019-212966

Received 14.09.2022.
Revised 10.10.2022.
Accepted 14.10.2022.

About the Authors:

Brou Kouame Amos, postgraduate of the Information Technology Department, Peoples' Friendship University of Russia (RUDN) (6, Miklikho-Maklaya St., Moscow, 117198, RF), broukouameamos9@gmail.com

Smirnov, Ivan V., associate professor of the Information Technology Department, Peoples' Friendship University of Russia (RUDN) (6, Miklikho-Maklaya St., Moscow, 117198, RF), Cand.Sci. (Phys.-Math.), associate professor, ORCID, Scopus, smirnov-iv@rudn.ru

Claimed contributorship:

Brou Kouame Amos: basic concept formulation; research objectives and tasks; data pre-processing; analysis of research results. I. V. Smirnov: work control; the text revision; correction of the conclusions.

Conflict of interest statement

The authors do not have any conflict of interest.

All authors have read and approved the final manuscript.

Advanced Engineering Research 2022. V. 22, no. 4. P. 384−390. ISSN 2687−1653

INFORMATION TECHNOLOGY, COMPUTER SCIENCE, AND MANAGEMENT

Check for updates

UDC 004.01

Original article

https://doi.org/10.23947/2687-1653-2022-22-4-384-390

Development of Architecture for Connecting a System Module for People with Disabilities

Alexey A. Baskakov✉**, Alexey G. Tarasov**

Moscow State University of Technology (MSUT "STANKIN"), 1, Vadkovsky Lane, Moscow, Russian Federation

✉ aleks.baskakov@mail.ru

Abstract

Introduction. To develop new system modules of software to help employees with disabilities, it is required to work out an architectural solution for the interaction of all parts of the system. As a result of the analysis and design, it is necessary to obtain a software architecture that must meet a number of standard requirements. First of all, it should be safe. To do this, you should take into account the error logging system, event auditing, the possibility of disabling the functionality immediately after putting it into commercial operation, internal mechanisms for validating client input requests and server responses. This study is aimed at the development of basic system maintenance options, the analysis of exception cases under interacting with the user for further evaluation of the architecture efficiency, and the direct project development.

Materials and Methods. The architectural decision was carried out using the Unified Modeling Language (UML), which helps to build visual images of the life cycle and interaction of all components of the system. The syntax of the UML deployment diagram was used to study the interaction of the main modules of the future system, and the syntax of the UML sequence diagram was used to process the lifecycle. A use case diagram was also applied to describe the main use cases. To study the interaction of the main modules of the future system, the UML deployment diagram syntax was used. For life cycle processing, the UML sequence diagram syntax was applied. In addition, a use case diagram was applied to describe the base use cases.

Results. An architecture that has a scheme for the interaction of individual modules and systems, as well as options for using the software package for the future implementation of the software product, has been developed. The proposed system architecture meets the requirements of security, reliability (fault tolerance), and performance. The authors have fixed the functional requirements of the system of assistance to employees of enterprises with hearing problems for the possibility of their employment and work on the telecommunication Internet. Basic variations of system maintenance have been developed.

Discussion and Conclusions. Building a competent architecture provides taking into account cases that go beyond the normal use of the system, and applying a fuzzy model to determine the system efficiency. Further in-depth description of deployment and operation options will enable to implement an efficient and productive system.

Keywords: UML deployment diagram, UML sequence diagram, software architecture, commercial software, UML use case diagram.

Acknowledgements. The authors would like to thank Yuri G. Kogan, Cand.Sci. (Engineering), associate professor of the Department of Information Technologies and Computing Systems, STANKIN Moscow State Technical University, who participated in the development of the system use cases as a subject matter expert.

For citation. A. A. Baskakov, A. G. Tarasov. Development of Architecture for Connecting a System Module for People with Disabilities. Advanced Engineering Research, 2022, vol. 22, no. 4, pp. 384–390. https://doi.org/10.23947/2687-1653-2022-22-4-384-390

Introduction. Previously, the causes of disability among the population with disabilities were investigated through expert evaluation using the method of pairwise comparisons by Thomas L. Saati. As a result, it has been discovered that for improving the ability to work, it is required to develop a comprehensive system that would solve the problem of hearing loss and make it possible to work in remote support centers, where understanding the interlocutor is mandatory [1]. Before evaluating the efficiency, you need to work out all possible options for system maintenance. This will determine the service architecture efficiency associated with the performance of each module of the desired level of service. To reduce labor costs at the development stage, it is required to determine in advance exception cases when the module is working with transcription.

The scientific novelty of this study is the efficiency of the architecture in terms of tasks to be solved (service options).

The assessment was carried out using a fuzzy model of expert opinions in this field. It goes beyond the scope of discussion of this article.

To develop the architecture, you need to consider the following parameters:

– cross-platform — the software product should cover the main operating systems;

– fault tolerance — the system should work stably in case of interruptions in operation;

– security — the system must support logging, monitoring and auditing of user events;

– horizontal scalability — with an increase in the number of clients, the software product must work at the same speed by increasing the number of servers;

– performance — the system should work without delays in real time.

Planning and describing the software architecture is an important and necessary step before the direct development of a client-server application. The system should have a module for speech recognition and translate it into text, thereby allowing people with hearing problems to work on remote support.

Materials and Methods.

UML is a special modeling language that is used in the development of the architecture of computing systems, software, network architecture, and in the construction of business processes[1] [2, 3].

The following schemes were used to describe the project architecture:

1. Sequence diagram describes the process of receiving calls and processing them from the point of view of an employee of the organization[2].

2. Use case diagram describes the use cases of the system.

3. Deployment diagram describes the architecture of the system.

[1] Khammatova LA. Universal UML Modeling Language, Basic Diagrams and Usage Problems. In: ‘Proryvnye nauchnye issledovaniya: problemy, zakonomernosti, perspektivy”, Coll. of Papers XIII Int. Sci.-Pract. Conf. Penza, 2019. P. 88–90. (In Russ.)
[2] Teslenko IB, Tsarev AO. Osobennosti informatsionnogo proektirovaniya s ispol'zovaniem yazyka UML. In: “Innovatsionnoe razvitie sotsial'no-ehkonomicheskikh sistem: usloviya, rezul'taty i vozmozhnosti”, Proc. V Int. Sci.-Pract. Conf. Orekhovo-Zuyevo, 2017. P. 174–177. (In Russ.)

Research Results. The construction of UML diagrams made it possible to determine the system service quality criteria, to take into account exception cases and ways of processing them, and the construction of a deployment diagram — to determine the system efficiency using a fuzzy model.

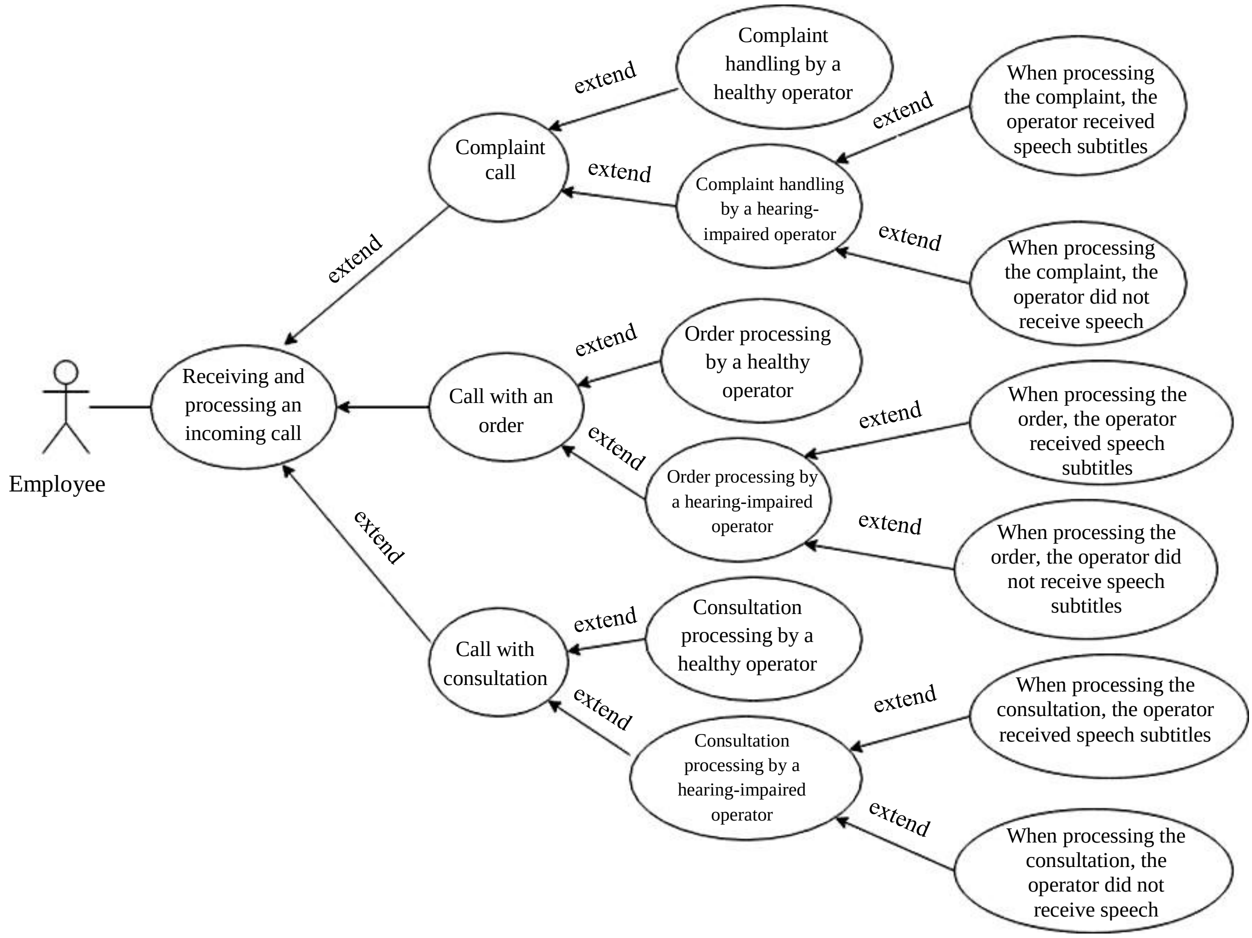

Fig. 1. Diagram of system use cases (the authors' figure)

Figure 1 shows a use case diagram developed by the authors of this article, which demonstrates that the main remote support requests come for the following reasons: complaints about the provision of services by the enterprise, consultation, and ordering services. At that, it should be borne in mind that the system of automatic generation of subtitles may work incorrectly for some reasons, i.e., it could not recognize speech, filtering of prohibited words was not passed, etc. In this case, you should switch the client to a robotic system or another operator.

The robotic system is an automatic voice generation module with its own life cycle, which enables to inform the client about technical problems during a call. The module also provides switching to another free operator at the will of the client or taking a queue in case of a heavy load at a given time.

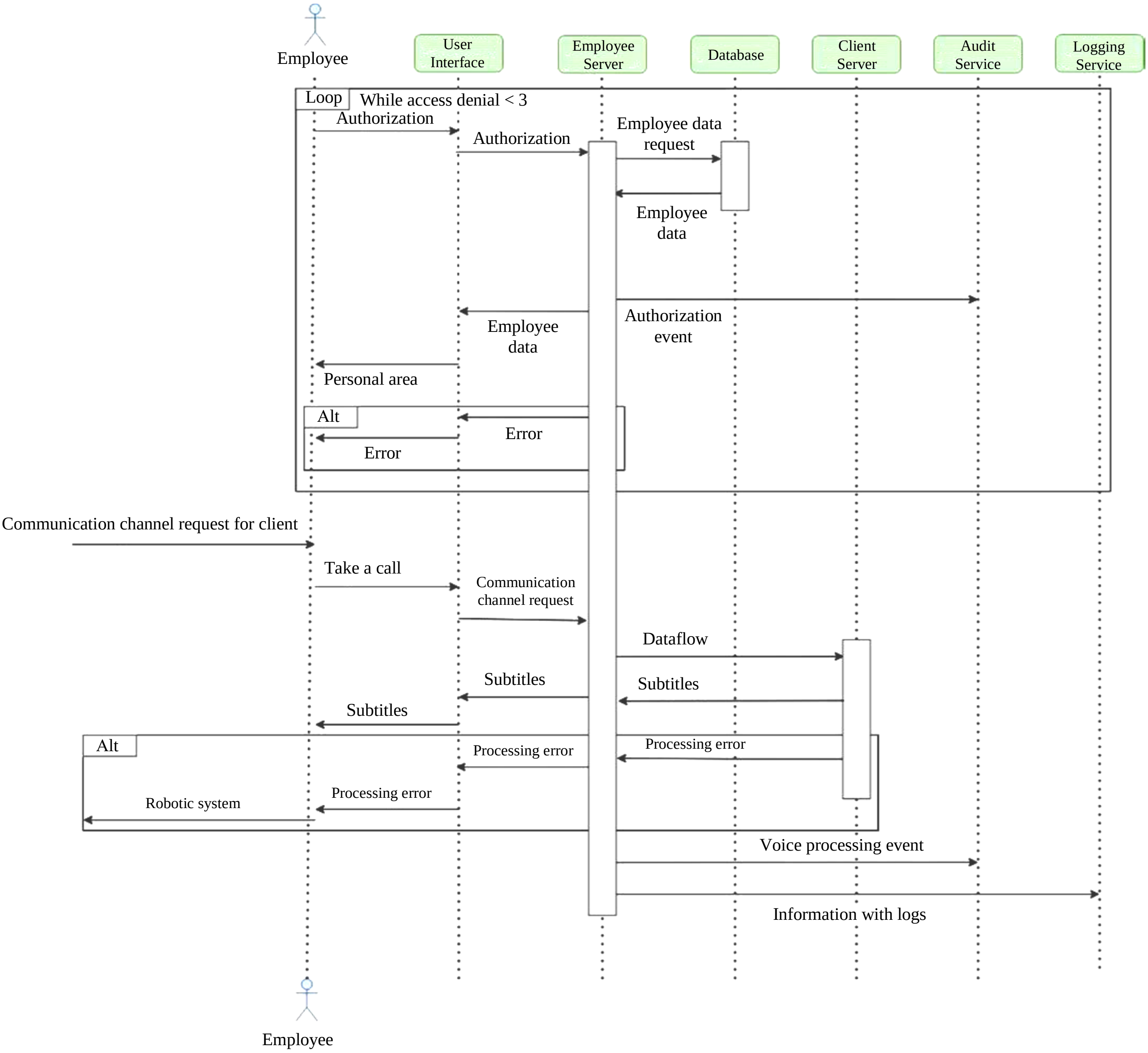

Fig. 2. Employee workflow diagram (the authors' figure)

igure 2 shows a workflow diagram from the point of view of an employee of the organization. After the standard authorization procedure, a call from the client may be received in the employee's personal account via a broadcast channel. If the call is accepted, a continuous information transmission channel is established between the client and the employee. The received data is transmitted in real time to the processing module, where text subtitles are generated using a set of transformations and methods.

In case of a conversion error, the client switches to a robotic system, and the employee is notified that voice processing is impossible. All actions (events) of the client and employee are marked in the speech recognition and logging module.

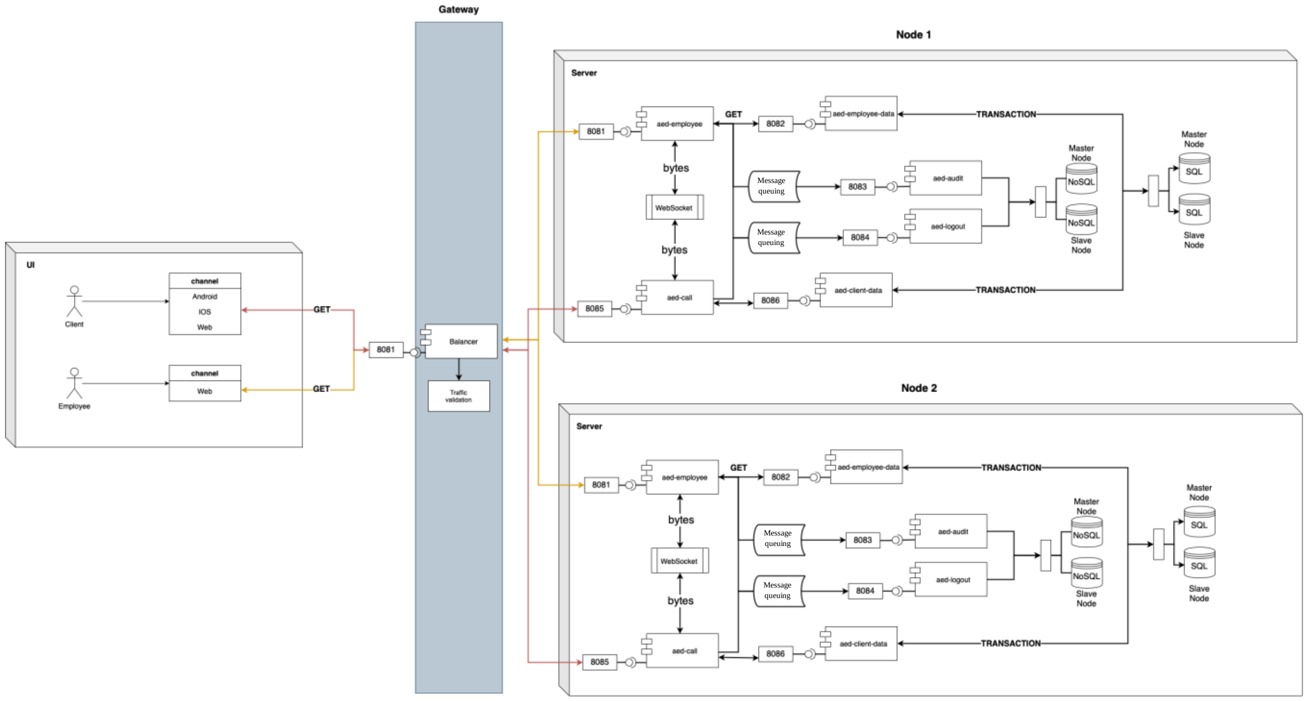

Fig. 3. System component deployment diagram (the authors' figure)

Figure 3 shows a microservice architecture project deployment diagram [4, 5], which consists of three blocks:

Internet. Visual modules for user-client interaction (User Interface, UI) are located on the Internet. It is worth noting that the client's channels for implementation are represented by three platforms: IOS, Android, Web; whereas the employee has only a Web channel. Principally, this is due to the fact that an employee does not usually need such applications for mobile operating systems because of the kind of work and security.

Data Gateway. The key task of the gateway is to provide the transfer of information from the Internet to the local network, where the primary servers are deployed, and back. This gives a number of advantages. First, there is a common point for transmitting all data. It is not possible to interact with the server bypassing the security gateway. Secondly, all requests can be checked for compliance with the originally laid format. Thirdly, the gateway allows load balancing between nodes, thereby achieving fault tolerance. If one node stops functioning, all requests are automatically distributed among other nodes. Fourthly, the system can be easily scaled. If the number of requests grows over time, it is enough to add a new node and the performance will remain at the same level.

Nodes. It is a complex system consisting of services interacting with each other. The major ones include services for receiving requests from a client and an employee. Their task is to receive a request, process it and set up interaction with each other using special components — sockets that allow data exchange in real time. These components receive data about the client and employee from special services that interact with a relational database using the SQL language [6]. For fault tolerance and speed, the database also has several nodes, but at least two. All user and client actions are transmitted to the speech recognition and logging services using message queues. This gives some advantages — asynchronous data transmission and safety of all information in case of a service failure. At that, storing such information in a relational database is impractical due to the uniformity and simplicity of the structure. For this reason, it is advisable to use a document-oriented NoSQL DBMS [7, 8][3]. It is worth noting that independent databases in each of the nodes provide high performance, and the consistency and relevance of data is implemented through a mechanism, whose replication will be described in detail in the following studies. The "Master-Slave" mechanism in

[3] Popov VB, Gavrikov IV. Tekhnologii "NOSQL" v algoritmakh analiza bol'shikh dannykh i iskusstvennom intellekte. In: "Problemy informatsionnoi bezopasnosti", Coll. of Papers V All-Russian Sci.-Pract. Conf. with international participation. Simferopol, Gurzuf, 2019. P. 158–160. (In Russ.)

relational and non-relational databases is required for possible vertical scaling and minimizing resource costs in case of an increase in the load on a single node.

All requests from the Internet to the local network occur over the HTTP protocol using the following methods:

– GET — in case of receiving information from any of the modules;

– POST — in case of creating records in any of the modules;

– PUT — in case of a change in any of the modules.

Requests to the stored information occur within transactions to provide data integrity [9–11].

Discussion and Conclusions. Architecture development, using the language of graphical description, enables to visually describe the functional requirements for the system, evaluate its effectiveness and reduce the number of errors.

The use case diagram made it possible to identify the need to develop a robotic system, as well as to identify many service options for a fuzzy model in case of exception situations during voice transcription. The deployment diagram helped to determine the effectiveness of the functions performed by each internal service, and the sequence diagram helped to determine the product lifecycle.

References

1. Baskakov AA, Tarasov AG. To the Problem of Using an Automated Workplace by People with Disabilities. Advanced Engineering Research. 2021;21:290–296. https://doi.org/10.23947/2687-1653-2021-21-3-290-296

2. Bazydto G, Adamski M, Węgrzyn M, et al. From UML State Machine Diagram into FPGA Implementation. IFAC Proceedings Volumes. 2013;46:298–303. https://doi.org/10.3182/20130925-3-CZ-3023.00061

3. Shailaja Uke, Ravindra Thool. UML Based Modeling for Data Aggregation in Secured Wireless Sensor Network. Procedia Computer Science. 2016;78:706–713. https://doi.org/10.1016/j.procs.2016.02.120

4. Saulo S de Toledo, Antonio Martini, Dag IK Sjøberg. Identifying Architectural Technical Debt, Principal, and Interest in Microservices: A Multiple-Case Study. Journal of Systems and Software. 2021;177:110968. https://doi.org/10.1016/j.jss.2021.110968

5. Nuno Mateus-Coelho, Manuela Cruz-Cunha, Luis Gonzaga Ferreira. Security in Microservices Architectures. Procedia Computer Science. 2021;181:1225–1236. https://doi.org/10.1016/j.procs.2021.01.320

6. Grigor'ev YuA, Matyukhin VG. Otsenka vremeni vypolneniya slozhnogo SQL-zaprosa v SUBD MS SQL SERVER 2000. Informatika i sistemy upravleniya. 2004;2:3–13. (In Russ.)

7. Davydov DA, Manylov PS. Evolution of NOSQL. Scientific and Technical Volga Region Bulletin. 2013;3:131–135.

8. Sharipova NN. About the Use of NOSQL Databases. Wschodnioeuropejskie czasopismo naukowe. 2016;9:73–76.

9. Chodak G, Suchacka G, Chawla Y. HTTP-Level E-Commerce Data Based on Server Access Logs for an Online Store. Computer Networks. 2020;183:107589. https://doi.org/10.1016/j.comnet.2020.107589

10. Okumura N, Ogata K, Shinoda Y. Formal Analysis of RFC 8120 Authentication Protocol for HTTP under Different Assumptions. Journal of Information Security and Applications. 2020;53:102529. https://doi.org/10.1016/j.jisa.2020.102529

11. Robert LR Mattson, Somnath Ghosh. HTTP-MPLEX: An Enhanced Hypertext Transfer Protocol and Its Performance Evaluation. Journal of Network and Computer Applications. 2009;32:925–939. https://doi.org/10.1016/j.jnca.2008.10.001

Received 26.09.2022.

Revised 24.10.2022.

Accepted 26.10.2022.

About the Authors:

Baskakov, Alexey A., post-graduate student of the Information Technologies and Computing Systems Department, Moscow State University of Technology (MSUT “STANKIN”) (1, Vadkovsky Lane, Moscow, 127055, RF), ORCID, aleks.baskakov@mail.ru

Tarasov, Alexey G., associate professor of the Information Technologies and Computing Systems Department, Moscow State University of Technology (MSUT “STANKIN”) (1, Vadkovsky Lane, Moscow, 127055, RF), Cand.Sci. (Eng.), ORCID, tarasov.ag@mail.ru

Claimed contributorship:

A. A. Baskakov: computational analysis; text preparation; search for scientific literature; formulation of conclusions. A. G. Tarasov: academic advising; research objectives and tasks setting; correction of the conclusions.

Conflict of interest statement

The authors do not have any conflict of interest.

All authors have read and approved the final manuscript.